The completion of this thesis
was supported by the

Randy Seeling Award

given, in his memory, to another
outstanding graduate student
of the Geology Department,
University of Minnesota, Duluth.

PETROGRAPHIC EVIDENCE FOR THE RECYCLING OF LATE PROTEROZOIC - EARLY PALEOZOIC QUARTZOSE ARENITES, SOUTHEASTERN MINNESOTA - SOUTHWESTERN WISCONSIN

A THESIS
SUBMITTED TO THE FACULTY OF THE GRADUATE SCHOOL
OF THE UNIVERSITY OF MINNESOTA
BY

AMY MARIE GALAROWICZ

IN PARTIAL FULFILLMENT OF THE REQUIREMENTS
FOR THE DEGREE OF
MASTER OF SCIENCE

DECEMBER 1997

ABSTRACT

The Late Proterozoic - Early Paleozoic arenites of southeastern Minnesota - southwestern Wisconsin are all mature, quartzose arenites. The Late Proterozoic Hinckley Sandstone was deposited as a rift fill sandstone. With the transgression of the Sauk Sea during Cambrian time, the continent was flooded. In southeastern Minnesota, the sea entered the Hollandale embayment. During this time of transgression and regressions, the quartzose Cambrian Mt. Simon Sandstone, Eau Claire Formation, Galesville Sandstone, Ironton Sandstone, Franconia Formation, Jordan Sandstone, and the New Richmond Sandstone of the Shakopee Formation were deposited. Following a major regression at the end of Shakopee time, the sea re-entered the continent. The Tippecanoe transgression was responsible for the widespread deposition of the St. Peter Sandstone during Middle Ordovician time.

All of the arenites of this study are quartzose in nature and highly mature. Almost 95 percent of all the framework grains consist of monocrystalline quartz; potassium feldspar and plagioclase are minor components. Two units, the Eau Claire Formation and the Franconia Formation, contain significantly higher amounts of feldspar, generally 11 to 15 percent. These two quartzose feldspathic units are in general finer grained than the other more quartzose units, an observation noted earlier by other workers.

Other detrital minerals include polycrystalline quartz and multicycle monocrystalline quartz. A decrease in the amount of polycrystalline quartz stratigraphically upward in the column suggests that this unstable mineral portion was eliminated by abrasion.

Multicycle quartz grains with abraded quartz overgrowths are present in all nine of the units. The presence of an abraded quartz overgrowth indicates that the grain was once previously cemented by quartz, and that through erosional processes, the grain was removed from its original environment of deposition and incorporated into a stratigraphically younger unit. The grain, with the original overgrowth intact, is then recemented with quartz, resulting in a euhedral overgrowth enclosing the abraded one.

The amount of unaltered and altered feldspar types can also be used to support the recycling of the quartzose arenites. Peaks of unaltered feldspar occur during Eau Claire and Franconia time, indicating that influxes of fresh sediment may have occurred during these times. Further evidence of the recycling of the quartzose arenites in relation to the feldspar concentrations can be found in the Ironton Sandstone, in which unaltered feldspar of Eau Claire time was reworked and recycled to the point that during Ironton time, the amount of altered feldspar surpassed the amount of unaltered feldspar.

A high mineralogical maturity in the arenites is also evidenced by the heavy mineral concentrations. All of the units contain similar heavy mineral concentrations, consisting mainly of rounded zircon, tourmaline, rutile, and garnet. As further evidence of the recycling of the arenites, all nine units also contain tourmaline grains with abraded overgrowths. Abraded tourmaline overgrowths form in the same manner that quartz overgrowths do, and are indicative of recycling.

In summary, it has long been speculated that the Late Proterozoic - Early Paleozoic quartz arenites are multicycle in origin because of the presence of clean quartz sand (e.g. Matsch and Ojakangas, 1982, p. 65; Dott and Batten, 1982, p. 283; Dott and Prothero, 1994, p. 236). This study now provides petrographic evidence that erosional processes during the Late Cambrian - Early Ordovician marine transgressions and regressions played a substantial role in the creation of these quartz arenites, thereby recycling grains from older exposed units within the Hollandale embayment.

ACKNOWLEDGMENTS

I would like to acknowledge the people who guided me, both academically and personally, toward the completion of this thesis. The advice and guidance of my advisor, Dr. Richard Ojakangas, is greatly appreciated. I would also like to thank my committee members, Dr. Howard Mooers and Dr. Tom Johnson, for their suggestions and revisions of the manuscript, the University of Minnesota Graduate School for providing partial funding of this project, and the Large Lakes Observatory for allowing me to extend my stay at the University. To those previous workers who have petrographically studied the units involved in this thesis, and the Minnesota Geological Survey, I am grateful for the use of the thin sections. To Tony Runkel, for his help with the location of outcrops. The Minnesota Department of Natural Resources, Division of Minerals Drill Core Library at Hibbing, Minnesota provided a portion of the drill core samples. My fellow graduate students and geology students of the University of Minnesota - Duluth are thanked for their support. A special thank you to my friends who helped me face the challenges that this thesis, Duluth, and life presented throughout the past few years. Finally, I would like to thank my family for their constant moral and financial support.

I have fought and kicked and fasted
and prayed and cursed and cried myself to the
point of existing. It has been like being born
again, literally. Just knowing
has meant everything to me. Knowing has
pushed me out into the world, into college,
into places, into people.
-Alice Walker

TABLE OF CONTENTS

FIGURES

TABLES

PLATES

PLATES

PLATES

PLATES

PLATES

CHAPTER I

INTRODUCTION

Late Cambrian seas flooded the north-central United States, transgressing northward in the Hollandale embayment, a broad lowland. The seas were confined to an area bordered by the Transcontinental arch to the north and west, by the Wisconsin dome to the northeast, and by the Wisconsin arch to the east (Figure 1). This vegetationless cratonic surface was weathered and eroded for the nearly half a billion years before Cambrian sedimentation began (Dott and Prothero, 1994, p. 236). Wind and rivers had distributed the Cambrian quartz-rich sands in widespread sheets and the Sauk transgression caused marine reworking of much of that sand (Dott and Prothero, 1994, p. 238). As the Late Cambrian seas transgressed and regressed, a sequence of quartzose arenites (Figure 2) was deposited upon a wide variety of Precambrian basement rocks.

Quartz arenites can be defined as sandstones containing 95 percent or more detrital quartz grains (Pettijohn, et al., 1987, p. 176), typically resulting from extensive periods of sediment reworking or recycling. Suttner (1981) determined that first cycle quartz arenites are produced through a specific and complex combination of extreme conditions consisting of a tropical climate, low relief, and slow sedimentation rates. Rarely are these conditions met, and therefore Suttner (1981) determined that a majority of quartz arenites are multicycle in origin. Pettijohn et al; (1987, p. 184) also noted that the presence of abraded overgrowths is indicative of a multicycle origin.

Also, it is not uncommon for multicycle quartz arenites to be associated with transitional sandstone types such as sub-lithic or sub-feldspathic arenites. Quartz arenites are usually viewed as "cleaned-up" sandstones, commonly showing a decrease in feldspar or rock fragments in stratigraphically younger units. It is this evolutionary progression that implies quartz arenites are multicycle sands (Pettijohn et al., 1987, p.178).

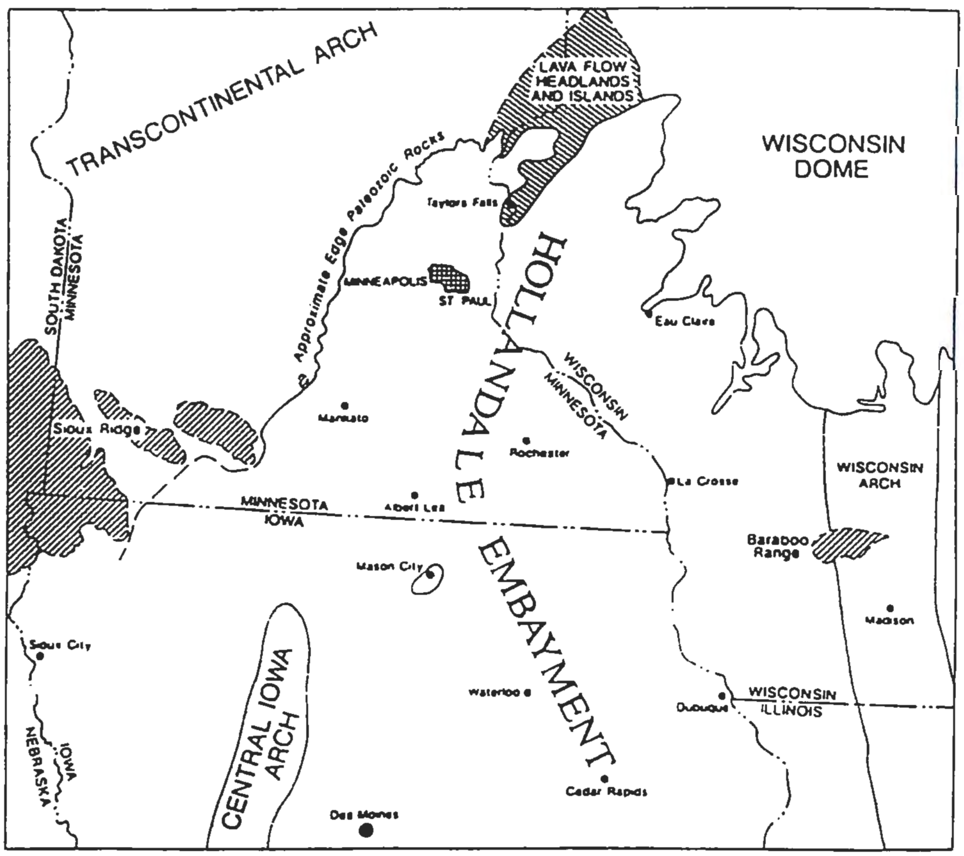

Fig. 1: Paleogeography of southeastern Minnesota and adjoining areas during Late Cambrian time. (From Mossler, 1992).

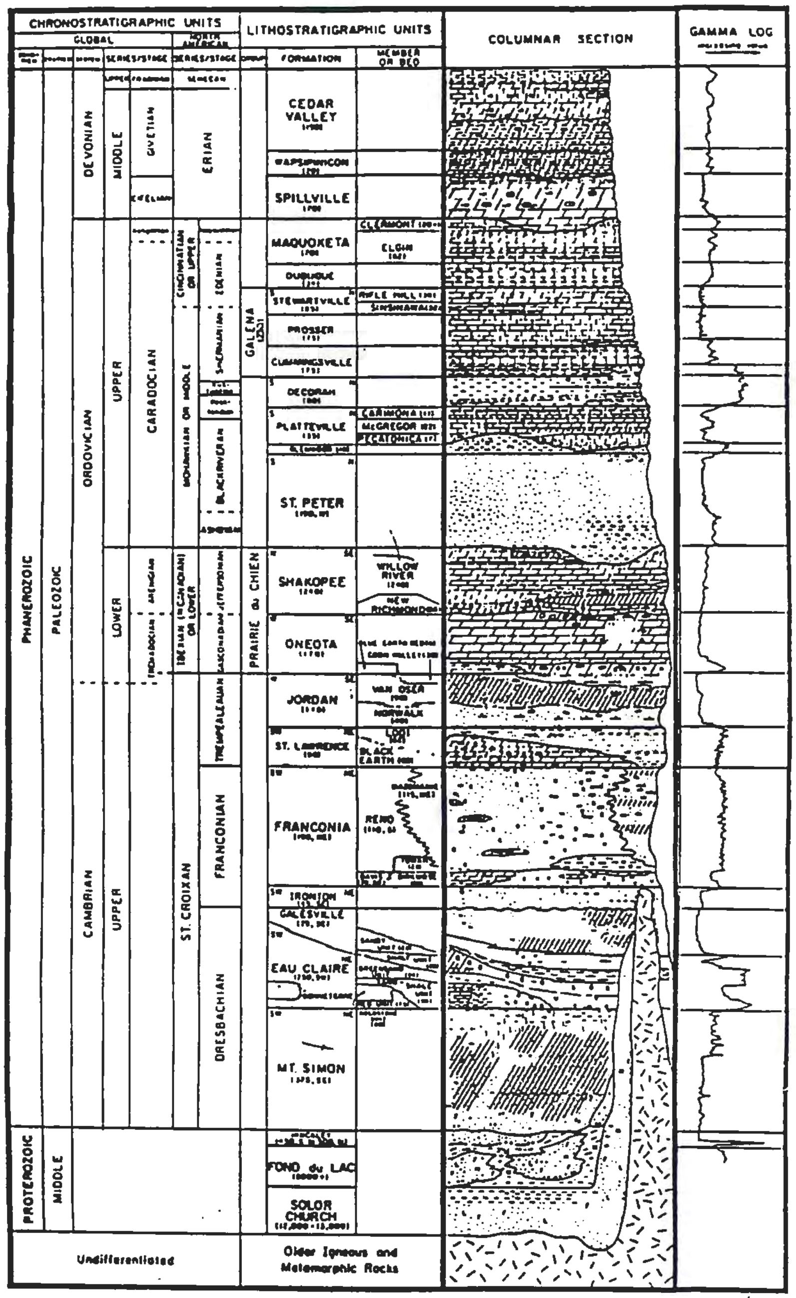

Fig. 2: Stratigraphic relationship of the Late Proterozoic - Early Paleozoic arenites. (From Mossler, 1987).

The Lower Paleozoic quartzose arenites (defined as quartz-rich arenites with a small, variable amount of feldspar present) of this study have undergone a significant amount of reworking and possible recycling in a marine environment, indicative of transgressing and regressing shorelines. During these transgressions and regressions, it is hypothesized that the quartzose arenites of the Hollandale embayment underwent a great deal of recycling. Several hypotheses may exist to explain the possible role of recycling in the production of these quartzose arenites. These include:

1) The stratigraphically older units were recycled to produce the stratigraphically younger units (Figure 2). An example of this hypothesis would be the recycling of the Hinckley Sandstone to produce a fraction of the Mt. Simon Sandstone.

2) The recycling occurred within each unit, and not from stratigraphically older units. This hypothesis is dependent upon the role of quartz cementation. An example of this hypothesis would be the recycling of the basal Mt. Simon to produce the upper Mt. Simon.

3) No recycling occurred. The abraded quartz overgrowths are actually products of possible dissolution rather than recycling.

By petrographically examining the quartzose arenites of the Late Proterozoic-Early Paleozoic stratigraphic column, evidence for the possible recycling of the quartzose arenites may be found in the presence of abraded quartz overgrowths, a decrease in polycrystalline quartz grains, and a decrease in feldspar content.

Purpose of the study:

Specific objectives of this study are to:

a) Integrate petrographic observations from nine drill cores and outcrop samples from southeastern Minnesota - southwestern Wisconsin to determine the recycling history of the sediments of the Late Proterozoic-Early Paleozoic quartz arenites.

b) Specifically determine and examine the presence, mineralogy, and abundance of quartz types in the quartz arenites to help determine mineralogical maturity by using consistent operational definitions for all units.

c) Determine the presence, mineralogy, and abundance of feldspar types in quartz arenites to help determine mineralogical maturity.

d) Examine the heavy mineral suites to help determine the mineralogical maturity of the quartz arenites.

e) Classify the various quartz arenites as first cycle or multicycle.

This study did not involve intensive stratigraphic or field studies of the Late Proterozoic-Early Paleozoic quartz arenites because several researchers have studied many of the arenites in detail. These researchers will be referred to where appropriate.

Location of the study area:

The Late Proterozoic-Early Paleozoic arenites are exposed in southeastern Minnesota and southwestern Wisconsin. All of the units included in this study were visited in the field and the visited outcrop locations are marked on Figure 3. Samples are from nine drill holes throughout the southeastern part of the state (Figure 3). Drill hole locations, ground elevations, depths, and units sampled are presented in the following pages, and Figure 4 shows a correlation of stratigraphy described in the drill holes.

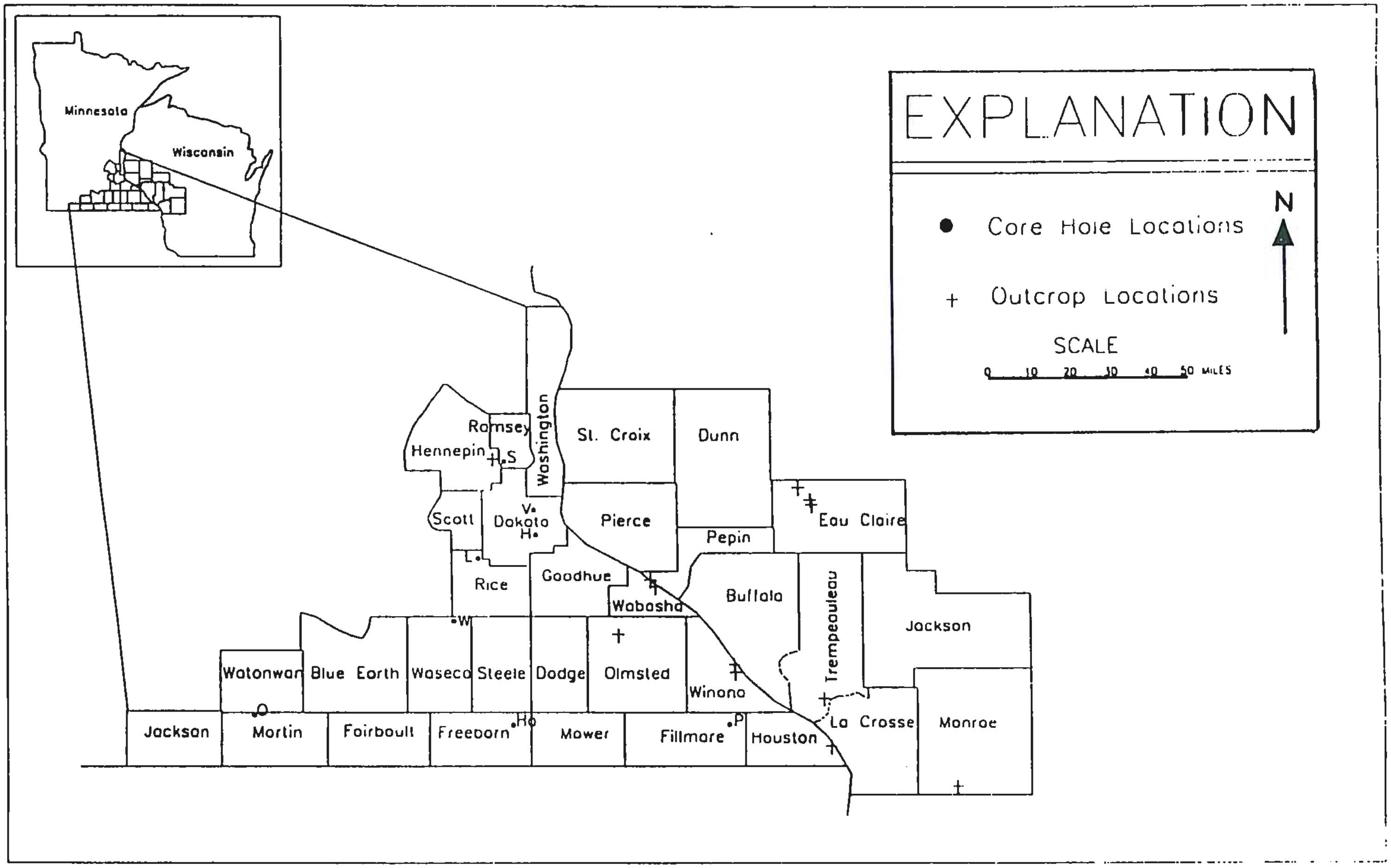

Fig. 3: Location map of study area.
Drill Hole Abbreviations:
O = Pan Ocean Oil, Ltd. **SQ-9**
Ho = Northern Natural Gas Hollandale 1-A **(H1A)**
L = N.N.G. Lonsdale 65-1 **(LH)**
V = N.N.G. Vermillion 66-2**(V66)**
W = Minnegasco **SCH-1**
P = New Jersey Zinc **B-1**
H = N.N.G. Hampton 65-1**(DH)**
S = University of Minnesota **AC-1, BC-1**

Drill Hole Data:

DH= Drill hole	L= Location	C= County
GE= Ground elevation	D= Depth	U= Units sampled

DH= Northern Natural Gas Hollandale 1-A (**H1A**)
L= SE1/4, SE1/4, SW1/4, sec. 7, T. 103N., R. 19W.
C= Freeborn
GE= 1202 ft.
D = 1905 ft.
U= Mt. Simon, Eau Claire, Galesville, Ironton, Franconia, St. Peter

DH= New Jersey Zinc **B-1**
L= NW1/4, SW 1/4, sec. 25, T. 104N., R. 32W.
C= Fillmore
GE= 800 ft.
D = 1124 ft.
U= Mt. Simon, Eau Claire, Galesville, Franconia

DH= Pan Ocean Oil, Ltd. **SQ-9**
L= SE1/4, SW 1/4, sec. 1, T. 104N., R. 32W.
C= Martin
GE= 1185 ft.
D = 703 ft.
U= Mt. Simon

DH= Minnegasco **SCH-1**
L= NW1/4, NE 1/4, sec. 6, T. 108N., R. 22W.
C= Waseca
GE= 1118 ft.
D = 2080 ft.
U= Mt. Simon

DH= University of Minnesota **AC-1**

L= SE1/4, SW 1/4, sec. 21, T. 113N., R. 23W.

C= Ramsey

GE= 950 ft.

D = 982.1 ft.

U= Mt. Simon, Eau Claire, Galesville, Franconia, St. Peter

DH= University of Minnesota **BC-1**

L= SE1/4, SW 1/4, sec. 21, T. 113N., R. 23W.

C= Ramsey

GE= 950 ft.

D = 982.1 ft.

U= Galesville, Ironton

DH= N.N.G. Hampton 65-1(**DH**)

L= NW 1/4, NW 1/4, sec. 4, T. 113N., R. 18W.

C= Dakota

GE= 980 ft.

D = 1374 ft.

U= Mt. Simon, Galesville

DH= N.N.G. Vermillion 66-2(**V66**)

L= SW 1/4, SW 1/4, sec. 8, T. 114N., R. 18W.

C= Dakota

GE= 920 ft.

D = 1115 ft.

U= Mt. Simon, Eau Claire, Galesville

DH= N.N.G. Lonsdale 65-1 (**LH**)

L= SW 1/4, SW 1/4, sec. 14, T. 112N., R. 21W.

C= Rice

GE= 1100 ft.

D = 2843 ft.

U= Mt. Simon, Eau Claire, Galesville

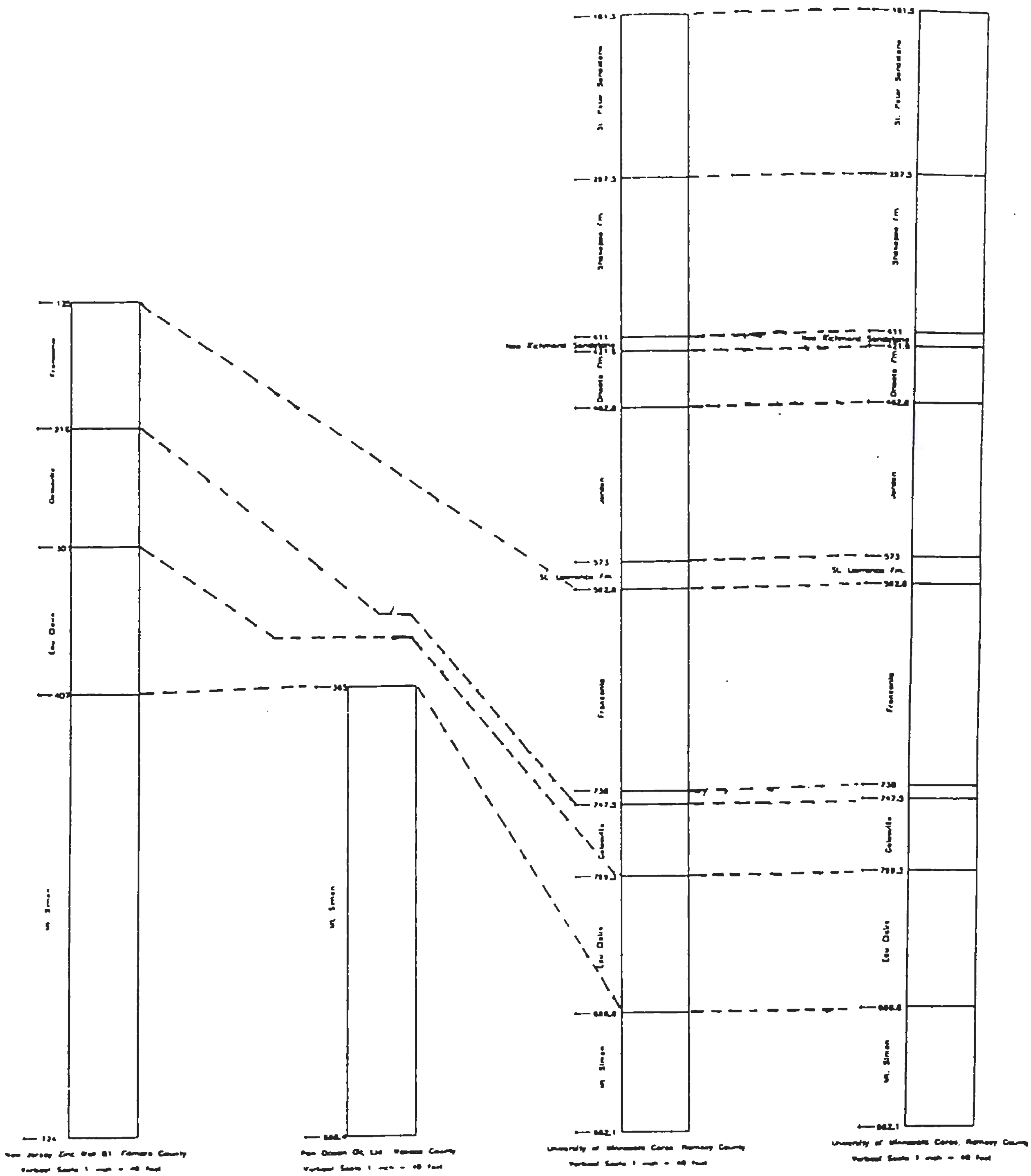

Fig. 4: Correlation of the drill holes.

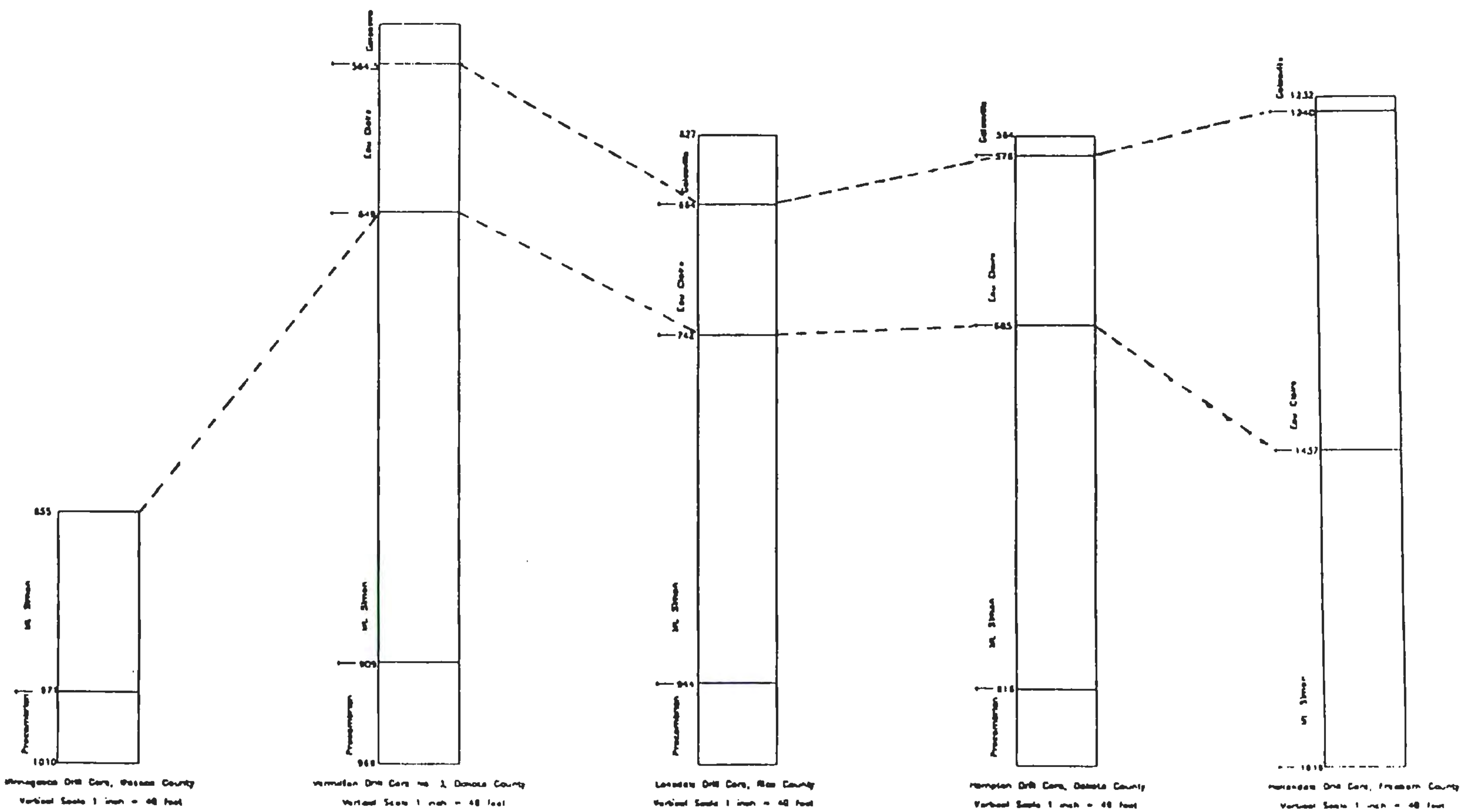

Fig. 4: Correlation of the drill holes.

Methods of study:

A total of 90 random samples were collected at the Minnesota Department of Natural Resources, Division of Minerals core library, Hibbing, Minnesota; the Minnesota Geological Survey, University of Minnesota Core Repository, Minneapolis, Minnesota; and several outcrop locations. A total of 137 thin sections from the Late Proterozoic Hinckley Sandstone, the Upper Cambrian Mt. Simon Formation, Eau Claire Sandstone, Galesville Sandstone, Ironton Sandstone, and Jordan Sandstone, and the Ordovician New Richmond Member of the Shakopee Formation and the St. Peter Sandstone were examined for mineralogical maturity using a petrographic microscope. Sixty-four of the 137 thin sections came from previous work: 9 from Uribe (1994), 7 from Squillace (1979), 15 from the Minnesota Geological Survey, 5 from Tryhorn and Ojakangas (1972), and 28 from Churchill (in prep.).

To distinguish orthoclase from untwinned plagioclase and dusky quartz, the thin sections were stained for potassium with sodium cobaltnitrite. The thin sections were also impregnated with blue epoxy to show pore space. Six random traverses of one hundred equally spaced points were counted, for a total of 600 points per thin section.

Thirty-four of the 90 random samples were prepared for heavy mineral analysis using tetrabromoethane (Density = 2.9 g/cm^2). When available, 300 non-opaque heavy minerals were identified and counted for each sample using the petrographic microscope.

Previous work:

Potter and Pryor (1961) compiled an extensive report on the possible dispersal centers of Paleozoic sediments. They provide evidence through integrated studies of petrography, stratigraphy, and paleocurrent indicators to suggest that the early Paleozoic arenites were recycled to produce the stratigraphically higher units. They concluded that the pre-Mississippian sandstones of the Upper Mississippi Valley and adjacent areas all had the same original source, the Precambrian rocks of the Lake Superior region.

Most of the units involved in this investigation have been studied extensively, but prior to this, no author examined all of the units using consistent operational definitions. Austin (1972), Mossler (1987), and Runkel (1994) give the most detailed descriptions of the Paleozoic units involved in this study.

Ojakangas (1963) completed a sedimentological study of the Upper Cambrian Lamotte Sandstone of Missouri, the basal Cambrian unit in that region. The Lamotte Sandstone is lithologically similar to the Mt. Simon Sandstone, but is diachronous, having been deposited earlier as the initial Late Cambrian sea transgressed northward. He concluded that there was evidence for a multicycle origin for the Lamotte.

Uribe (1994) did a petrographic and diagenetic study of the Upper Cambrian Mt. Simon Sandstone of southeastern Minnesota. Churchill (in prep.) studied the Upper Cambrian Mt. Simon Sandstone, Eau Claire Formation, and Galesville Sandstone. He examined the texture, mineralogy, and maturity of these units. Distefano (1973) focused on the mineralogy and petrology of the Eau Claire Formation. Andrew (1965) studied the Ironton Sandstone, focusing on grain size and heavy minerals. Pride (1966) did a grain size analysis and heavy mineral study of the New Richmond Member of the Shakopee Formation. Squillace (1979) also studied the geology of the Lower Ordovician New Richmond Member of the Shakopee Formation, focusing on paleocurrent analysis, grain size analysis, and petrography; he concluded that the New Richmond was multicycle in origin due to the presence of abraded quartz overgrowths. Parham (1970) examined the petrography of the St. Peter Sandstone.

CHAPTER II

REGIONAL GEOLOGY

Precambrian basement framework:

In Potter and Pryor's (1961) study of the dispersal centers of Paleozoic sediments of this region and adjacent regions, they concluded that the southerly direction of sediment movement and the slope of the craton persisted through the Paleozoic to the present. They suggested that uniformity over such a long period of time and over such an extensive region reflects tectonic control by the basement rocks of the craton. It is this tectonic control that explains the existence of persistent paleoslopes, of recycling, and of the location and orientation of major clastic deposits derived from distant tectonic lands.

The Late Proterozoic-Early Paleozoic arenites of the northern Midcontinent region were deposited upon Archean and Proterozoic igneous, sedimentary, and metamorphic rocks, thus establishing a major unconformity recognized throughout the Midcontinent region. The sediments were deposited on a craton on which there were active intracratonic basins as well as scattered arches and domes (Ostrom, 1970). During Late Cambrian and Early and Middle Ordovician time, the existing highlands in the Upper Mississippi Valley were the Transcontinental arch, the Wisconsin dome, and the Wisconsin arch (Figure 1). As the major marine transgression flooded the continent, it entered the Hollandale embayment. The embayment is bordered by these highlands: the Transcontinental arch to the north and west, the Wisconsin arch to the northeast, and the Wisconsin dome to the east. The Transcontinental arch is composed of a variety of igneous and metamorphic rocks while the Wisconsin dome and the Wisconsin arch are composed of granite and undifferentiated igneous and metamorphic rocks (Ostrom, 1981).

Structural geology of the study area:

Precambrian:

Several episodes of deformation have affected the Precambrian rocks in this region, the latest of these being the Midcontinent rifting that occurred during Keweenawan time, 1.1 billion years ago. The Midcontinent Rift System extends from Lake Superior to northern and eastern

Kansas, and forms a midcontinent gravity high because of the large gravity anomaly that extends along the same trend.

With the rifting and extrusion of the mafic volcanics, formation of the Lake Superior Syncline started (Craddock, 1972). The syncline continued to subside during Late Keweenawan time with thousands of feet of sediment being deposited. Undergoing a period of compressive deformation, axial horsts were then uplifted relative to the adjacent blocks, allowing for the possible simultaneous subsidence of the flanking basins.

The St. Croix horst in southeastern Minnesota is the most prominent Precambrian structural feature of southeastern Minnesota, and the relationship between the sedimentary units of the Late Proterozoic - Early Paleozoic is both complex and largely dependent upon the present geometry of the St. Croix horst (Figure 5) (Craddock, 1972). A second horst exists near the Iowa border where the midcontinent gravity high is well-developed and is described by Craddock (1972).

The Belle Plaine fault separates the two horsts and is defined by Sloan and Danes (1962) on the basis of well data and gravity measurements. Chase and Gilmore (1973) concluded that the Belle Plaine fault is a left-lateral transform fault which developed during the Keweenawan rifting.

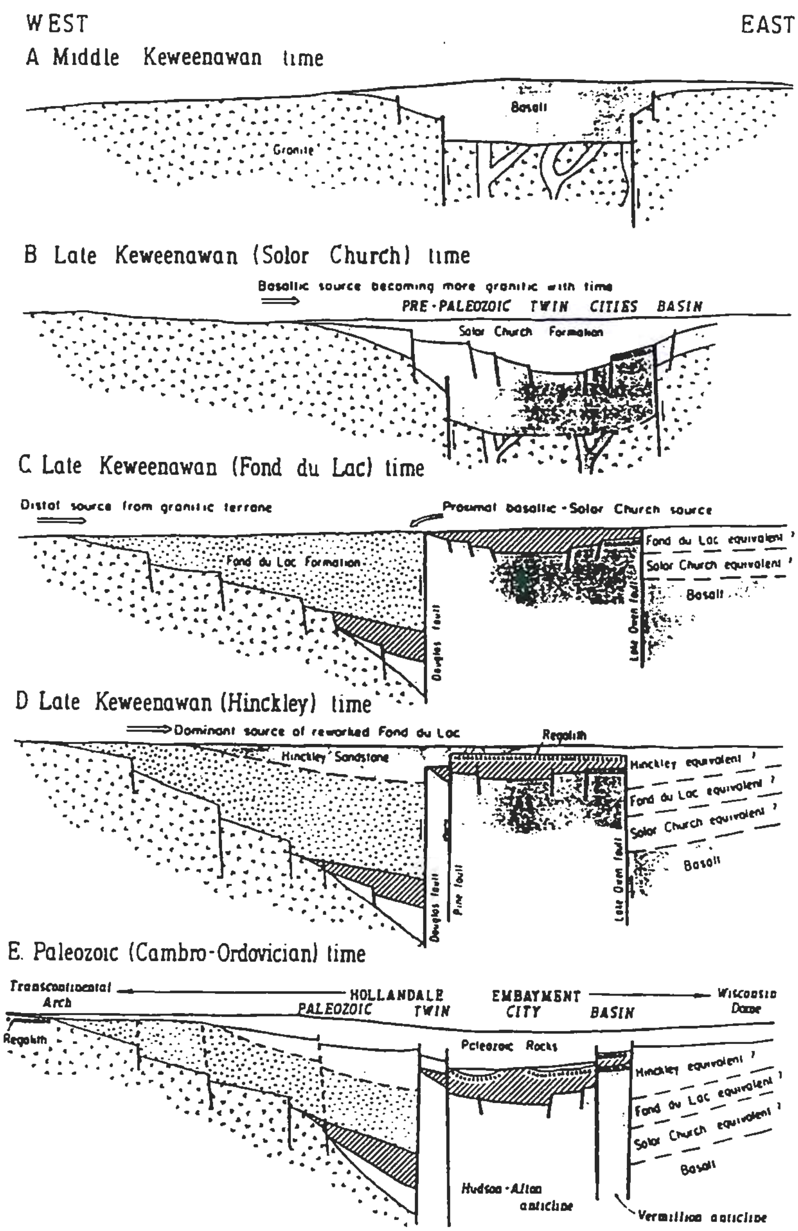

Fig. 5: Structural geology of southeastern Minnesota. (From Morey, 1972).

Paleozoic:

In southeastern Minnesota - southwestern Wisconsin, rocks of the Hollandale embayment overlie the older horsts and faults. The Hollandale embayment exists as a depression that is in part located over the underlying Keweenawan Midcontinent Rift system.

When the structure contour lines on top of the Mt. Simon Sandstone and the Eau Claire Formation (Figures 6 and 7) are compared with their respective isopach contour lines (Figures 8 and 9), there is little correlation between the two (Churchill, in prep.). This indicates that the embayment was not a governing feature during Dresbachian time and had limited effect on the sedimentation (Churchill, in prep.).

Clear definition of the Hollandale embayment and the other smaller structural features of the study area was not present until Early Ordovician time (Austin, 1972). The distribution of the Red Unit of the Eau Claire Formation defined the presence of the Hollandale embayment in Early Ordovician time (Austin, 1972). The Red Unit of the Eau Claire Formation occurs along the western edge of the embayment and as the basal unit near the center of the embayment (Austin, 1972). The absence of the Red Unit on the Wisconsin arch indicates that the Transcontinental arch was a highland to the west, contributing sediment into the early embayment (Austin, 1972).

The Dresbachian and younger rocks that were deposited within the embayment are mostly flat-lying units deposited in the transgressing and regressing sea. However, the attitudes of these units may have been affected by smaller structural features which are believed to be a continuation of Precambrian structural activity associated with the rift system (Bunker, 1988).

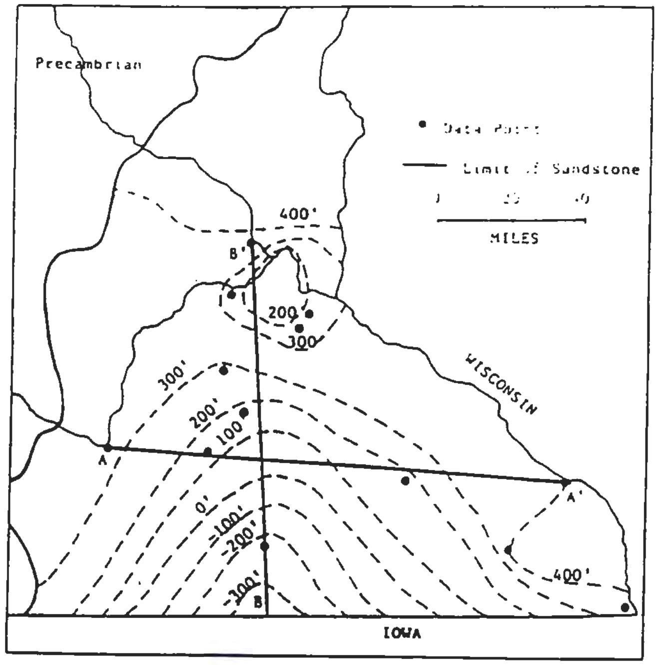

Fig. 6: Structure contour lines of the Mt. Simon Sandstone. (From Churchill, in prep.).

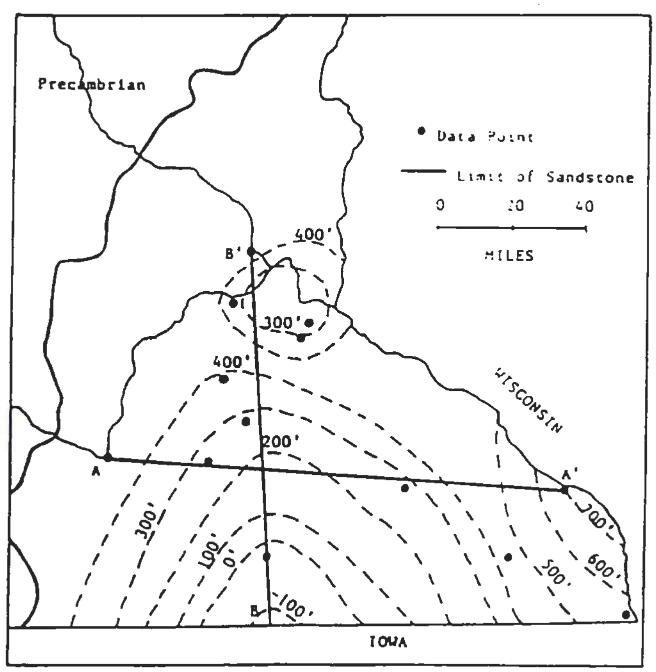

Fig. 7: Structure contour lines of the Eau Claire Formation. (From Churchill, in prep.).

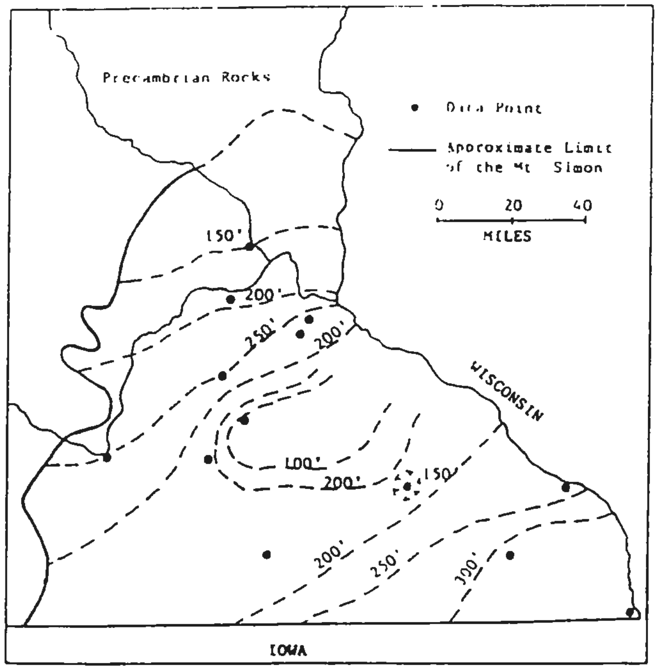

Fig. 8: Isopach contour lines of the Mt. Simon Sandstone. (From Churchill, in prep.).

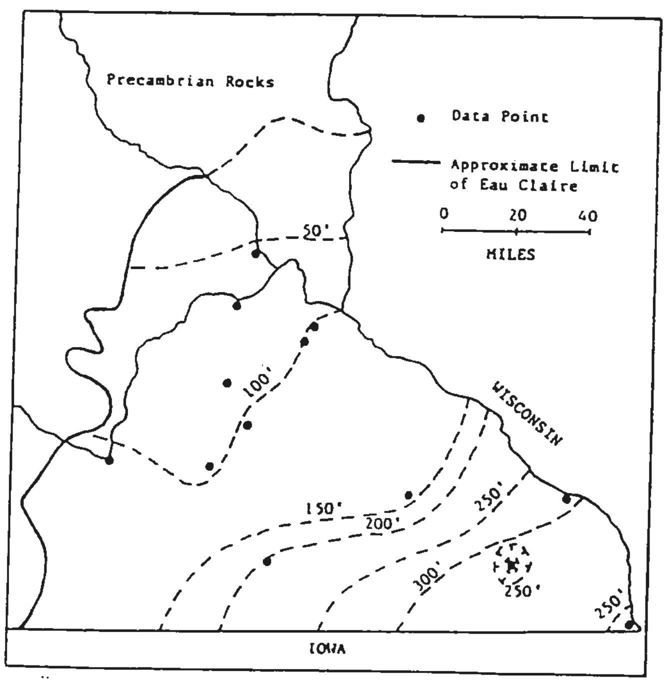

Fig. 9: Isopach contour lines of the Eau Claire Formation. (From Churchill, in prep.).

The Twin Cities basin is a structural basin located in the northern section of the Hollandale embayment and overlies the southern end of the St. Croix horst (Austin, 1972). Sedimentation in the Twin Cities basin was limited during Early Ordovician time, as evidenced by the isopach contours of the Prairie du Chien Group (Figure 10). The Precambrian fault zones that had initially formed the St. Croix horst now were responsible for the formation of the subsiding basin. The possible isostatic readjustment of the Midcontinent Rift System may have reactivated these fault zones, forming a series of en-enchelon anticlines that helped to define the edges of the basin (Miller, 1970, in Austin, 1972). The basin is bordered to the southwest by the upthrown northeast block of the Belle Plaine fault, while the northern margin is formed by onlap onto the Precambrian sedimentary rocks (Mossler, 1992).

During Paleozoic time, isostatic adjustments along Precambrian faults to the east and south of the Twin Cities basin produced the Hudson-Afton anticline and the Vermillion anticline (Austin, 1972). Movement within the Vermillion anticline appears to have been continuous throughout Mt. Simon to Jordan time, ending prior to the Early Ordovician (Austin, 1972).

Austin (1972) stated that the effect that the Red Wing - Rochester anticline had on the sedimentation of the Paleozoic is unclear, and that it is most likely a post-Ordovician feature caused by downwarping of the underlying units during subsidence of the Hollandale embayment.

Lithostratigraphy and depositional environments:

Hinckley Sandstone:

The uppermost Late Proterozoic unit in the Midcontinent Rift is the Hinckley Sandstone of Minnesota, which correlates with the Devils Island Sandstone of the Bayfield Group in Wisconsin and consists of pale-brown to light-gray, medium- to coarse-grained quartz sand (Morey and Ojakangas, 1982). The grains are moderately to well-rounded and the degree of sorting and cementation is variable. The mineralogical and textural maturity of the Hinckley Sandstone is indicative of a high-energy environment, and the presence of multicycle quartz

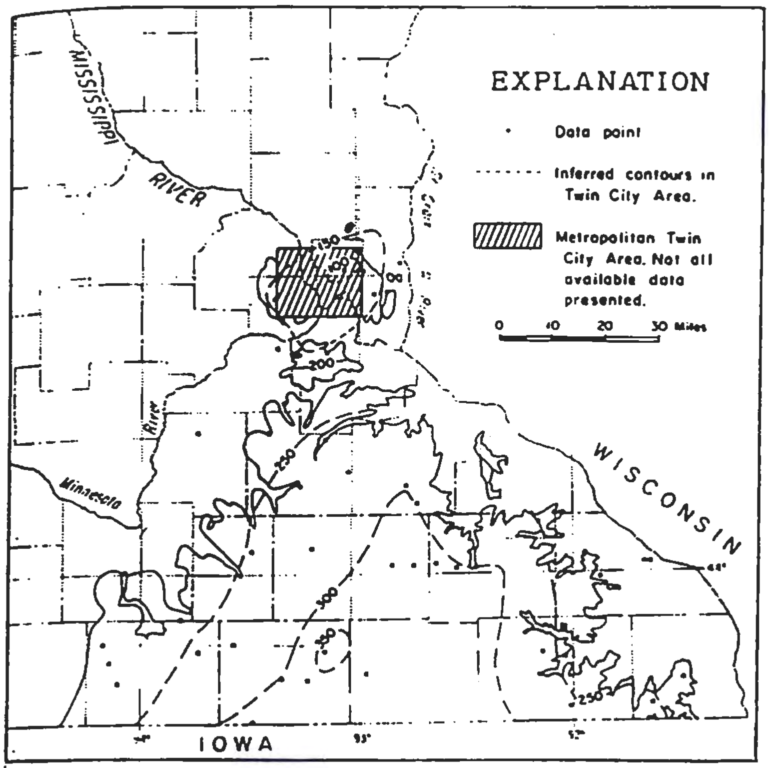

Fig. 10: Isopach contour lines (in feet) of the Prairie du Chien Group. (From Austin, 1972).

grains suggests recycling of the underlying Fond du Lac formation (Tryhorn and Ojakangas, 1972). In east-central Minnesota, the Hinckley Sandstone has a maximum thickness of 500 feet. However, it thins progressively southward and is about 150 feet thick near Minneapolis-St. Paul (Morey, 1972).

Mt. Simon Sandstone:

The Mt. Simon Sandstone consists of medium- to coarse-grained feldspathic sandstone with minor interbeds of shale, fine-grained quartz sandstone, and conglomeratic sandstone. The degree of rounding is grain-size dependent; as the Mt. Simon is moderately to well-sorted and the grains are primarily rounded to well-rounded in the medium- to coarse-grained fraction, and subrounded to angular in the fine-grained fraction (<0.125 mm) (Uribe, 1994).

Mossler (1992) interpreted the depositional environments of the Mt. Simon Sandstone as follows:

-Basal conglomerate: Braided fluvial deposit

-Lower Mt. Simon Sandstone (medium- to coarse-grained sandstone): Braid plain, braid delta, and littoral deposits.

-Middle Mt. Simon Sandstone (fine- to medium-grained sandstone and shale beds): Distal braid delta deposits.

-Upper Mt. Simon Sandstone: Sand shoals and tidal flat deposits.

The Mt. Simon Sandstone extends laterally into Wisconsin, Iowa, Illinois, and the lower peninsula of Michigan. It can be traced as far south as Tennessee, where it has been dated as Early Cambrian in age . In Wisconsin, the Mt. Simon Sandstone is considered to be Late Cambrian. The difference in age is attributed to transgression during deposition (Ostrom, 1966).

Eau Claire Formation:

The Eau Claire Formation has been informally divided into 6 units representing different lithofacies (Mossler, 1992), as follows:

-Basal red unit: red-colored quartzose sandstone and shale with abundant brachiopods.

-Dolostone unit: Pale-olive-gray dolostone with pale-red shale partings; overlies the red unit in Faribault and Jackson Counties.

-Sand-shale unit: In areas where the basal red unit and dolostone unit are missing, this unit forms the base of the Eau Claire, typified by thin alternating layers of shale and finely laminated sandstone.

-Greensand unit: Light-olive-gray highly glauconitic silty sandstone with some gray-green shale.

-Shaly unit: Siltstone with interbeds of slightly glauconitic sandstone and gray-green shale.

-Sandy unit: Fine-grained, slightly glauconitic, quartzose sandstone with interbeds of shale.

The Eau Claire Formation was once believed to have been deposited seaward of the littoral environment, in a shelf environment similar to the Northwest Gulf of Mexico (Ostrom, 1966). However, Byers and Huber (1976) have interpreted the Eau Claire Formation to represent a tidal flat environment based on the presence of fine-grained sediments and abundant fossils. Mossler (1992) supported this interpretation and has identified the depositional environments of the Eau Claire Formation as follows:

-Basal red unit: tidal flat deposit.

-Dolostone unit: shallow subtidal origin.

-Sand-shale unit: mixed sand/mud tidal flat.

-Greensand unit: shallow marine sandstone.

-Shaly unit: lagoonal sediment with smaller amounts of tidal flat sediment.

-Sandy unit: tidal flat.

Galesville Sandstone:

The Galesville Sandstone consists of a light gray to white, moderately well-sorted quartzose sandstone. It is medium- to coarse-grained, with interbeds of fine-grained quartzose sand at its base (Austin, 1972). Austin (1972) noted that in the Hollandale embayment, where the entire Galesville-Ironton succession is present, the bottom part of the Galesville is regressive and the upper part is transgressive. Mossler (1992) interpreted the sediments of the Galesville Formation as foreshore, shoreface, and tidal channel deposits, indicative of a marine transgression. Austin (1972) had similar interpretations for sediments deposited away from the center of the embayment, such as those deposited along the Wisconsin arch (Austin, 1972). The Galesville rests disconformably on the Eau Claire Formation in western Wisconsin (Austin, 1972).

Ironton Sandstone:

Austin (1972) noted that the entire Galesville - Ironton succession is present in the center of the Hollandale embayment. The Ironton and Galesville derived sediment of similar grain size from the same source (Austin, 1972). The Ironton Sandstone is generally composed of medium- to coarse-grained, light-gray to white quartzose sand. It is moderately well- to poorly-sorted and can be slightly glauconitic. Generally, the formation is burrow mottled and poorly bedded, although cross-bedding can be found at some localities. The quartz-rich Ironton sand is classified as a lower energy sandstone, lying directly on the higher energy Galesville (Austin, 1972). The Ironton is less well-sorted than the Galesville and commonly contains silt (Austin, 1972).

A sharp contact may exist at the Galesville - Ironton boundary. This may be due to a change in current activity or the possible rejuvenation of Precambrian structures during Cambrian time (Austin, 1972). Movement along Precambrian faults may also be responsible for the unconformity between the Galesville and Ironton that was previously noted by Berg (1954) and Berg et al (1956).

Franconia Sandstone:

The Franconia Sandstone consists of four members originally named by Berg (1954); Mossler (1992) noted the presence of a fifth member, the Davis Member.

-Birkmose Member (basal): Green-gray, highly glauconitic feldspathic sandstone.

-Davis Member: Dolostone unit that resembles the Davis Formation of Missouri, a unit that extends into Iowa and possibly Illinois.

-Tomah Member: Light brown-gray feldspathic siltstone interbedded with thin beds of green-gray shale.

-Reno Member: Light gray to green-gray feldspathic sandstone with minor interbeds of shale and siltstone.

-Mazomanie Member: Intertongues with the Reno Member; yellow-gray sandstone similar to the Tomah Member, no shale interbeds present.

Austin (1972) noted that the Tomah Member is the dominant unit near the center of the Hollandale embayment and suggested that the more glauconitic members are located in the more shoreward and basinward accumulations. The distribution of the Tomah Member allows the development of the embayment to be defined by the distribution patterns of the members of the Franconia Formation.

Jordan Sandstone:

The Jordan Sandstone consists of three members:

-Basal Norwalk Member: White to light-gray to gray-orange feldspathic sandstone, containing some thin gray-green shale partings. It is confined to the fringes of the Hollandale embayment (Austin, 1972).

-Van Oser Member: Tan to gray-orange, fine- to coarse-grained, supermature quartzose sandstone. It is the thickest, most resistant unit of the Jordan, and is the only member of the Jordan present in the Twin Cities basin (Austin, 1972).

-Coon Valley Member: Buff to tan, medium-grained quartzose sandstone with minor amounts of dolostone and fine-grained feldspathic sandstone (Mossler, 1992). Mossler (1992) reported that the Coon Valley Member is gradational with the overlying Oneota Dolomite and Austin (1972) noted that the east-west trend in sedimentation is similar to that of the underlying St. Lawrence Formation, indicating that the Hollandale embayment opened seaward to the west and southwest during deposition of the sediments of the Trempealeauan Stage.

Runkel (1994) recently interpreted the Jordan lithofacies as representing a regressive sequence deposited as part of a shoreline system that prograded across the Hollandale embayment.

New Richmond (Sandstone) Member of the Shakopee Formation:

The New Richmond Sandstone consists of two lithofacies that were informally named by Austin (1971):

Prairie Island facies: Gray-orange to yellow-brown quartzose sandstone and sandy dolostone containing ripple marks and cross-beds (Squillace, 1979).

Root Valley facies: White to light gray quartzose sandstone with well-developed cross-bedding (Austin, 1972).

According to Austin (1972), the New Richmond thins to the west and north from extreme southeastern Minnesota. He interpreted the New Richmond to represent a remnant of the east-west trend in sedimentation of the underlying Trempealeauan Stage in the Lower Ordovician (Austin, 1972).

St. Peter Sandstone:

The St. Peter consists of white to light-gray, fine- to medium-grained, well-sorted quartzose sandstone. It is poorly cemented and typically massive. A noticeable unconformity exists between the St. Peter and the underlying Shakopee Formation, indicating a significant break in sediment deposition (Mossler, 1992).

The St. Peter was deposited during a Middle Ordovician transgression (Mazzullo, 1988). He suggested that changes in the grain size of the St. Peter are due to the repetitive smaller transgressions and regressions of the Middle Ordovician sea.

CHAPTER III

THIN SECTION PETROGRAPHY

A total of 137 thin sections from drill cores and outcrop samples of the nine arenites studied were examined for mineralogical maturity using a petrographic microscope. Sixty-four of the 137 thin sections came from previous work: 9 from Uribe (1994), 7 from Squillace (1979), 15 from the Minnesota Geological Survey, 5 from Tryhorn and Ojakangas (1972), and 28 from Churchill (in prep.). Six random traverses (perpendicular to the bedding) of one hundred equally spaced points were counted for a total of 600 points per thin section. Most of the thin sections were prepared with blue epoxy to aid in the identification of pore spaces, and were also stained for potassium feldspar (using sodium cobaltnitrite).

Table 1 shows the modal analyses of the arenites chosen for this study.

Operational definitions:

The following are descriptions of the rock-forming minerals in the Late Proterozoic-Early Paleozoic arenites as seen in thin section. The abbreviations for each constituent are used in Table 1.

Framework grains:

Common quartz (CQTZ): Single crystals with straight to slightly undulose extinction (<5° on conventional flat stage) (Plate 1-A). Inclusions of needle-shaped rutile are common. Zircon, tourmaline, and apatite inclusions are rare.

Polycrystalline quartz (PQTZ): Aggregates of several crystals (Plate 1-B). A vast majority of grains included in this category have mostly straight contacts between crystals (i.e., recrystallized metamorphic quartz), although a few grains consist of slightly sutured elongate crystals (i.e., stretched metamorphic quartz).

Vein quartz (VQTZ): Unit grains that show abundant fluid inclusions, either randomly or in planes. Under one polar, vein quartz grains have a cloudy appearance (Plate 1-C). Vein quartz grains are scarce throughout the stratigraphic column.

Multicycle quartz (RQTZ): Grains included in this category have apparent subrounded to rounded quartz overgrowths beneath younger overgrowths (Plate 2A-I).

Plagioclase (UA PLAG, A PLAG): Both altered (A) and unaltered (UA) varieties of all feldspar types were counted. Unstained feldspar grains (i.e. did not stain with sodium colbaltnitrite) and grains showing albite twinning were counted as plagioclase (Plate 1D).

Potassium Feldspar (UA ORTH, A ORTH): Stained feldspar grains with no twinning were counted as orthoclase (Plate 1E).

Microcline (UA MICRO, A MICRO): Stained grains that show apparent cross-hatching were counted as microcline (Plate 1F).

Detrital Core (DETR CORE): Feldspar grains which are surrounded by an authigenic feldspar overgrowth were counted as detrital cores. No effort was made to count the core type under its specific category (i.e. if the core was altered plagioclase, it was counted as a detrital core, not as an altered plagioclase grain) (Plate 1G).

Plutonic rock fragments (PRF): Grains counted as plutonic rock fragments are grains comprised of coarse quartz and feldspar (Plate 1H).

Muscovite: Muscovite (MUSC) is present in trace amounts. The muscovite grains are typically elongate and large and are more common in finer-grained samples with a clayey matrix (Plate 3A).

Glauconite (GLAUC): Green to dark-green pellets (up to 0.4mm in size) showing an internal aggregate structure of randomly oriented micron-sized crystals (Plate 3B).

Matrix:

Matrix is defined herein as all detrital particles less than 62.5 microns (0.0625mm) in diameter (Plate 3C). Also considered as matrix are clayey layers and lenses (<2 mm thick) and discontinuous patches or remnants compacted after burial; however, silt grains were not considered as matrix, but rather as mineral fragments. Matrix is common in some samples (as much as 72.1 percent), although the amount of matrix was not considered when the rocks were classified. A majority of the matrix is most likely potassium-rich clay (illitic?) as suggested by the yellow colbaltnitrite staining.

Cement:

Quartz (QTZ): Quartz overgrowths are considered to be quartz cement (Plate 3D). In many samples, quartz cement is considered to be present along the boundaries between adjacent quartz grains, although it is not easily seen as overgrowths.

Feldspar (FELD): Feldspar cement was counted as those authigenic (?) overgrowths that cemented 2 or more grains together (Plate 3E). In most samples, feldspar cement was considered to be present along the boundaries between adjacent feldspar grains, although it was difficult to see a defined overgrowth. The overgrowths on detrital cores make up most of the feldspar cement.

Calcite (CAL): Carbonate cement with no characteristic crystal habit (i.e. anhedral) was counted as calcite (Plate 3F). Replacement of grains (primarily quartz) by calcite is common.

Dolomite (DOL): Carbonate cement with a characteristic rhombohedral crystal habit was counted as dolomite (Plate 3G).

Siderite (SID): In a very few thin sections, fine rhombohedral-shaped grains with dark, hematitic centers are present (Plate 3H).

Kaolinite (KAOL): Randomly oriented "books" (vermicular kaolinite) are present as pore-filling kaolinite cement (Plate 4A).

Hematite (HEM): Hematite cement is optically opaque but is red in reflected light (Plate 4B). It has coated some grains and filled some pores.

Fossils:

Inarticulate brachiopod shell fragments are found in several units. Collophane (COLL) is the main component of the shells (Plate 4C).

CLASSIFICATION OF UNITS:

Through petrographic evidence analysis of the thin sections, two main rock types are present (see Figure 11 and Table 1). Seventy-one percent of the samples (n = 98 samples) are classified as quartz sandstones (quartz arenites according to Pettijohn, et al., 1987, p. 145). A quartz sandstone is defined as a sandstone containing 95 percent or more quartz. The other major rock type (28.2 percent of all samples), is feldspathic sandstone (subarkose according to

Pettijohn, et al., 1987, p. 145). The feldspar content of these sandstones ranges between 5 and 25 percent detrital feldspar. The two sandstone types contain very few rock fragments.

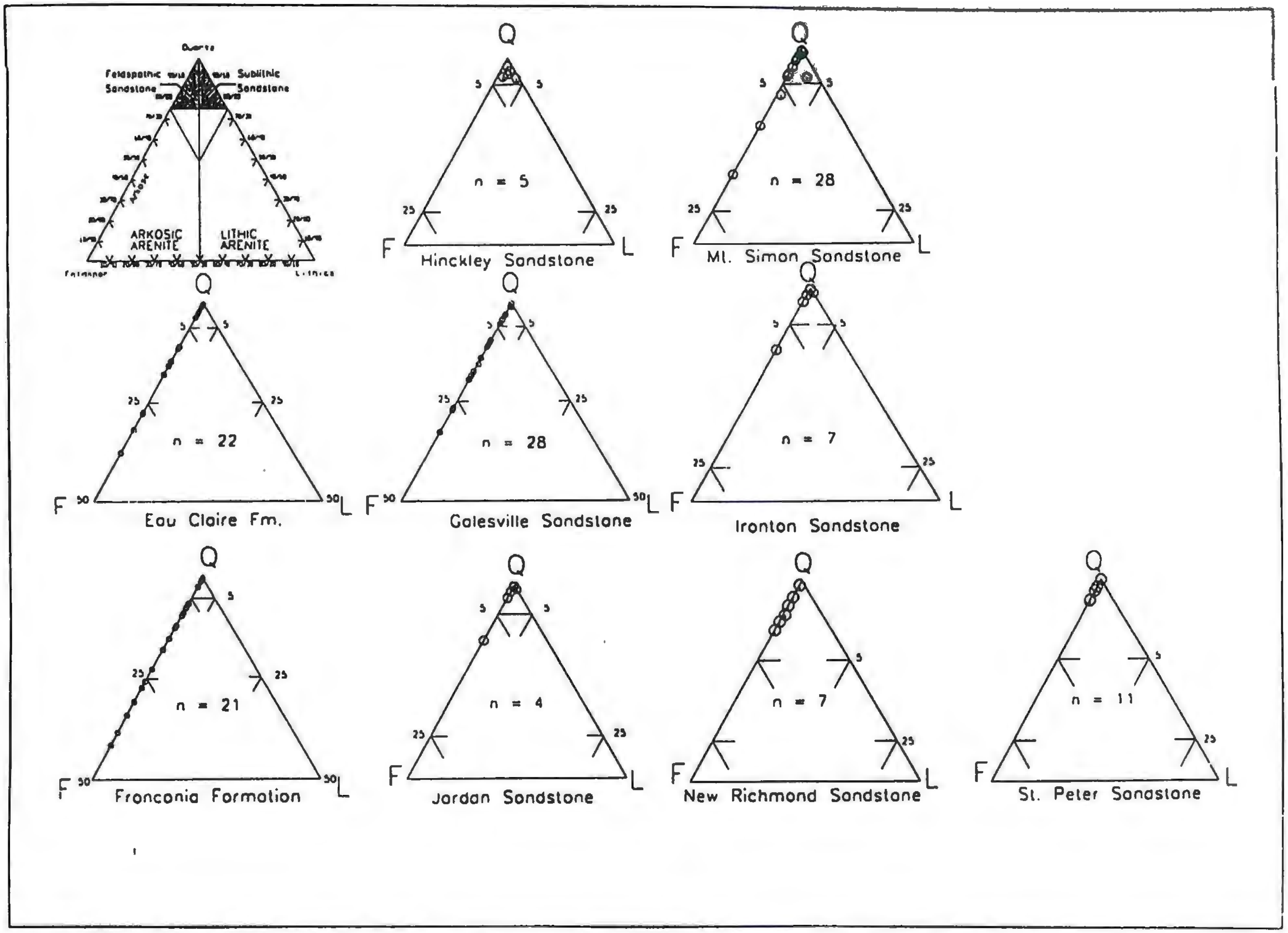

Fig. 11: Classification of the arenites. "Q" includes common, polycrystalline, multicycle, and vein quartz grains. "F" includes all unaltered and altered detrital feldspar. "L" includes rare chert and rare plutonic rock fragments.

		QUARTZ					FELDSPAR			
Unit	Sample#	CQTZ	PQTZ	VQTZ	RQTZ	TOTAL QTZ	UA PLAG	A PLAG	UA ORTH	A ORTH
Hinckley	PHN-9	92.1	2.7	0.2	3.5	98.5	0.0	0.4	0.0	0.2
Hinckley	PHN-23	87.9	1.8	2.7	4.3	96.7	0.0	0.2	0.0	0.2
Hinckley	PHH-5	93.7	1.1	0.4	2.2	97.4	0.0	0.2	0.0	1.1
Hinckley	PHH-7	91.5	3.5	0.5	1.4	96.9	0.0	0.0	0.2	1.9
Hinckley	PHH-8	89.1	4.2	0.9	3.8	98.0	0.0	0.0	0.0	0.7
AVERAGE		90.9	2.7	0.9	3.0	97.5	0.0	0.2	0.0	0.8
Mt. Simon	AG-AC1-972	96.7	1.0	0.0	1.0	98.7	0.0	0.0	0.5	0.0
Mt. Simon	AG-AC1-927	93.7	3.3	0.0	1.6	98.6	0.0	0.0	0.9	0.0
Mt. Simon	AG-B1-604	88.3	0.0	0.0	0.0	88.3	0.0	1.9	0.0	0.3
Mt. Simon	RU-SCH-834	98.7	0.0	0.0	1.1	99.8	0.2	0.0	0.0	0.0
Mt. Simon	RU-SQ9-474	84.1	3.8	0.3	11.0	99.2	0.0	0.0	0.8	0.0
Mt. Simon	RU-SQ9-545	86.9	2.8	0.0	10.3	100.0	0.0	0.0	0.0	0.0
Mt. Simon	RU-SQ9-554	89.5	2.5	0.0	5.8	97.8	0.6	0.3	0.3	0.0
Mt. Simon	RU-SQ9-595	90.0	3.8	0.0	6.2	100.0	0.0	0.0	0.0	0.0
Mt. Simon	RU-SQ9-630	84.5	10.5	0.7	0.0	95.7	0.2	0.0	1.1	0.2
Mt. Simon	RU-SQ9-666	87.4	3.4	0.0	9.0	99.8	0.0	0.2	0.0	0.0
Mt. Simon	RU-SQ9-672	84.1	10.4	0.0	5.5	100.0	0.0	0.0	0.0	0.0
Mt. Simon	RU-SQ9-678	88.0	1.5	0.0	10.5	100.0	0.0	0.0	0.0	0.0
Mt. Simon	CH-V66-3	89.2	8.9	0.0	1.9	100.0	0.0	0.0	0.0	0.0
Mt. Simon	CH-V66-5	97.4	2.2	0.2	0.0	99.8	0.0	0.2	0.0	0.0
Mt. Simon	CH-V66-8	80.1	19.7	0.0	0.2	100.0	0.0	0.0	0.0	0.0
Mt. Simon	CH-V66-11	90.7	5.7	0.0	1.0	97.4	0.0	1.0	0.0	0.0
Mt. Simon	CH-V66-12	94.5	0.7	0.0	0.7	95.9	0.0	2.4	0.0	0.0
Mt. Simon	CH-V66-14	85.7	7.6	1.2	5.1	99.6	0.0	0.0	0.0	0.0
Mt. Simon	CH-H1A-1617	96.3	0.0	0.0	0.0	96.3	0.0	3.0	0.0	0.0
Mt. Simon	CH-H1A-1526	94.2	3.8	0.0	0.2	98.2	0.0	1.5	0.0	0.0
Mt. Simon	CH-H1A-1521.5	93.2	4.1	0.0	0.3	97.5	0.0	1.8	0.0	0.0
Mt. Simon	CH-H1A-1488	98.9	0.5	0.0	0.0	99.3	0.0	0.5	0.0	0.0
Mt. Simon	CH-H1A-1467	100.0	0.0	0.0	0.0	100.0	0.0	0.0	0.0	0.0
Mt. Simon	CH-DH-3	98.2	1.6	0.0	0.0	99.8	0.0	0.0	0.0	0.0
Mt. Simon	CH-DH-5	91.3	6.4	0.0	0.0	97.7	0.0	0.0	0.0	0.0
Mt. Simon	CH-DH-9	96.7	2.1	0.4	0.0	99.2	0.0	0.2	0.0	0.0
Mt. Simon	94-WI-07	79.7	0.3	0.0	0.8	80.9	1.4	1.1	12.5	0.0
Mt. Simon	94-WI-01	83.2	9.7	0.0	0.2	93.2	0.0	0.0	5.4	0.0
AVERAGE		90.8	4.2	0.1	2.6	97.6	0.1	0.5	0.8	0.0
Eau Claire	CH-V66-15	96.3	0.0	0.0	1.1	97.4	0.0	0.9	0.0	0.0
Eau Claire	CH-V66-16	97.4	2.4	0.0	0.0	99.8	0.0	0.0	0.0	0.0
Eau Claire	CH-V66-17	95.7	4.0	0.0	0.3	100.0	0.0	0.0	0.0	0.0
Eau Claire	CH-V66-21	89.3	0.0	0.0	0.0	89.3	0.0	5.5	0.0	0.0
Eau Claire	CH-LH-9	87.3	10.8	0.0	0.0	98.1	0.0	0.0	0.0	0.0
Eau Claire	AG-B1-310	82.2	0.0	0.0	0.0	82.2	0.0	6.4	0.0	0.5
Eau Claire	AG-H1A-1416	88.3	0.3	0.0	0.0	88.6	0.0	4.1	0.0	0.3
Eau Claire	AG-H1A-1333	89.2	0.0	0.0	0.0	89.2	2.2	3.3	0.0	0.0
Eau Claire	CH-H1A-1328	97.8	0.0	0.0	0.0	97.8	0.0	1.4	0.0	0.0
Eau Claire	CH-H1A-1306	99.3	0.0	0.0	0.0	99.3	0.4	0.0	0.0	0.0
Eau Claire	CH-H1A-1303	99.1	0.0	0.0	0.0	99.1	0.0	0.0	0.0	0.0
Eau Claire	AG-H1A-1298	97.9	0.0	0.0	0.0	97.9	0.0	0.9	0.0	0.0
Eau Claire	AG-H1A-1241	94.5	0.2	0.0	1.8	96.5	0.0	0.9	0.0	1.1
Eau Claire	CH-H1A-1238	94.3	0.3	0.3	1.6	96.5	0.0	1.3	0.0	0.0
Eau Claire	94-WI-05	71.2	0.0	0.0	0.3	71.5	2.1	0.3	22.5	0.0

Table 1. Modal analyses.

ABBREVIATIONS:

CQTZ: Common quartz
PQTZ: Polycrystalline quartz
VQTZ: Vein (?) quartz
RQTZ: Recycled quartz
UA PLAG: Unaltered plagioclase
A PLAG: Altered plagioclase
UA ORTH: Unaltered orthoclase
A ORTH: Altered orthoclase
UA MICR: Unaltered microcline
A MICR: Altered microcline
DETR CORE: Detrital core
AUTH FELD: Authigenic feldspar
PRF: Plutonic rock fragment
GLAUC: Glauconite
Q: Quartz
F: Feldspar
L: Lithics (Rock fragments)
QTZSS: Quartz sandstone
FLDSS: Feldspathic sandstone

FELDSPAR							
UA MICR	A MICR	DETR CORE	AUTH FELD	TOTAL UA FELD	TOTAL A FELD	TOTAL CORE+AUTH	TOTAL FELD
0.0	0.0	0.2	0.2	0.0	0.6	0.3	0.7
0.0	0.0	0.0	0.0	0.0	0.4	0.0	0.4
0.0	0.0	0.0	0.0	0.0	1.3	0.0	1.3
0.0	0.0	0.2	0.0	0.2	1.9	0.2	2.2
0.0	0.0	0.0	0.0	0.0	0.7	0.0	0.7
0.0	0.0	0.1	0.0	0.0	1.0	0.1	1.1
0.0	0.0	0.8	1.5	0.5	0.0	2.3	1.3
0.0	0.0	0.5	1.0	0.9	0.0	1.5	1.4
0.0	0.0	9.5	19.2	0.0	2.2	28.7	11.7
0.0	0.0	0.0	0.0	0.2	0.0	0.0	0.2
0.0	0.0	0.0	0.0	0.8	0.0	0.0	0.8
0.0	0.0	0.0	0.0	0.0	0.0	0.0	0.0
0.0	0.0	0.0	0.0	0.8	0.3	0.0	1.1
0.0	0.0	0.0	0.0	0.0	0.0	0.0	0.0
0.0	0.0	0.0	0.0	1.3	0.2	0.0	1.5
0.0	0.0	0.0	0.0	0.0	0.2	0.0	0.2
0.0	0.0	0.0	0.0	0.0	0.0	0.0	0.0
0.0	0.0	0.0	0.0	0.0	0.0	0.0	0.0
0.0	0.0	0.0	0.0	0.0	0.0	0.0	0.0
0.0	0.0	0.2	0.2	0.0	0.0	0.3	0.2
0.0	0.0	0.0	0.0	0.0	0.0	0.0	0.0
0.0	0.0	1.7	2.0	0.0	1.0	3.7	2.7
0.0	0.0	1.7	4.3	0.0	2.4	6.0	4.1
0.0	0.0	0.0	1.4	0.0	0.0	1.4	0.0
0.0	0.4	0.4	0.5	0.0	3.4	0.9	3.7
0.0	0.0	0.3	0.7	0.0	1.5	1.0	1.8
0.0	0.0	0.7	0.7	0.0	1.8	1.3	2.5
0.0	0.0	0.2	0.2	0.0	0.5	0.3	0.7
0.0	0.0	0.0	0.0	0.0	0.0	0.0	0.0
0.0	0.0	0.2	0.0	0.0	0.0	0.2	0.2
0.0	0.0	1.5	1.0	0.0	0.0	2.5	1.5
0.0	0.0	0.2	0.8	0.0	0.2	1.0	0.4
0.0	0.3	3.9	1.6	13.9	1.4	5.5	19.2
0.0	0.0	1.0	1.2	5.4	0.0	2.2	6.4
0.0	0.0	0.8	1.3	0.9	0.5	2.1	2.2
0.0	0.9	0.8	5.2	0.0	1.8	6.0	2.6
0.0	0.0	0.2	0.0	0.0	0.0	0.2	0.2
0.0	0.0	0.0	0.0	0.0	0.0	0.0	0.0
0.0	0.0	5.2	18.2	0.0	5.5	23.4	10.7
0.0	1.9	0.0	0.0	0.0	1.9	0.0	1.9
0.0	0.5	10.4	13.1	0.0	7.4	23.5	17.8
0.0	0.0	7.0	10.8	0.0	4.4	17.8	11.4
0.3	0.3	4.7	0.0	2.5	3.6	4.7	10.8
0.5	0.0	0.3	3.3	0.5	1.4	3.6	2.2
0.0	0.0	0.3	3.3	0.4	0.0	3.6	0.7
0.0	0.0	0.9	7.9	0.0	0.0	8.8	0.9
0.0	0.0	1.2	2.0	0.0	0.9	3.2	2.1
0.0	0.0	1.5	0.8	0.0	2.0	2.3	3.5
0.0	1.0	1.2	4.1	0.0	2.3	5.3	3.5
0.3	0.0	3.3	2.8	24.9	0.3	6.1	28.5

Table 1. Modal analyses.

Unit	Sample#	CHERT	PRF	TOTAL LITHICS	Muscovite	MATRIX	Silica	Feldspar	Calcite	Dolomite	Siderite
Hinckley	PHN-9	0.8	0.0	0.8		1.4	1.9	1.0			
Hinckley	PHN-23	0.9	2.0	2.9		0.2	1.0	0.2			
Hinckley	PHH-5	0.8	0.6	1.3		0.2	0.2	0.6			
Hinckley	PHH-7	0.0	0.9	0.9	0.2	0.2	0.5	0.6			
Hinckley	PHH-8	0.4	0.9	1.3			1.6	1.6			
AVERAGE		0.6	0.9	1.4							
Mt. Simon	AG-AC1-972	0.0	0.0	0.0				1.3			
Mt. Simon	AG-AC1-927	0.0	0.0	0.0				0.3			
Mt. Simon	AG-B1-604	0.0	0.0	0.0					1.2		
Mt. Simon	RU-SCH-834	0.0	0.0	0.0						6.1	
Mt. Simon	RU-SQ9-474	0.0	0.0	0.0					0.2		
Mt. Simon	RU-SQ9-545	0.0	0.0	0.0	0.4		0.2		0.2		
Mt. Simon	RU-SQ9-554	1.1	0.0	1.1					21.1		
Mt. Simon	RU-SQ9-595	0.0	0.0	0.0			4.8				
Mt. Simon	RU-SQ9-630	0.0	2.8	2.8		1.6	2.6		0.4	1.6	
Mt. Simon	RU-SQ9-666	0.0	0.0	0.0			3.0				
Mt. Simon	RU-SQ9-672	0.0	0.0	0.0			2.9		0.2		
Mt. Simon	RU-SQ9-678	0.0	0.0	0.0			1.6				
Mt. Simon	CH-V66-3	0.0	0.0	0.0					1.4		
Mt. Simon	CH-V66-5	0.0	0.0	0.0		2.2					
Mt. Simon	CH-V66-8	0.0	0.0	0.0					17.2		
Mt. Simon	CH-V66-11	0.0	0.0	0.0					0.2		
Mt. Simon	CH-V66-12	0.0	0.0	0.0							
Mt. Simon	CH-V66-14	0.0	0.4	0.4		1.4	0.8				
Mt. Simon	CH-H1A-1617	0.0	0.0	0.0	0.4	40.5			0.2		
Mt. Simon	CH-H1A-1526	0.0	0.0	0.0	0.2				6.1		
Mt. Simon	CH-H1A-1521.5	0.0	0.0	0.0		33.5					
Mt. Simon	CH-H1A-1488	0.0	0.0	0.0		1.5					
Mt. Simon	CH-H1A-1467	0.0	0.0	0.0		2.0	0.3				
Mt. Simon	CH-DH-3	0.0	0.0	0.0		5.8			31.0		
Mt. Simon	CH-DH-5	0.8	0.0	0.8		8.1					
Mt. Simon	CH-DH-9	0.0	0.4	0.4							
Mt. Simon	94-WI-07	0.0	0.0	0.0	1.0	1.0	0.2	1.0			
Mt. Simon	94-WI-01	0.0	0.5	0.5			0.5	0.2			
AVERAGE		0.1	0.1	0.1							
Eau Claire	CH-V66-15	0.0	0.0	0.0		0.3					
Eau Claire	CH-V66-16	0.0	0.0	0.0					26.1		
Eau Claire	CH-V66-17	0.0	0.0	0.0					10.2		
Eau Claire	CH-V66-21	0.0	0.0	0.0		6.4	0.3		1.5		
Eau Claire	CH-LH-9	0.0	0.0	0.0					25.2		
Eau Claire	AG-B1-310	0.0	0.0	0.0					12.4		
Eau Claire	AG-H1A-1416	0.0	0.0	0.0					1.3		6.3
Eau Claire	AG-H1A-1333	0.0	0.0	0.0	0.5			8.8	3.5		
Eau Claire	CH-H1A-1328	0.0	0.0	0.0					42.3		
Eau Claire	CH-H1A-1306	0.0	0.0	0.0					1.2		
Eau Claire	CH-H1A-1303	0.0	0.0	0.0	0.1				2.0		
Eau Claire	AG-H1A-1296	0.0	0.0	0.0				0.2	19.4		
Eau Claire	AG-H1A-1241	0.0	0.0	0.0				0.7	3.3		
Eau Claire	CH-H1A-1238	0.0	0.0	0.0	0.2	27.2					
Eau Claire	94-WI-05	0.0	0.0	0.0	0.3			3.6			

Table 1. Modal analyses.

CEMENT		FOSSILS								
Kaolinite	Hematite	COLL	Pyritic	Carbonate	GLAUC	PORES	R NAME	Q	F	L
2.1						11.0	QTZSS	98.5	0.7	0.8
1.1	0.6					9.0	QTZSS	96.7	0.4	2.9
	9.7					4.9	QTZSS	97.4	1.3	1.3
3.3						6.1	QTZSS	96.9	2.2	0.9
4.0						7.6	QTZSS	98.0	0.7	1.3
								97.5	1.1	1.4
						30.3	QTZSS	98.7	1.3	0.0
	0.2					26.8	QTZSS	98.6	1.4	0.0
					17.2	1.2	QTZSS	88.3	11.7	0.0
		1.6				18.4	QTZSS	99.8	0.2	0.0
25.6	0.6					18.4	QTZSS	99.2	0.8	0.0
18.6						19.8	QTZSS	100.0	0.0	0.0
11.6						11.3	QTZSS	97.8	1.1	1.1
18.0						9.9	QTZSS	100.0	0.0	0.0
0.6	0.2					22.2	QTZSS	95.7	1.5	2.8
10.4						16.3	QTZSS	99.8	0.2	0.0
7.3						12.7	QTZSS	100.0	0.0	0.0
4.7						18.7	QTZSS	100.0	0.0	0.0
						18.3	QTZSS	100.0	0.0	0.0
						14.8	QTZSS	99.8	0.2	0.0
						3.2	QTZSS	100.0	0.0	0.0
						25.8	QTZSS	97.4	2.7	0.0
						24.2	QTZSS	95.9	4.1	0.0
						17.8	QTZSS	99.6	0.0	0.4
	9.1	0.2				3.8	QTZSS	96.3	3.7	0.0
						14.1	QTZSS	98.2	1.8	0.0
		0.2				4.8	QTZSS	97.5	2.5	0.0
		0.5				30.0	QTZSS	99.3	0.7	0.0
						22.4	QTZSS	100.0	0.0	0.0
		0.3				4.5	QTZSS	99.8	0.2	0.0
						9.3	QTZSS	97.7	1.5	0.8
						20.6	QTZSS	99.2	0.4	0.4
					1.4	31.4	FLDSS	80.9	19.2	0.0
						27.4	FLDSS	93.2	6.4	0.5
								97.6	2.2	0.2

Table 1. Modal analyses.

		QUARTZ					FELDSPAR			
Unit	Sample#	CQTZ	PQTZ	VQTZ	RQTZ	TOTAL QTZ	UA PLAG	A PLAG	UA ORTH	A ORTH
Eau Claire	AG-AC1-897	83.0	1.0	0.0	0.4	84.4	1.1	0.0	12.3	0.0
Eau Claire	AG-AC1-892	71.3	1.4	0.0	0.0	72.7	2.3	0.3	21.6	0.0
Eau Claire	AG-AC1-878	62.4	0.0	0.0	0.0	62.4	2.2	0.8	30.2	0.0
Eau Claire	AG-AC1-845	97.3	0.9	0.0	0.0	98.2	0.0	0.0	1.8	0.0
Eau Claire	AG-AC1-840	72.0	0.3	0.0	0.0	72.3	0.9	0.3	22.7	0.0
Eau Claire	AG-AC1-815	85.3	0.3	0.0	0.0	85.6	1.6	0.5	8.6	0.0
Eau Claire	AG-TRIP1-5A	66.7	1.2	0.0	0.4	68.3	3.2	0.4	23.0	0.0
AVERAGE		87.2	1.0	0.0	0.3	88.5	0.7	1.2	6.5	0.1
Galesville	AG-TRIP1-2L	98.3	0.4	0.0	1.3	100.0	0.0	0.0	0.0	0.0
Galesville	AG-TRIP1-2U	92.6	2.5	0.6	3.9	99.6	0.0	0.0	0.0	0.0
Galesville	AG-B1-220	73.3	0.0	0.0	0.0	73.3	3.8	1.2	12.2	0.3
Galesville	AG-B1-299	66.7	0.0	0.0	0.9	67.6	0.0	11.9	0.0	11.1
Galesville	CH-H1A-1208	81.7	1.3	0.0	1.8	84.8	0.0	5.5	0.8	3.7
Galesville	CH-H1A-1208	97.9	1.1	0.0	0.2	99.2	0.0	0.2	0.0	0.0
Galesville	CH-V66-22	89.7	0.3	0.0	0.3	90.2	0.0	3.3	0.0	1.0
Galesville	CH-DH-17	88.9	0.3	0.0	0.0	89.1	0.0	2.0	0.0	0.0
Galesville	CH-LH-14	89.5	0.0	0.0	0.0	89.5	2.2	0.0	0.0	0.0
Galesville	MGS-BC1-765.8	95.6	0.3	0.0	0.0	95.9	0.0	0.5	0.0	0.0
Galesville	MGS-BC1-759.4	97.8	0.2	0.0	1.8	99.8	0.0	0.0	0.0	0.0
Galesville	MGS-BC1-759.1	93.6	0.0	0.0	1.3	94.9	0.0	1.3	0.0	0.0
Galesville	MGS-BC1-737.7	96.5	0.9	0.0	0.0	97.4	0.0	0.9	0.0	0.0
Galesville	MGS-AC1-781.9	96.8	0.2	0.0	2.6	99.6	0.0	0.0	0.0	0.0
Galesville	MGS-AC1-771.5	95.5	0.0	0.0	1.1	96.6	0.0	0.0	2.9	0.0
Galesville	MGS-AC1-763.0	91.3	5.9	0.0	2.8	100.0	0.0	0.0	0.0	0.0
Galesville	MGS-AC1-762.9	95.6	1.2	0.0	2.7	99.5	0.0	0.2	0.0	0.0
Galesville	MGS-AC1-762.9	95.5	3.1	0.0	0.6	99.2	0.0	0.8	0.0	0.0
Galesville	MGS-AC1-762.8	90.0	2.7	0.0	4.3	97.0	0.0	1.3	0.0	0.0
Galesville	AG-AC1-760	86.0	7.9	0.0	3.1	97.0	1.7	0.0	0.8	0.0
Galesville	AG-CTYF-GALE2	80.6	0.0	0.0	0.3	80.8	0.8	0.8	15.9	0.0
Galesville	AG-CTYF-GALES	83.0	0.0	0.0	0.0	83.0	1.1	0.9	12.1	0.0
Galesville	AG-CTYF-GAEC	90.8	0.0	0.0	0.0	90.8	1.4	0.7	4.9	0.0
Galesville	AG-TRIP1-1LA	73.2	0.0	0.0	0.3	73.5	1.4	0.5	18.8	0.0
Galesville	AG-TRIP1-1LB	80.4	0.6	0.0	0.9	81.9	0.0	0.3	12.8	0.0
Galesville	AG-TRIP1-5AU	81.6	0.7	0.0	0.7	83.0	5.1	0.0	10.2	0.0
Galesville	AG-TRIP1-5AU*	85.2	0.0	0.0	1.1	86.3	1.3	0.0	9.3	0.0
Galesville	AG-TRIP1-4A	96.7	0.0	0.0	3.3	100.0	0.0	0.0	0.0	0.0
AVERAGE		88.7	1.1	0.0	1.3	91.0	0.7	1.2	3.6	0.6
Ironton	AG-H1A-1206	90.1	1.3	0.0	0.0	91.4	0.0	2.3	0.2	4.5
Ironton	AG-H1A-1204	96.0	3.1	0.0	0.0	99.1	0.0	0.4	0.0	0.0
Ironton	MGS-BC1-718.1	95.8	1.8	0.0	1.8	99.4	0.0	0.0	0.0	0.0
Ironton	MGS-BC1-718.1	91.4	5.3	0.0	3.3	100.0	0.0	0.0	0.0	0.0
Ironton	MGS-BC1-717.9	92.9	0.2	0.0	6.6	99.8	0.0	0.2	0.0	0.0
Ironton	AG-TRIP1-5B	90.4	8.1	0.0	0.7	99.1	0.9	0.0	0.0	0.0
Ironton	AG-TRIP1-5B*	88.8	5.8	0.0	3.5	98.1	1.7	0.0	0.0	0.0
AVERAGE		92.2	3.7	0.0	2.3	98.1	0.4	0.4	0.0	0.6
Franconia	MGS-AC1-741.5	97.3	1.9	0.0	0.4	99.6	0.0	0.0	0.0	0.0
Franconia	MGS-AC1-734.2	98.2	0.0	0.0	0.9	99.1	0.0	0.6	0.0	0.0
Franconia	AG-B1-213.5	90.1	0.0	0.0	0.3	90.4	0.0	2.5	0.0	0.0
Franconia	AG-B1-179	99.1	0.6	0.0	0.0	99.7	0.3	0.0	0.0	0.0
Franconia	AG-B1-167	84.8	0.0	0.0	0.0	84.8	0.0	4.6	0.0	6.7
Franconia	AG-B1-135.5	60.7	0.0	0.0	0.9	61.6	0.0	13.7	0.5	17.4
Franconia	AG-H1A-1062	58.4	0.0	0.0	0.0	58.4	3.4	0.0	32.3	1.0
Franconia	AG-H1A-1163.5	95.7	0.0	0.0	4.3	100.0	0.0	0.0	0.0	0.0
Franconia	AG-AC1-730	84.5	3.0	0.0	5.6	93.1	1.3	0.0	4.3	0.0
Franconia	AG-AC1-710	65.5	0.0	0.0	0.3	65.9	3.0	0.0	24.9	0.0
Franconia	AG-AC1-685	77.2	0.0	0.0	0.0	77.2	3.7	0.7	15.9	0.0
Franconia	AG-AC1-665	90.8	0.0	0.0	0.0	90.8	6.5	0.7	30.4	0.0
Franconia	AG-AC1-655	73.7	0.0	0.0	0.4	74.1	3.3	0.8	17.6	0.0
Franconia	AG-AC1-645.6	97.9	0.0	0.0	0.0	97.9	0.6	0.0	0.0	0.0
Franconia	AG-AC1-635	87.7	0.0	0.0	0.4	88.1	2.9	0.4	5.4	0.0
Franconia	AG-AC1-618	90.2	0.4	0.0	0.7	91.3	3.3	0.4	1.0	0.0
Franconia	AG-AC1-603	91.8	0.7	0.0	0.0	92.5	1.3	0.7	4.7	0.0
Franconia	AG-AC1-601.5	82.1	0.0	0.0	0.0	82.1	4.0	1.7	9.0	0.0
Franconia	AG-TRIP1-3	85.0	0.0	0.0	2.5	87.5	1.2	0.5	7.9	0.0
Franconia	AG-TRIP1-3*	69.1	0.0	0.0	0.0	69.1	5.6	0.0	19.0	0.0
Franconia	AG-TRIP1-3L	72.1	0.0	0.0	0.5	72.6	2.6	0.5	18.5	0.0
AVERAGE		83.4	0.3	0.0	0.8	84.6	2.0	1.3	9.1	1.2
Jordan	AG-TRIP1-4B	92.9	2.0	0.0	1.5	96.4	0.3	0.0	2.3	0.0
Jordan	AG-TRIP1-4B2	97.2	1.1	0.0	0.0	98.3	0.0	0.0	1.4	0.0
Jordan	AG-TRIP1-5C1	97.7	0.5	1.3	0.0	99.5	0.0	0.0	0.5	0.0
Jordan	AG-TRIP1-5C2	97.7	0.7	0.0	0.9	99.3	0.0	0.0	0.7	0.0
AVERAGE		96.3	1.1	0.3	0.6	98.4	0.1	0.0	1.2	0.0

Table 1. Modal analyses.

FELDSPAR							
UA MICR	A MICR	DETR CORE	AUTH FELD	TOTAL UA FELD	TOTAL A FELD	TOTAL CORE+AUTH	TOTAL FELD
0.7	0.0	1.5	1.7	14.1	0.0	3.2	15.6
0.0	0.0	3.1	3.1	23.9	0.3	6.2	27.3
0.6	0.6	3.2	2.1	33.0	1.4	5.3	37.6
0.0	0.0	0.0	0.0	1.8	0.0	0.0	1.8
0.0	0.0	3.8	0.7	23.6	0.3	4.5	27.7
0.0	0.0	3.7	2.4	10.2	0.5	6.1	14.4
0.0	0.0	5.1	1.1	26.2	0.4	6.2	31.7
0.1	0.2	2.6	3.8	7.3	1.6	6.4	11.5
0.0	0.0	0	0.0	0.0	0.0	0.0	0.0
0.0	0.0	0	0.0	0.0	0.0	0.0	0.0
0.3	0.9	8.1	0.0	16.3	2.4	8.1	26.8
0.0	0.0	9.4	6.6	0.0	23.0	16.0	32.4
0.0	0.3	4.8	0.0	0.8	9.5	4.8	15.1
0.0	0.0	0.23	0.0	0.0	0.2	0.2	0.5
0.0	0.3	5.3	10.1	0.0	4.6	15.4	9.9
0.0	1.5	7.4	11.4	0.0	3.5	18.8	10.9
0.0	1.6	6.7	14.8	2.2	1.6	21.5	10.5
0.0	0.0	3.6	15.5	0.0	0.5	19.1	4.1
0.0	0.0	0.16	0.5	0.0	0.0	0.7	0.2
0.0	0.2	3.6	6.5	0.0	1.5	10.1	5.1
0.0	0.2	1.5	8.2	0.0	1.1	9.7	2.6
0.0	0.0	0	0.3	0.0	0.0	0.3	0.0
0.0	0.0	0.33	1.3	2.9	0.0	1.6	3.2
0.0	0.0	0	0.0	0.0	0.0	0.0	0.0
0.0	0.0	0.32	0.5	0.0	0.2	0.8	0.5
0.0	0.0	0	0.0	0.0	0.8	0.0	0.8
0.0	0.0	1.7	1.2	0.0	1.3	2.9	3.0
0.3	0.0	0.17	0.3	2.8	0.0	0.5	3.0
0.3	0.0	1.4	1.6	17.0	0.8	3.0	19.2
0.0	0.0	3	1.0	13.2	0.9	4.0	17.1
0.0	0.0	2.2	0.2	6.3	0.7	2.4	9.2
0.5	0.0	5	2.3	20.7	0.5	7.3	26.2
0.0	0.0	5	2.4	12.8	0.3	7.4	18.1
0.0	0.0	1.7	0.8	15.3	0.0	2.5	17.0
0.0	0.0	3.1	1.3	10.6	0.0	4.4	13.7
0.0	0.0	0	0.0	0.0	0.0	0.0	0.0
0.0	0.2	2.7	3.1	4.3	1.9	5.8	8.9
0.0	0.0	1.6	0.0	0.2	6.8	1.6	8.6
0.2	0.2	0.0	0.0	0.2	0.7	0.0	0.9
0.0	0.0	0.0	0.0	0.0	0.0	0.0	0.0
0.0	0.0	0.0	0.0	0.0	0.0	0.0	0.0
0.0	0.0	0.0	0.0	0.0	0.2	0.0	0.2
0.0	0.0	0.0	0.0	0.9	0.0	0.0	0.9
0.0	0.0	0.2	0.0	1.7	0.0	0.2	1.9
0.0	0.0	0.3	0.0	0.4	1.1	0.3	1.8
0.0	0.2	0.2	1.3	0.0	0.2	1.5	0.4
0.0	0.0	0.3	0.2	0.0	0.6	0.5	0.9
0.0	0.3	6.8	8.1	0.0	2.8	14.9	9.6
0.0	0.0	0.0	0.0	0.3	0.0	0.0	0.3
0.0	0.7	3.2	0.0	0.0	12.0	3.2	15.2
0.0	0.9	5.9	0.0	0.5	32.0	5.9	38.4
1.0	0.3	3.6	0.0	36.7	1.3	3.6	41.6
0.0	0.0	0.0	0.0	0.0	0.0	0.0	0.0
0.0	0.0	0.8	0.2	5.6	0.0	1.0	6.4
0.3	0.0	5.9	1.8	28.2	0.0	7.7	34.1
0.4	0.0	2.1	2.1	20.0	0.7	4.2	22.8
0.0	0.0	3.0	1.5	5.5	0.7	4.5	9.2
0.4	0.0	3.8	2.3	21.3	0.8	6.1	25.9
1.1	0.0	0.5	0.2	1.7	0.0	0.7	2.2
0.0	0.8	2.3	2.5	8.3	1.3	4.8	11.9
1.9	0.4	1.8	1.6	6.2	0.7	3.4	8.7
0.0	0.0	0.8	0.7	6.0	0.7	1.5	7.5
1.7	0.0	1.5	1.3	14.7	1.7	2.8	17.9
0.0	0.0	2.9	1.6	9.1	0.5	4.5	12.5
1.0	0.0	5.3	3.3	25.6	0.0	8.6	30.9
1.0	0.0	4.8	2.0	22.1	0.5	6.8	27.4
0.4	0.2	2.6	1.5	10.1	2.7	4.1	15.4
0.0	0.0	0.8	0.0	2.6	0.0	0.8	3.4
0.0	0.0	0.3	0.3	1.4	0.0	0.7	1.7
0.0	0.0	0.0	0.0	0.5	0.0	0.0	0.5
0.0	0.0	0.0	0.0	0.7	0.0	0.0	0.7
0.0	0.0	0.3	0.1	1.3	0.0	0.4	1.6

Table 1. Modal analyses.

			ROCK FRAGMENTS		MICAS				CEMENT		
Unit	Sample#	CHERT	PRF	TOTAL LITHICS	Muscovite	MATRIX	Silica	Feldspar	Calcite	Dolomite	Siderite
Eau Claire	AG-AC1-897	0.0	0.0	0.0		25.7			1.5		
Eau Claire	AG-AC1-892	0.0	0.0	0.0	0.2	9.9		0.3	2.0		
Eau Claire	AG-AC1-878	0.0	0.0	0.0	0.3	1.0		0.7			
Eau Claire	AG-AC1-845	0.0	0.0	0.0		0.2			9.9		
Eau Claire	AG-AC1-840	0.0	0.0	0.0	0.2			1.3	1.0		
Eau Claire	AG-AC1-815	0.0	0.0	0.0							
Eau Claire	AG-TRIP1-5A	0.0	0.0	0.0	1.1	2.8		0.2	0.3		
AVERAGE		0.0	0.0	0.0							
Galesville	AG-TRIP1-2L	0.0	0.0	0.0		0.0	0.2				
Galesville	AG-TRIP1-2U	0.4	0.0	0.4		0.0		1.1			
Galesville	AG-B1-220	0.0	0.0	0.0		0.0		7.5	2.0		
Galesville	AG-B1-299	0.0	0.0	0.0	0.5	0.0			3.6		
Galesville	CH-H1A-1208	0.0	0.2	0.2	0.3	0.0		11.7	1.2		
Galesville	CH-H1A-1208	0.0	0.4	0.4		18.7					
Galesville	CH-V66-22	0.0	0.0	0.0	0.6	7.0			0.6		
Galesville	CH-DH-17	0.0	0.0	0.0	0.2	3.1	0.2				
Galesville	CH-LH-14	0.0	0.0	0.0	0.3	14.8					
Galesville	MGS-BC1-765.8	0.0	0.0	0.0		0.0	2.5				
Galesville	MGS-BC1-759.4	0.0	0.0	0.0		0.0	2.0	0.3			
Galesville	MGS-BC1-759.1	0.0	0.0	0.0		1.6	0.5	0.7			
Galesville	MGS-BC1-737.7	0.0	0.0	0.0	0.2	0.0	1.1				
Galesville	MGS-AC1-781.9	0.4	0.0	0.4		0.0	0.2				
Galesville	MGS-AC1-771.5	0.2	0.0	0.2	0.2	0.0		0.2			
Galesville	MGS-AC1-763.0	0.0	0.0	0.0		21.0					
Galesville	MGS-AC1-762.9	0.0	0.0	0.0		15.9	0.8	2.2			
Galesville	MGS-AC1-762.9	0.0	0.0	0.0		12.0	2.4				
Galesville	MGS-AC1-762.8	0.0	0.0	0.0		34.2					
Galesville	AG-AC1-760	0.0	0.0	0.0	0.2	34.6					
Galesville	AG-CTYF-GALE2	0.0	0.0	0.0		0.0	0.2	2.2			
Galesville	AG-CTYF-GALES	0.0	0.0	0.0		0.0	0.5	1.3			
Galesville	AG-CTYF-GAEC	0.0	0.0	0.0		19.3			1.3		
Galesville	AG-TRIP1-1LA	0.3	0.0	0.3		0.0		2.0			
Galesville	AG-TRIP1-1LB	0.0	0.0	0.0		0.0		3.4			
Galesville	AG-TRIP1-5AU	0.0	0.0	0.0		3.5		0.3	0.3		
Galesville	AG-TRIP1-5AU*	0.0	0.0	0.0	0.2	13.8		0.7			
Galesville	AG-TRIP1-4A	0.0	0.0	0.0		3.1	0.2	0.2			
AVERAGE		0.0	0.0	0.0							
Ironton	AG-H1A-1208	0.0	0.0	0.0		0.0		8.4			
Ironton	AG-H1A-1204	0.0	0.0	0.0		0.0	0.8		2.9		
Ironton	MGS-BC1-718.1	0.0	0.6	0.6		12.8	3.5				
Ironton	MGS-BC1-718.1	0.0	0.0	0.0	0.2	22.3	1.0				
Ironton	MGS-BC1-717.9	0.0	0.0	0.0		18.8	2.0	2.8			
Ironton	AG-TRIP1-5B	0.0	0.0	0.0		9.3		0.3			
Ironton	AG-TRIP1-5B*	0.0	0.0	0.0	0.2	70.8					
AVERAGE		0.0	0.1	0.1							
Franconia	MGS-AC1-741.5	0.0	0.0	0.0			1.8				
Franconia	MGS-AC1-734.2	0.0	0.0	0.0		8.3	1.8				
Franconia	AG-B1-213.5	0.0	0.0	0.0				0.7	0.5		
Franconia	AG-B1-179	0.0	0.0	0.0							
Franconia	AG-B1-167	0.0	0.0	0.0				1.0	20.4		
Franconia	AG-B1-135.5	0.0	0.0	0.0	0.3			9.0	13.8		
Franconia	AG-H1A-1062	0.0	0.0	0.0	0.1			15.3	9.2		
Franconia	AG-H1A-1163.5	0.0	0.0	0.0					85.3		
Franconia	AG-AC1-730	0.4	0.0	0.4					3.8		
Franconia	AG-AC1-710	0.0	0.0	0.0	2.0	1.6			3.6		
Franconia	AG-AC1-685	0.0	0.0	0.0				0.5	17.2		
Franconia	AG-AC1-665	0.0	0.0	0.0	0.5	439.0		1.0	7.7		
Franconia	AG-AC1-655	0.0	0.0	0.0					18.6		
Franconia	AG-AC1-645.6	0.0	0.0	0.0				1.5	11.4		
Franconia	AG-AC1-635	0.0	0.0	0.0		12.0			25.5		
Franconia	AG-AC1-618	0.0	0.0	0.0		11.3		0.3	13.8		
Franconia	AG-AC1-603	0.0	0.0	0.0					49.7		
Franconia	AG-AC1-601.5	0.0	0.0	0.0		8.8			37.7		
Franconia	AG-TRIP1-3	0.0	0.0	0.0				0.2	1.1		
Franconia	AG-TRIP1-3*	0.0	0.0	0.0	0.3			0.5	1.5		
Franconia	AG-TRIP1-3L	0.0	0.0	0.0	0.2	0.2		1.1	25.9		
AVERAGE		0.0	0.0	0.0							
Jordan	AG-TRIP1-4B	0.3		0.3					31.6		
Jordan	AG-TRIP1-4B2	0.0		0.0			0.2		34.9		
Jordan	AG-TRIP1-5C1	0.0		0.0					35.3		
Jordan	AG-TRIP1-5C2	0.0		0.0					2.3		
AVERAGE		0.1		0.1							

Table 1. Modal analyses.

CEMENT		FOSSILS								
Kaolinite	Hematite	Collophane	Pyritic	Carbonate	GLAUC	PORES	R NAME	Q	F	L
					9.8	12.4	FLDSS	84.4	15.6	0.0
		3.9			0.8	19.4	FLDSS	72.7	27.3	0.0
		1.5			1.9	31.0	FLDSS	62.4	37.6	0.0
		4.6			62.0	4.8	QTZSS	98.2	1.8	0.0
		0.3			4.4	32.6	FLDSS	72.3	27.7	0.0
						18.5	FLDSS	85.6	14.4	0.0
	19.6	0.2			0.8	28.0	FLDSS	68.3	31.7	0.0
								88.5	11.5	0.0
						24.3	QTZSS	100.0	0.0	0.0
						18.7	QTZSS	99.6	0.0	0.4
		5.2				21.2	FLDSS	73.3	26.8	0.0
				0.3	14.4	27.9	FLDSS	67.6	32.4	0.0
				3.1		17.5	FLDSS	84.8	15.1	0.2
						8.9	QTZSS	99.2	0.5	0.4
	1.1	2.3				11.7	QTZSS	90.2	9.9	0.0
		1.6			0.3	10.5	QTZSS	89.1	10.9	0.0
		0.3				11.3	QTZSS	89.5	10.5	0.0
		0.2				13.9	QTZSS	95.9	4.1	0.0
		0.5				14.6	QTZSS	99.8	0.2	0.0
		1.0			1.3	8.6	QTZSS	94.9	5.1	0.0
						13.9	QTZSS	97.4	2.6	0.0
		0.2				15.9	QTZSS	99.6	0.0	0.4
		0.8				12.9	QTZSS	96.6	3.2	0.2
						2.7	QTZSS	100.0	0.0	0.0
						2.9	QTZSS	99.5	0.5	0.0
		0.2				2.8	QTZSS	99.2	0.8	0.0
						1.0	QTZSS	97.0	3.0	0.0
						6.0	QTZSS	97.0	3.0	0.0
	0.3				11.3	22.2	FLDSS	80.8	19.2	0.0
	0.7	0.3			14.5	21.3	FLDSS	83.0	17.1	0.0
	6.2				19.5	6.1	QTZSS	90.8	9.2	0.0
		0.3				30.6	FLDSS	73.5	26.2	0.3
	0.2	1.8			1.3	30.4	FLDSS	81.9	18.1	0.0
	4.4	1.3			2.7	20.2	FLDSS	83.0	17.0	0.0
	0.2	0.5			1.1	17.1	FLDSS	86.3	13.7	0.0
	0.2					21.6	QTZSS	100.0	0.0	0.0
							FLDSS	91.0	8.9	0.1
		0.7				20.3	FLDSS	91.4	8.6	0.0
						25.9	QTZSS	99.1	0.9	0.0
		0.3				3.0	QTZSS	99.4	0.0	0.6
						1.3	QTZSS	100.0	0.0	0.0
						9.0	QTZSS	99.8	0.2	0.0
	0.2					14.4	QTZSS	99.1	0.9	0.0
						0.5	QTZSS	98.1	1.9	0.0
							QTZSS	98.1	1.8	0.1
						18.1	QTZSS	99.6	0.4	0.0
		2.1			25.8	4.9	QTZSS	99.1	0.9	0.0
	0.5	2.3			0.3	22.1	QTZSS	90.4	9.6	0.0
	2.0			3.4	17.0	24.0	QTZSS	99.7	0.3	0.0
					27.1	1.0	QTZSS	84.8	15.2	0.0
		0.8			12.2	22.0	FLDSS	61.6	38.4	0.0
					11.7	22.8	FLDSS	58.4	41.6	0.0
	0.8				9.2	0.8	QTZSS	100.0	0.0	0.0
		0.3			44.1	12.3	QTZSS	93.1	6.4	0.4
					6.7	29.2	FLDSS	65.9	34.1	0.0
					10.1	23.3	FLDSS	77.2	22.8	0.0
					41.8	17.0	FLDSS	90.8	9.2	0.0
					15.3	19.6	FLDSS	74.1	25.9	0.0
	0.3	0.5			54.4	2.1	QTZSS	97.9	2.2	0.0
					9.1	9.2	FLDSS	88.1	11.9	0.0
					7.6	19.2	FLDSS	91.3	8.7	0.0
					6.9	17.2	FLDSS	92.5	7.5	0.0
		0.2			14.0	8.3	FLDSS	82.1	17.9	0.0
	1.3		0.2		7.2	19.3	FLDSS	87.5	12.5	0.0
					10.5	31.9	FLDSS	69.1	30.9	0.0
					14.1	19.7	FLDSS	72.6	27.4	0.0
							FLDSS	84.6	15.4	0.0
						2.0	QTZSS	96.4	3.4	0.3
						2.7	QTZSS	98.3	1.7	0.0
	1.1					1.3	QTZSS	99.5	0.5	0.0
	2.1					25.3	QTZSS	99.3	0.7	0.0
							QTZSS	98.4	1.6	0.1

Table 1. Modal analyses.

		QUARTZ					FELDSPAR			
Unit	Sample#	CQTZ	PQTZ	VQTZ	RQTZ	TOTAL QTZ	UA PLAG	A PLAG	UA ORTH	A ORTH
New Richmond	PS-LN-10-17	93.8	0.5	0.0	1.5	95.8	0.0	0.0	3.0	0.5
New Richmond	PS-LN-10-16	94.5	0.5	0.0	0.0	95.0	0.5	0.5	3.0	0.5
New Richmond	PS-LN-10-14	96.0	0.5	0.0	0.5	97.0	0.0	0.5	2.0	0.5
New Richmond	PS-LN-10-12	93.8	0.2	0.0	0.0	94.0	0.5	0.5	4.0	0.5
New Richmond	PS-LW-16-5	99.5	0.0	0.0	0.0	99.5	0.2	0.0	0.2	0.0
New Richmond	PS-LW-16-4	97.8	0.2	0.0	0.0	98.0	0.5	0.0	0.5	0.5
New Richmond	PS-LW-16-6	97.0	0.5	0.0	0.5	98.0	0.0	0.0	1.0	1.0
AVERAGE		96.1	0.3	0.0	0.4	96.8	0.2	0.2	2.0	0.5
St. Peter	AG-H1-473	100.0	0.0	0.0	0.0	100.0	0.0	0.0	0.0	0.0
St. Peter	AG-H1-533	97.1	0.0	0.0	2.9	100.0	0.0	0.0	0.0	0.0
St. Peter	AG-H1-539	93.5	0.0	0.0	3.6	97.1	0.0	0.0	2.5	0.0
St. Peter	AG-H1-626	95.0	1.5	0.0	1.0	97.5	0.5	0.3	1.5	0.0
St. Peter	AG-AC1-191.5	98.2	1.6	0.0	0.2	100.0	0.0	0.0	0.0	0.0
St. Peter	AG-AC1-181.5	100.0	0.0	0.0	0.0	100.0	0.0	0.0	0.0	0.0
St. Peter	95-MNT-STP1	99.1	0.2	0.0	0.7	100.0	0.0	0.0	0.0	0.0
St. Peter	95-MNT-STP2	98.6	0.7	0.0	0.7	100.0	0.0	0.0	0.0	0.0
St. Peter	95-MNT-STP3	99.3	0.0	0.0	0.7	100.0	0.0	0.0	0.0	0.0
St. Peter	AG-TRIP1-6	97.1	1.8	0.0	0.0	98.9	0.0	0.0	0.9	0.0
St. Peter	AG-TRIP1-6A	97.6	0.7	0.2	0.0	98.6	0.0	0.0	1.4	0.0
AVERAGE		97.8	0.6	0.0	0.9	99.3	0.0	0.0	0.6	0.0

Table 1. Modal analyses.

FELDSPAR							
UA MICR	A MICR	DETR CORE	AUTH FELD	TOTAL UA FELD	TOTAL A FELD	TOTAL CORE+AUTH	TOTAL FELD
0.5	0.0	0.0	0.0	3.5	0.5	0.0	4.0
0.0	0.5	0.0	0.0	3.5	1.5	0.0	5.0
0.0	0.0	0.0	0.0	2.0	1.0	0.0	3.0
0.5	0.0	0.0	0.0	5.0	1.0	0.0	6.0
0.2	0.0	0.0	0.0	0.5	0.0	0.0	0.5
0.5	0.0	0.0	0.0	1.5	0.5	0.0	2.0
0.0	0.0	0.0	0.0	1.0	1.0	0.0	2.0
0.2	0.1	0.0	0.0	2.4	0.8	0.0	3.2
0.0	0.0	0.0	0.0	0.0	0.0	0.0	0.0
0.0	0.0	0.0	0.0	0.0	0.0	0.0	0.0
0.0	0.2	0.2	0.0	2.5	0.2	0.2	2.9
0.0	0.3	0.0	0.0	2.0	0.5	0.0	2.5
0.0	0.0	0.0	0.0	0.0	0.0	0.0	0.0
0.0	0.0	0.0	0.0	0.0	0.0	0.0	0.0
0.0	0.0	0.0	0.0	0.0	0.0	0.0	0.0
0.0	0.0	0.0	0.0	0.0	0.0	0.0	0.0
0.0	0.0	0.0	0.0	0.0	0.0	0.0	0.0
0.0	0.0	0.2	0.0	0.9	0.0	0.2	1.1
0.0	0.0	0.0	0.0	1.4	0.0	0.0	1.4
0.0	0.0	0.0	0.0	0.6	0.1	0.0	0.7

Table 1. Modal analyses.

			ROCK FRAGMENTS		MICAS		CEMENT				
Unit	Sample#	CHERT	PRF	TOTAL LITHICS	Muscovite	MATRIX	Silica	Feldspar	Calcite	Dolomite	Siderite
New Richmond	PS-LN-10-17	0.0	0.2	0.2			0.2				
New Richmond	PS-LN-10-16	0.0		0.0			0.2	0.2			
New Richmond	PS-LN-10-14	0.0		0.0							
New Richmond	PS-LN-10-12	0.0		0.0							
New Richmond	PS-LW-16-5	0.0		0.0			0.2	0.2			
New Richmond	PS-LW-16-4	0.0		0.0			0.2	0.2			
New Richmond	PS-LW-16-6	0.0		0.0				0.2			
AVERAGE		0.0		0.0							
St. Peter	AG-H1-473	0.0		0.0							
St. Peter	AG-H1-533	0.0		0.0			0.5				
St. Peter	AG-H1-539	0.0		0.0			3.1				
St. Peter	AG-H1-628	0.0		0.0			4.5			7.1	
St. Peter	AG-AC1-191.5	0.0		0.0							
St. Peter	AG-AC1-181.5	0.0		0.0		29.3					
St. Peter	95-MNT-STP1	0.0		0.0							
St. Peter	95-MNT-STP2	0.0		0.0							
St. Peter	95-MNT-STP3	0.0		0.0			0.2		0.2		
St. Peter	AG-TRIP1-6	0.0		0.0			0.2				
St. Peter	AG-TRIP1-6A	0.0		0.0							
AVERAGE		0.0		0.0							

Table 1. Modal analyses.

CEMENT		FOSSILS								
Kaolinite	Hematite	Collophane	Pyritic	Carbonate	GLAUC	PORES	R NAME	Q	F	L
0.2	0.2					25.0	QTZSS	95.8	4.0	0.2
0.2	0.2					25.0	QTZSS	95.0	5.0	0.0
						25.0	QTZSS	97.0	3.0	0.0
	0.2					19.0	QTZSS	94.0	6.0	0.0
						28.0	QTZSS	99.5	0.5	0.0
						22.0	QTZSS	98.0	2.0	0.0
				7.0		28.0	QTZSS	98.0	2.0	0.0
								96.8	3.2	0.0
	7.0					19.7	QTZSS	100.0	0.0	0.0
	4.2					25.1	QTZSS	100.0	0.0	0.0
	1.7					25.0	QTZSS	97.1	2.9	0.0
						26.8	QTZSS	97.5	2.5	0.0
						26.2	QTZSS	100.0	0.0	0.0
						7.5	QTZSS	100.0	0.0	0.0
						25.6	QTZSS	100.0	0.0	0.0
						29.6	QTZSS	100.0	0.0	0.0
						29.7	QTZSS	100.0	0.0	0.0
						27.6	QTZSS	98.9	1.1	0.0
						30.4	QTZSS	98.6	1.4	0.0
							QTZSS	99.3	0.7	0.0

Table 1. Modal analyses.

PLATE 1

A. Sample AG-TRIP1-2U, Galesville Sandstone. Photomicrograph of common quartz (CQ). Crossed polarizers, field of view 1.5 mm across.

B. Sample 94-WI-01, Mt. Simon Sandstone. Photomicrograph of polycrystallin quartz (PQ) and common quartz. Crossed polarizers, field of view 1.5 mm across.

C. Sample CH-V66-14, Mt. Simon Sandstone. Photomicrograph of vein quartz (VQ). Crossed polarizers, field of view 1.5 mm across.

D. Sample AG-AC1-878, Eau Claire Formation. Photomicrograph of rounded detrital plagioclase (PL). Crossed polarizers, field of view 0.8 mm across.

E. Sample AG-CTYF-GALES, Galesville Sandstone. Photomicrograph of rounded detrital orthoclase (OR). Crossed polarizers, field of view 0.8 mm across.

F. Sample AG-AC1-665, Franconia Formation. Photomicrograph of rounded detrital microcline (MC). Crossed polarizers, field of view 0.8 mm across.

G. Sample AG-AC1-655, Franconia Formation. Photomicrograph of detrital core (DC) with authigenic feldspar overgrowth (AU). Crossed polarizers, field of view 0.8 mm across.

H. Sample 94-WI-01, Mt. Simon Sandstone. Photomicrograph of a plutonic rock fragment (PRF). Crossed polarizers, field of view 0.8 mm across.

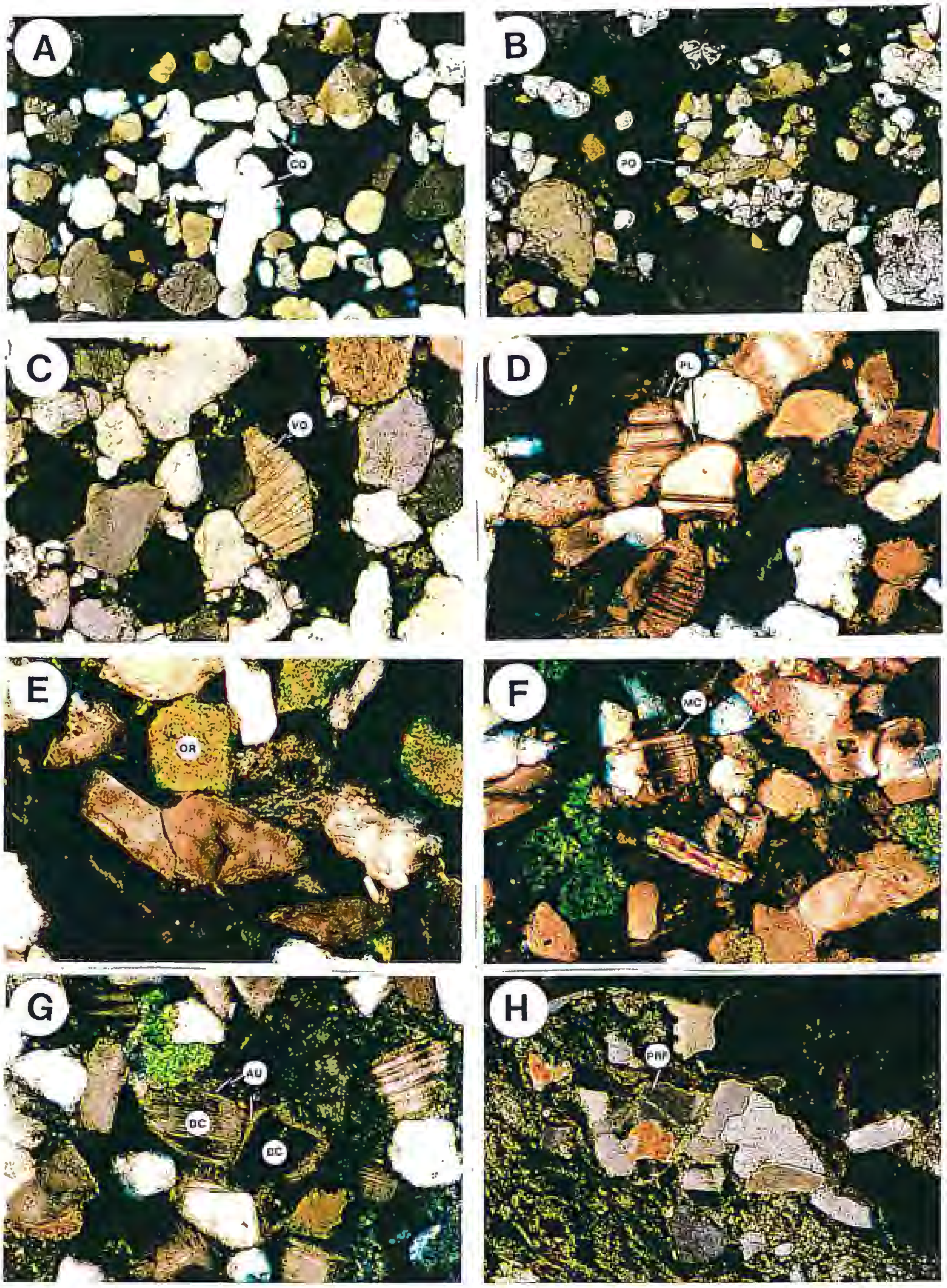
A
CQ
B
PQ
C
VQ
D
PL
E
OR
F
MC
G
AU
DC
EC
H
PRF

PLATE 2

A. Sample PH-CX-2. Photomicrograph of multicycle Hinckley quartz grain (RQ). Crossed polarizers, field of view 0.4 mm across.

B. Sample 94-WI-01. Photomicrograph of multicycle Mt. Simon quartz grain (RQ). Crossed polarizers, field of view 0.8 mm across.

C. Sample CH-V66-15. Photomicrograph of multicycle Eau Claire quartz grain (RQ). Crossed polarizers, field of view 0.8 mm across.

D. Sample AG-TRIP1-2U. Photomicrograph of multicycle Galesville quartz grain (RQ). Crossed polarizers, field of view 0.4 mm across.

E. Sample MGS-BC1-717.9. Photomicrograph of multicycle Ironton quartz grain (RQ). Crossed polarizers, field of view 0.8 mm across.

F. Sample AG-AC1-730. Photomicrograph of multicycle Franconia quartz grain (RQ). Crossed polarizers, field of view 0.8 mm across.

G. Sample AG-TRIP1-4B. Photomicrograph of multicycle Jordan quartz grain (RQ). Crossed polarizers, field of view 0.8 mm across.

H. Sample PS-LN-10-17. Photomicrograph of multicycle New Richmond quartz grain (RQ). Crossed polarizers, field of view 0.8 mm across.

I. Sample AG-H1-533. Photomicrograph of multicycle St. Peter quartz grain (RQ). Crossed polarizers, field of view 0.8 mm across.

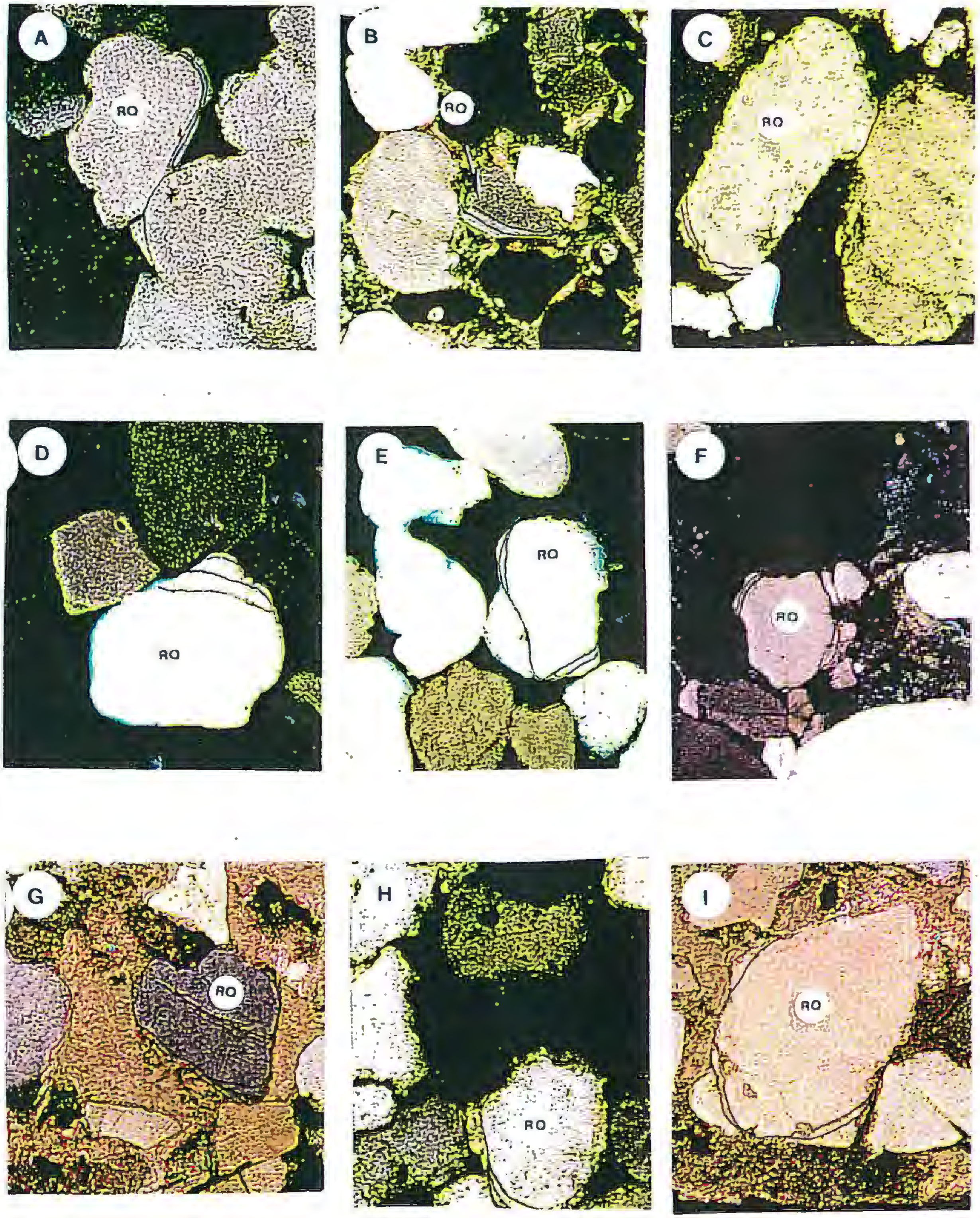
A
RQ
B
RQ
C
RQ
D
RQ
E
RQ
F
RQ
G
RQ
H
RQ
I
RQ

PLATE 3

A. Sample AG-AC1-665, Franconia Formation. Photomicrograph of detrital muscovite (MU). Crossed polarizers, field of view 0.4 mm across.

B. Sample AG-AC1-645.5, Franconia Formation. Photomicrograph of glauconite pellets (GL) and common quartz. Crossed polarizers, field of view 0.8 mm across.

C. Sample AG-TRIP1-5B*, Ironton Sandstone. Photomicrograph of primary matrix (MA) and common quartz. Crossed polarizers, field of view 0.8 mm across.

D. Sample AG-TRIP1-4B2, Jordan Sandstone. Photomicrograph of quartz (QTZ) cement. Crossed polarizers, field of view 0.4 mm across.

E. Sample AG-AC1-665, Franconia Formation. Photomicrograph of authigenic feldspar (AU) and adjacent detrital common quartz grains (CQ). Crossed polarizers, field of view 0.8 mm across.

F. Sample AG-AC1-655, Franconia Formation. Photomicrograph of calcite cement (CAL). Crossed polarizers, field of view 0.8 mm across.

G. Sample RU-SCH-834, Mt. Simon Sandstone. Photomicrograph of authigenic rhombohedral dolomite cement (DOL). Crossed polarizers, 0.8 mm across.

H. Sample AG-H1A-1416, Eau Claire Formation. Photomicrograph of detrital quartz grains partially cemented with siderite (SID) cement (?). Crossed polarizers, field of view 0.8 mm across.

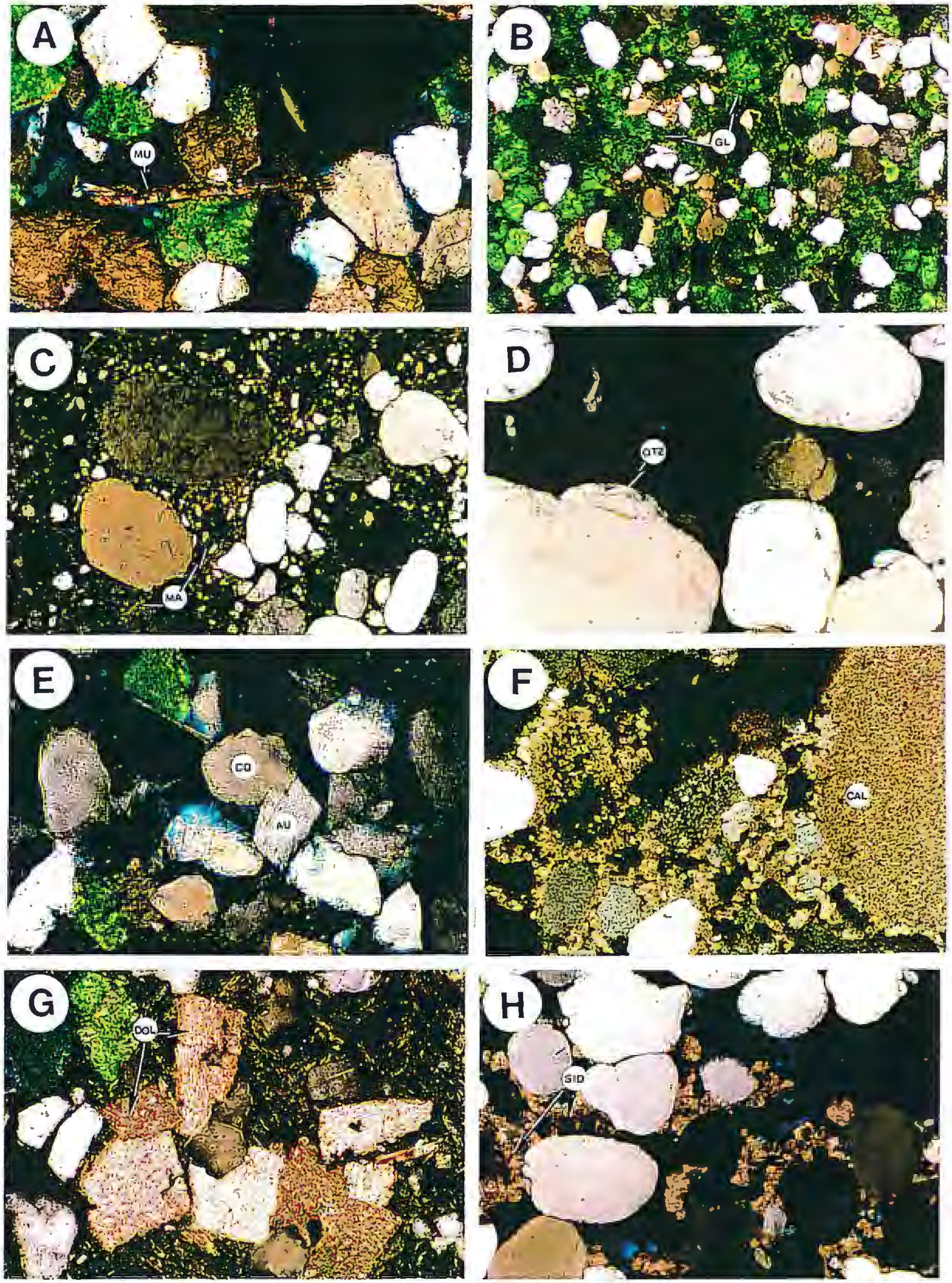

A
MU
B
GL
C
MA
D
QTZ
E
CO
AU
F
CAL
G
DOL
H
SID

PLATE 4

A. Photomicrograph of authigenic kaolinite (KAL). Sample RU-SQ9-474, Mt. Simon Sandstone. Crossed polarizers, field of view 0.8 mm across.

B. Photomicrograph of authigenic hematite cement. Sample CH-V66-22, Galesville Sandstone. Plain polarized light, field of view 0.8 mm across.

C. Photomicrograph of brachiopod (BR) shell fragments. Sample AG-B1-220, Galesville Sandstone. Plain polarized light, field of view 0.8 mm across.

D. Photomicrograph of garnet (Ga) surface etching. Sample AG-AC1-603, Franconia Formation. Plain polarized light, field of view 0.4 mm across.

E. Photomicrograph of zoned zircon (Z) grain. Sample AG-AC1-845, Eau Claire Formation. Plain polarized light, field of view 0.4 mm across.

F. Photomicrograph of unzoned zircon (Z) grain. Sample AG-AC1-972, Mt. Simon Sandstone. Plain polarized light, field of view 0.4 mm across.

G. Photomicrograph of a rutile (R) grain. Sample 94-WI-01, Mt. Simon Sandstone. Plain polarized light, field of view 0.4 mm across.

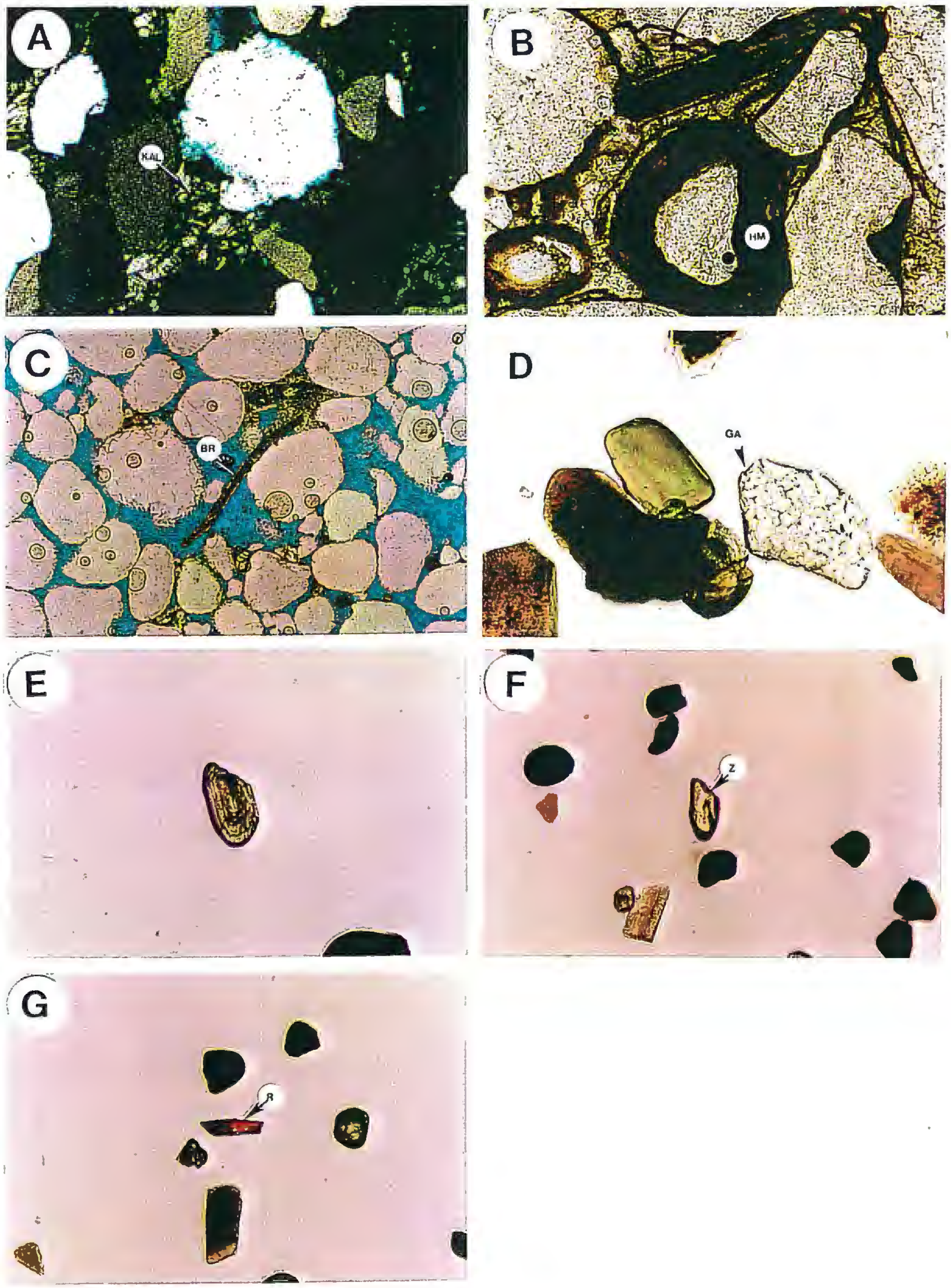
A
KAL
B
HM
C
BR
D
GA
E
F
Z
G
R

CHAPTER IV

HEAVY ACCESSORY MINERALS

Fifty-five representative samples from all nine units involved in this study from drill holes and outcrops were selected for heavy mineral analysis. Samples were selected on the quantity of grains that could be obtained, as most samples contained an inadequate amount of grains suitable for analysis. Thirty-three heavy mineral mounts were quantitatively studied (see Table 2). Those heavy mineral mounts excluded from the study contained a high portion of opaques; therefore, too few non-opaque grains were present to provide comparative percentages.

The main objective of the heavy mineral analysis is to determine the mineralogical maturity of the quartzose arenites using the ZTR index (Hubert, 1962). The ZTR index is defined as the total combined percentage of zircon, tourmaline, and rutile in the transparent heavy minerals excluding micas and authigenic minerals. A correlation can then be made between the mineralogical maturity of the quartz arenite with the relative amounts of zircon, tourmaline, and rutile. High ZTR indices are representative of intense weathering at the source and abrasion during transport, which may well have occurred during the recycling of the Late Proterozoic - Early Paleozoic quartzose arenites. Morton (1985) also stated that the zircon-tourmaline-rutile (ZTR) index can be a useful tool in examining the amount of sediment recycling.

Sample preparation:

Samples were prepared as follows:

1. Disaggregation by ceramic mortar and pestle of the arenite, allowing for liberation of the grains. Care was taken not to grind the samples, so as to leave the grains intact.
2. Sieving of disaggregated sediment, separating the coarse fraction by using a U.S. standard sieve mesh number 35 (0.5mm) on an ultrasonic sifter.
3. Coarse fraction analyzed under binocular scope to confirm the lack of heavy minerals.

4. Using distilled water, repeatedly washed the sample to dislodge any clay particles or loose iron oxides.
5. Gravity separation of heavy minerals in separatory funnels using tetrabromoethane, a heavy liquid with a density of 2.9 g/cm^2. Periodically, the samples were stirred to ensure separation.
6. The heavy residue was cleaned using acetone and subsequently dried. The washings were collected for future recycling of the heavy liquid.
7. With a hand magnet, the highly magnetic opaque portion was separated.
8. The heavy mineral residue was then split into two or four portions if a substantial number of grains were obtained. For petrographic analysis, the grains were then mounted in Canada balsam (n = 1.54).

<u>Counting procedure:</u>

All fifty-five heavy mineral mounts were analyzed with a petrographic microscope and thirty-three mounts were chosen for analysis. Only small core samples and outcrop samples were available for heavy mineral analysis, and the thirty-three of the fifty-five mounts chosen for analysis contained enough grains for analysis. When available, a total of 300 non-opaque grains were identified and counted. All of the grains present within the field of view were counted and tabulated on a spreadsheet, allowing for calculation of individual mineral percentages. The results are displayed in Table 2.

<u>Mineral descriptions:</u>

The percentages listed below are based on the total averages of non-opaque heavy mineral grains in the thirty-four mounts analyzed.

Non-opaques:

GARNET: Garnet is the most abundant non-opaque heavy mineral in all of the units of this study (average = 51.1%). Garnet grains were classified according to roundness (rounded and subrounded/subangular) and color (colorless and pink-brown). Approximately 30 percent of the grains are subrounded to subangular, 22 percent are rounded, and no angular garnet grains are present. Most of the grains (74 percent) are colorless. Etch-facets and surface pits are dissolution features found on most grains (Plate 4D).

ZIRCON: Zircon is the second most abundant non-opaque heavy mineral in all nine units of this study (average = 27.7 percent). Zircon grains were classified into two main categories, rounded grains and subrounded/subangular grains. These two categories were then further separated by the presence or lack of zonation in the grains (Plate 4E, 4F). A majority of the grains are unzoned and rounded. In some of the zircon grains, inclusions were observed. Most of the grains are colorless to pink prisms, 0.1 to 0.2 mm in length.

TOURMALINE: Tourmaline is the third most abundant non-opaque mineral present (average = 17 percent). Both the degree of roundness as well as the color/pleochroism were taken into consideration for the classification of the tourmaline grains (Plate 4G). A majority of grains are rounded (90 percent). They are ellipsoidal to spherical in shape, with a grain size ranging from 0.15 to 0.3mm.; a few are euhedral. A majority of the grains are green-brown in color (67 percent). The remaining 33 percent are varieties of green, blue, black, pink, and violet color. Inclusions are present in many grains. Abraded overgrowths are present on a few tourmaline grains. These abraded overgrowths serve a purpose similar to the abraded quartz overgrowths, as they are indicative of multicyclicity. Plate 5A-I shows tourmaline grains with abraded overgrowths from all nine units.

RUTILE: Rutile is present in almost half of the heavy mineral mounts analyzed. The amount is variable, ranging from 0.5 - 20 percent (average = 1.7 percent). Rutile was classified according to the degree of roundness (rounded, subrounded/subangular) and color (yellow or red) (Plate 4H). The ratio of rounded to subrounded rutile is approximately 1:1, while the ratio of yellow:red is 1:2. The average rutile grain size is between 0.1 and 0.2mm.

APATITE: Apatite is present in trace amounts in only four mounts. In three of the four samples (one mount each from the Galesville, Franconia, and St. Peter), the apatite grains are subrounded and colorless, while the fourth grain mount (from the St. Peter) contains rounded colorless grains. Some ragged edges are present on the apatite grains due to dissolution processes.

PYROXENE: (Augite/diopside): One sample (PS-LW-16-B) contains an augite grain. The grain was identified by its moderate birefringence and its inclined extinction of 30°- 40°.

EPIDOTE: Subrounded epidote is found in two samples (AG-MNT-STP2, AG-AC1-972) in trace amounts. It is identified by its irregular morphology and high relief.

STAUROLITE: Staurolite is present in three samples (AG-AC1-685, AG-TRIP1-5B, and AG-MNT-STP1). The grains are mainly subangular to angular and are approximately 0.1- 0.2mm. in diameter. Pleochroism, high relief, and quartz inclusions are features used to identify staurolite.

ANATASE: Anatase is present in two samples (AG-TRIP1-4B2, AG-TRIP1-5C2). Blue and yellow shades of anatase along with a distinct rectangular shape were noted. Anatase is clearly authigenic as it has not been abraded.

Opaques:

The opaque minerals in the nine units involved in this study were not counted. However, magnetite, pyrite, and hematite are the three most common opaque minerals seen. Magnetite was removed with a hand magnet prior to the mounting of the grains with Canada balsam.

Mineralogical maturity

The maturity of a sandstone can be determined by its mineral concentration, specifically, the ratio of quartz + chert to feldspar + rock fragments. Another method of determining mineralogical maturity is to examine the heavy mineral maturity, using Hubert's (1962) zircon = tourmaline - rutile (ZTR) maturity index for sandstones. Typically, the detrital heavy mineral assemblages are a function of the proportions of the various heavy minerals derived from the source area and serve as an indicator of the degree of modification of the detritus by sorting and abrasion during transportation and deposition (Hubert, 1962).

The ZTR index was calculated for the thirty-three heavy mineral mounts of this study. Of the thirty-three samples, eleven were classified as feldspathic sandstones, while the remaining twenty-two were identified as quartz sandstones. All thirty-three samples showed a relatively low ZTR index (below 86 percent, average = 47 percent) because of the high concentrations of garnet. The ratio of garnet:zircon is 2:1, garnet:tourmaline is 3:1, and garnet:rutile is 18:1. Garnet is a fairly stable heavy mineral; it is resistant to both abrasion and chemical attack (Tucker, 1991, p. 44). Therefore, in this study, a ZTRG index was also calculated for each of the thirty-four mounts.

All of the samples show ZTRG indices of approximately 100 percent (average = 98.5 percent), indicating a high mineralogical maturity. A high ZTRG index supports the mineralogical maturity of the sandstones indicated by their light mineral concentrations, with high concentrations of quartz and low amounts of feldspar and rock fragments.

		ZIRCON							TOURMALINE								
		ROUND		TOTAL	SUBROUND		TOTAL	TOTAL	SUBROUND TOURMALINE						TOTAL	ROUND TRM	
UNIT	SAMPLE #	ZONE	UNZONE	RND ZIRC	ZONE	UNZONE	SBRND ZIRC	ZIRCON	GRN-BRWN	GRN	BLUE	PINK	BLACK	VIOLET	SBRND TRM	GRN-BRWN	GREEN
Mt. Simon	94-WI-03	0.0	5.3	5.3	0.0	19.5	19.5	24.8	0.0	0.0	0.0	0.3	0.0	0.0	0.3	0.0	0.0
Mt. Simon	94-WI-04	1.8	24.5	26.4	0.9	7.3	8.2	34.5	21.8	0.9	0.0	17.3	0.0	0.0	40.0	0.9	0.0
Mt. Simon	AG-AC1-927	8.3	25.0	33.3	0.0	5.6	5.6	38.9	5.6	5.6	0.0	11.1	0.0	0.0	22.2	0.0	0.0
Mt. Simon	AG-AC1-972	0.6	45.6	46.3	0.3	0.0	0.3	46.6	23.0	0.0	1.0	13.3	0.0	0.0	37.2	0.0	0.0
Mt. Simon	94-WI-01	0.0	28.9	28.9	0.0	2.2	2.2	31.1	20.0	4.4	0.0	6.7	0.0	0.0	31.1	0.0	0.0
Mt. Simon	94-WI-07	0.0	17.4	17.4	0.0	4.3	4.3	21.7	8.7	2.2	0.0	2.2	0.0	0.0	13.0	2.2	0.0
AVERAGE				26.3			6.7	32.9							24.0		
Eau Claire	94-WI-05	5.7	35.2	40.9	0.0	0.0	0.0	40.9	23.9	4.5	0.0	2.3	0.0	0.0	30.7	0.0	1.1
Eau Claire	AG-AC1-845	4.5	4.5	9.1	9.1	0.0	9.1	18.2	0.0	0.0	0.0	0.0	0.0	0.0	0.0	0.0	0.0
Eau Claire	AG-AC1-878	4.4	25.6	30.0	1.1	15.6	16.7	46.7	4.4	3.3	0.0	0.0	0.0	0.0	7.8	1.1	0.0
Eau Claire	AG-AC1-892	0.6	37.3	38.0	0.0	5.1	5.1	43.0	0.0	1.9	0.0	4.4	0.0	0.0	6.3	0.6	0.0
AVERAGE				29.5			7.7	37.2							11.2		
Gale/Iron	AG-TRIP1-2L	0.0	6.5	6.5	3.2	25.8	29.0	35.5	3.2	0.0	0.0	0.0	0.0	0.0	3.2	3.2	0.0
Gale/Iron	AG-TRIP1-2U	4.4	43.3	47.8	0.0	0.0	0.0	47.8	23.3	0.0	0.0	8.9	0.0	0.0	32.2	1.1	0.0
Gale/Iron	AG-TRIP1-5B	5.1	7.7	12.8	0.0	7.7	7.7	20.5	2.6	0.0	0.0	2.6	0.0	0.0	5.1	0.0	0.0
Gale/Iron	AG-CTYF-Gales	0.0	8.3	8.3	3.6	0.0	3.6	11.9	7.3	0.0	0.0	0.7	0.0	0.0	7.9	0.3	0.0
Gale/Iron	AG-CTYF-Gale2	13.7	4.0	17.7	0.0	0.0	0.0	17.7	6.7	0.3	0.3	2.3	0.3	0.0	10.0	0.0	0.0
Gale/Iron	AG-TRIP1-4A	0.0	9.3	9.3	0.0	0.8	0.8	10.1	3.1	0.0	0.0	0.0	0.0	0.0	3.1	0.0	0.0
AVERAGE				17.0			6.9	23.9							10.3		
Franconia	AG-AC1-801.5	0.0	15.6	15.6	2.7	9.0	11.7	27.3	1.8	0.0	0.0	3.3	0.0	0.0	5.1	0.3	0.0
Franconia	AG-AC1-803	0.0	3.0	3.0	0.0	0.7	0.7	3.6	3.3	0.0	0.0	0.0	0.0	0.0	3.3	31.8	0.0
Franconia	AG-AC1-818	1.9	26.0	28.0	1.0	14.1	15.1	43.1	2.3	0.0	0.0	2.9	0.0	0.0	5.1	0.3	0.0
Franconia	AG-AC1-885	0.0	6.5	6.5	1.6	3.2	4.8	11.3	1.6	0.0	0.0	0.0	0.0	0.0	1.6	0.0	0.0
AVERAGE				13.3			8.1	21.3							3.8		
Jordan	AG-TRIP1-4B1	3.8	3.8	7.7	3.8	19.2	23.1	30.8	0.0	0.0	0.0	0.0	0.0	0.0	0.0	0.0	0.0
Jordan	AG-TRIP1-4B2	0.0	16.0	16.0	0.0	17.0	17.0	33.0	1.0	3.0	0.0	0.0	0.0	0.0	4.0	0.0	0.0
Jordan	AG-TRIP1-5B	0.0	23.5	23.5	0.0	0.0	0.0	23.5	23.5	0.0	0.0	0.0	0.0	0.0	23.5	0.0	0.0
Jordan	AG-TRIP1-5C	0.3	0.0	0.3	0.0	0.0	0.0	0.3	0.0	0.0	0.0	0.3	0.0	0.0	0.3	0.0	0.3
Jordan	AG-TRIP1-5C2	0.0	8.3	8.3	0.0	41.7	41.7	50.0	0.0	0.0	0.0	0.0	0.0	0.0	0.0	0.0	0.0
AVERAGE				11.2			16.3	27.5							5.6		
New Richmond	PS-LW-16-O	0.0	2.0	2.0	0.0	0.0	0.0	2.0	6.0	3.0	0.0	0.5	2.0	0.0	11.5	0.0	0.0
New Richmond	PS-LW-16-B	5.0	14.0	19.0	0.0	0.0	0.0	19.0	17.0	8.0	0.0	0.0	3.0	0.0	28.0	0.0	0.0
New Richmond	PS-LN-11-2	1.0	19.0	20.0	0.0	0.0	0.0	20.0	10.0	4.0	0.0	1.0	1.0	0.0	16.0	0.0	0.0
New Richmond	PS-LN-11-3	3.0	19.0	22.0	0.0	0.0	0.0	22.0	21.0	6.0	0.0	0.0	1.0	0.0	28.0	0.0	0.0
AVERAGE				15.8			0.0	15.8							20.9		
St. Peter	AG-MNT-STP1	0.0	30.0	30.0	0.0	6.7	6.7	36.7	23.3	0.0	0.0	3.3	0.0	0.0	26.7	0.0	0.0
St. Peter	AG-MNT-STP2	0.0	21.3	21.3	1.6	0.0	1.6	23.0	36.1	3.3	1.6	4.1	0.0	0.0	45.1	0.0	0.0
St. Peter	AG-TRIP1-6	1.0	54.8	55.7	0.0	0.0	0.0	55.7	14.1	1.0	0.0	3.6	0.0	0.0	18.7	0.0	0.0
St. Peter	AG-AC1-181.5	0.7	13.1	13.8	0.0	0.0	0.0	13.8	10.3	2.1	0.0	0.7	0.0	0.0	13.1	0.0	0.0
AVERAGE				30.2			2.1	32.3							25.9		

Table 2: Petrographic summary of the heavy minerals in the arenites.

<u>ABBREVIATIONS</u>:

SBRND: Subround
ZIRC: Zircon
RUT: Rutile
ANAT: Anatase
PYROX: Pyroxene
UNZONE: No zonation present
RND: Round
TRM: Tourmaline
GRNT: Garnet
HB SERIES: Hornblende
STAUR: Staurolite
TREM/ACT: Tremolite/Actinolite
SUBANG: Subangular
GRN-BRWN: Green-brown
COLRLESS: Colorless
AUG/DIOP: Augite/Diopside
ZONE: Zonation present

		TOURMALINE					RUTILE					GARNET					
		RND TRM			TOTAL	TOTAL	ROUND RUT		SUBRND-SUBANG RUT		TOTAL	RND GRNT		SUBRND-SUBANG		ANGULAR	TOTAL
UNIT	SAMPLE #	PINK	BLACK	VIOLET	RND TRM	TRM	YELLOW	RED	YELLOW	RED	RUTILE	COLRLESS	PINK-BRWN	COLRLESS	PINK-BRWN	COLRLESS	GARNET
Mt. Simon	94-WI-03	0.0	0.0	0.0	0.0	0.3	0.0	0.0	0.0	0.7	0.7	4.0	0.0	69.6	0.7	0.0	74.3
Mt. Simon	94-WI-04	0.9	0.0	0.0	1.8	41.8	0.0	3.6	0.0	0.9	4.5	3.6	13.6	0.0	1.8	0.0	19.1
Mt. Simon	AG-AC1-927	5.6	0.0	0.0	5.6	27.8	0.0	0.0	0.0	0.0	0.0	8.3	16.7	8.3	0.0	0.0	33.3
Mt. Simon	AG-AC1-972	0.0	0.0	0.0	0.0	37.2	0.0	2.6	0.0	0.0	2.6	5.5	8.1	0.0	0.0	0.0	13.6
Mt. Simon	94-WI-01	0.0	0.0	0.0	0.0	31.1	2.2	0.0	0.0	0.0	2.2	2.2	33.3	0.0	0.0	0.0	35.6
Mt. Simon	94-WI-07	0.0	0.0	0.0	2.2	15.2	0.0	0.0	0.0	0.0	0.0	19.6	4.3	39.1	0.0	0.0	63.0
AVERAGE					1.6	25.6					1.7						39.8
Eau Claire	94-WI-05	0.0	0.0	0.0	0.0	30.7	0.0	1.1	0.0	0.0	1.1	12.5	10.2	3.4	1.1	0.0	27.3
Eau Claire	AG-AC1-845	0.0	0.0	0.0	0.0	0.0	0.0	0.0	0.0	4.5	4.5	9.1	0.0	68.2	0.0	0.0	77.3
Eau Claire	AG-AC1-878	0.0	0.0	0.0	1.1	8.9	0.0	0.0	0.0	0.0	0.0	3.3	3.3	36.7	1.1	0.0	44.4
Eau Claire	AG-AC1-892	0.6	0.0	0.0	1.3	7.6	0.0	0.0	0.0	0.6	0.6	17.1	1.9	27.8	1.9	0.0	48.7
AVERAGE						11.8					1.6						49.4
Gale/Iron	AG-TRIP1-2L	6.5	0.0	0.0	9.7	12.9	0.0	0.0	3.2	0.0	3.2	0.0	0.0	48.4	0.0	0.0	48.4
Gale/Iron	AG-TRIP1-2U	0.0	0.0	0.0	1.1	33.3	0.0	0.0	0.0	0.0	0.0	13.3	4.4	1.1	0.0	0.0	18.9
Gale/Iron	AG-TRIP1-5B	0.0	0.0	0.0	0.0	5.1	0.0	0.0	10.3	2.6	12.8	7.7	10.3	41.0	2.6	0.0	61.5
Gale/Iron	AG-CTYF-Gales	0.0	0.0	0.3	0.7	8.6	0.0	0.0	0.0	0.0	0.0	17.5	4.0	56.1	2.0	0.0	79.5
Gale/Iron	AG-CTYF-Gale2	0.0	0.0	0.0	0.0	10.0	0.0	0.0	0.0	0.0	0.0	16.7	2.3	51.7	1.7	0.0	72.3
Gale/Iron	AG-TRIP1-4A	0.0	0.0	0.0	0.0	3.1	0.0	8.5	0.0	0.0	8.5	6.2	71.3	0.0	0.8	0.0	78.3
AVERAGE						12.2					4.1						59.8
Franconia	AG-AC1-601.5	0.6	0.0	0.0	0.9	6.0	0.0	0.0	0.0	0.0	0.0	19.2	3.9	42.0	1.5	0.0	66.7
Franconia	AG-AC1-603	0.0	0.0	0.0	31.8	35.1	0.0	0.0	0.0	0.0	0.0	9.3	6.6	38.1	7.3	0.0	61.3
Franconia	AG-AC1-618	1.0	0.0	0.0	1.3	6.4	0.0	0.0	0.0	0.6	0.6	8.0	1.3	39.5	1.0	0.0	49.8
Franconia	AG-AC1-685	0.0	0.0	0.0	0.0	1.6	0.0	0.0	0.0	3.2	3.2	6.5	0.0	77.4	0.0	0.0	83.9
AVERAGE						12.3					1.0						65.4
Jordan	AG-TRIP1-4B1	1.9	0.0	0.0	1.9	1.9	0.0	1.9	0.0	0.0	1.9	3.8	0.0	61.5	0.0	0.0	65.4
Jordan	AG-TRIP1-4B2	0.0	0.0	0.0	0.0	4.0	3.0	2.0	13.0	1.0	19.0	8.0	4.0	29.0	3.0	0.0	44.0
Jordan	AG-TRIP1-5B	0.0	0.0	0.0	0.0	23.5	0.0	20.6	0.0	0.0	20.6	0.0	32.4	0.0	0.0	0.0	32.4
Jordan	AG-TRIP1-5C	0.0	0.0	0.0	0.0	0.3	0.0	0.0	0.0	0.0	0.0	4.9	69.1	1.6	23.7	0.0	99.3
Jordan	AG-TRIP1-5C2	0.0	0.0	0.0	0.0	0.0	0.0	0.0	0.0	4.2	4.2	4.2	0.0	41.7	0.0	0.0	45.8
AVERAGE						6.0					9.1						57.4
New Richmond	PS-LW-16-O	0.0	0.0	0.0	0.0	11.5	0.0	0.0	0.0	0.0	0.0	23.0	7.0	54.0	2.0	0.0	86.0
New Richmond	PS-LW-16-B	0.0	0.0	0.0	0.0	28.0	0.0	0.0	0.0	0.0	0.0	8.0	8.0	37.0	0.0	0.0	53.0
New Richmond	PS-LN-11-2	0.0	0.0	0.0	0.0	16.0	0.0	0.0	0.0	0.0	0.0	5.0	10.0	10.0	0.0	0.0	25.0
New Richmond	PS-LN-11-3	0.0	0.0	0.0	0.0	28.0	0.0	0.0	0.0	1.0	1.0	4.0	10.0	26.0	0.0	0.0	40.0
AVERAGE						20.9					0.3						51.0
St. Peter	AG-MNT-STP1	0.0	0.0	0.0	0.0	26.7	3.3	3.3	0.0	0.0	6.7	6.7	10.0	13.3	0.0	0.0	30.0
St. Peter	AG-MNT-STP2	0.0	0.0	0.0	0.0	45.1	0.0	2.5	0.0	0.0	2.5	12.3	15.6	1.6	0.0	0.0	29.5
St. Peter	AG-TRIP1-6	0.0	0.0	0.0	0.0	18.7	0.0	0.0	0.0	0.0	0.0	17.0	8.2	0.3	0.0	0.0	25.6
St. Peter	AG-AC1-181.5	0.0	0.0	0.0	0.0	13.1	0.0	0.0	0.0	0.0	0.0	53.8	19.3	0.0	0.0	0.0	73.1
AVERAGE						25.9					2.3						39.5

Table 2: Petrographic summary of the heavy minerals in the quartz arenites.

		APATITE		AMPHIBOLE		PYROX	EPIDOTE	STAUR	ANAT	RX TYPE	Z+T+R	Z+T+R+G
		ROUND	SUBANG									
UNIT	SAMPLE#	COLRLESS	COLRLESS	HB SERIE	TREM/ACT	AUG/DIOP	SUBANG					
Mt. Simon	94-WI-03									FLDSS	25.7	100.0
Mt. Simon	94-WI-04									QTZSS	80.9	100.0
Mt. Simon	AG-AC1-927									QTZSS	66.7	100.0
Mt. Simon	AG-AC1-972						1.0			QTZSS	86.4	99.0
Mt. Simon	94-WI-01									FLDSS	64.4	100.0
Mt. Simon	94-WI-07									FLDSS	37.0	100.0
AVERAGE												99.8
Eau Claire	94-WI-05									FLDSS	72.7	100.0
Eau Claire	AG-AC1-845									QTZSS	22.7	100.0
Eau Claire	AG-AC 1-878									FLDSS	55.6	100.0
Eau Claire	AG-AC1-892									FLDSS	51.3	100.0
AVERAGE												100.0
Gale/Iron	AG-TRIP1-2L									QTZSS	51.6	100.0
Gale/Iron	AG-TRIP1-2U									QTZSS	81.1	100.0
Gale/Iron	AG-TRIP1-5B							3.0		QTZSS	38.5	97.0
Gale/Iron	AG-CTYF-Gales		3.0							FLDSS	20.5	97.0
Gale/Iron	AG-CTYF-Gale2									FLDSS	27.7	100.0
Gale/Iron	AG-TRIP1-4A									QTZSS	21.7	100.0
AVERAGE												99.0
Fraconia	AG-AC1-601.5									FLDSS	33.3	100.0
Fraconia	AG-AC1-603		2.0							FLDSS	38.7	98.0
Fraconia	AG-AC1-618									FLDSS	50.2	100.0
Fraconia	AG-AC1-685							4.0		FLDSS	16.1	96.0
AVERAGE												98.5
Jordan	AG-TRIP1-4B1									QTZSS	34.6	100.0
Jordan	AG-TRIP1-4B2								1.0	QTZSS	56.0	99.0
Jordan	AG-TRIP1-5B									QTZSS	67.6	100.0
Jordan	AG-TRIP1-5C									QTZSS	0.7	100.0
Jordan	AG-TRIP1-5C2								1.0	QTZSS	54.2	99.0
AVERAGE												99.6
New Richmond	PS-LW-16-0									QTZSS	13.5	99.5
New Richmond	PS-LW-16-B					1.0				QTZSS	47.0	99.0
New Richmond	PS-LN-11-2									QTZSS	36.0	61.0
New Richmond	PS-LN-11-3									QTZSS	51.0	91.0
AVERAGE												87.6
St. Peter	AG-MNT-STP1		1.0					1.0		QTZSS	70.0	98.0
St. Peter	AG-MNT-STP2	2.0					2.0			QTZSS	70.5	96.0
St. Peter	AG-TRIP1-6									QTZSS	74.4	100.0
St. Peter	AG-AC1-181.5									QTZSS	26.9	100.0
AVERAGE												98.5

Table 2: Petrographic summary of the heavy minerals in the quartz arenites.

PLATE 5

A. Photomicrograph of multicycle Mt. Simon tourmaline (T) grain. Sample 94-WI-07. Plain polarized light, field of view 0.4 mm across.

B. Photomicrograph of multicycle Eau Claire tourmaline (T) grain. Sample AG-AC1-878. Plain polarized light, field of view 0.4 mm across.

C. Photomicrograph of multicycle Galesville/Ironton tourmaline (T) grain. Sample AG-TRIP1-2L. Plain polarized light, field of view 0.4 mm across.

D. Photomicrograph of multicycle Franconia tourmaline (T) grain. Sample AG-AC1-603. Plain polarized light, field of view 0.4 mm across.

E. Photomicrograph of multicycle Jordan tourmaline (T) grain. Sample AG-TRIP1-5B. Plain polarized light, field of view 0.4 mm across.

F. Photomicrograph of multicycle New Richmond tourmaline (T) grain. Sample PS-LW-16-O. Plain polarized light, field of view 0.4 mm across.

G. Photomicrograph of multicycle St. Peter tourmaline (T) grain. Sample AG-AC1-181.5. Plain polarized light, field of view 0.4 mm across.

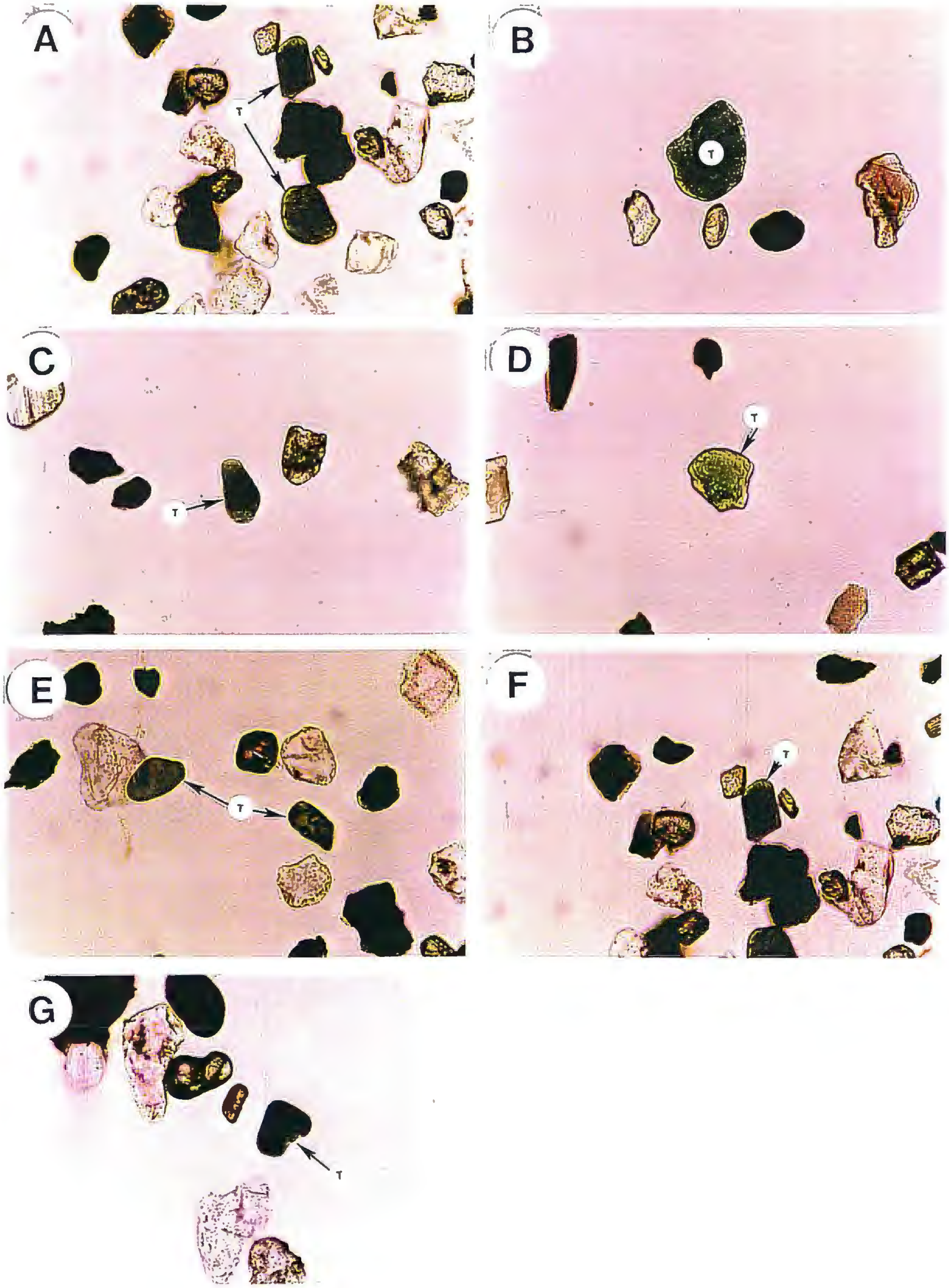
A
B
C
D
E
F
G
T

CHAPTER V

THE RECYCLING QUESTION

Why have I focused on the possible recycling of the quartzose arenites? It may indeed provide another piece of evidence (or perhaps a unique twist) to the cyclic sedimentation described by Ostrom (1964) and Austin (1972). Both authors describe four recurrent lithotopes of the region indicating five cycles of sedimentation (Figure 12): 1) well-sorted quartz arenite, 2) poorly sorted unit of mixed lithology, 3) shale or argillaceous sandstone, and 4) carbonate. The cycles developed because of repeated emergence caused by the reactivation of tectonically unstable highland cratonic areas and submergence caused by the submergence of the Appalachian geosynclinal basin (Austin, 1972).

Recurrent lithotopes were likely the result of the cyclic differences of the amount, mineralogy, and grain size of the clastic influx into the embayment and reflect the environment and proximity of the source area (Austin, 1972). Is it possible to even further support the concept of cyclic sedimentation by providing evidence of multicyclicity of the arenites? Perhaps the older units were recycled and contributed to the production of the stratigraphically younger units (Figure 13).

The possibility also exists that all of the textures of each unit may be explained by the recycling of that unit within itself. However, in order for this to be a realistic possiblity, one must consider that the sediment would have had to have been deposited and cemented with silica, then exposed to erosional processes, only to be recemented with silica again toward the stratigraphical top of the unit. This may indeed be the case. However, for the purposes of this study, it was hypothesized that the stratigraphically older quartz arenites were recycled to produce the stratigraphically younger quartz arenites. In order to determine if recycling of one unit itself was responsible for the textures, in-depth studies of each unit would have to be conducted.

In order to effectively discuss the possible multicyclicity of the units involved in this study, it is important to first address the issue of mineralogic maturity of the arenites. By

Depositional Environments				
Cycles	Beach-nearshore	Nearshore shelf	Depositional shelf	Reef
5	St. Peter Fm.	Nokomis Mbr.	Harmony Hill Mbr.	Ottawa Group
4	New Richmond Mbr.	?	Present, but unnamed	Shakopee Fm.
3	Jordan Fm.	Madison Fm.	Blue Earth Mbr.	Oneota Fm.
2	Galesville Fm.	Ironton Fm.	Fraconia Fm. and Lodi Mbr.	Black Earth Mbr.
1	Mt. Simon Fm.	Upper Mt. Simon	Eau Claire Fm.	Bonneterre Fm.

Fig. 12: Strata comprising five pre-Cincinnatian Paleozoic sedimentary cycles in the study area (after Austin, 1972).

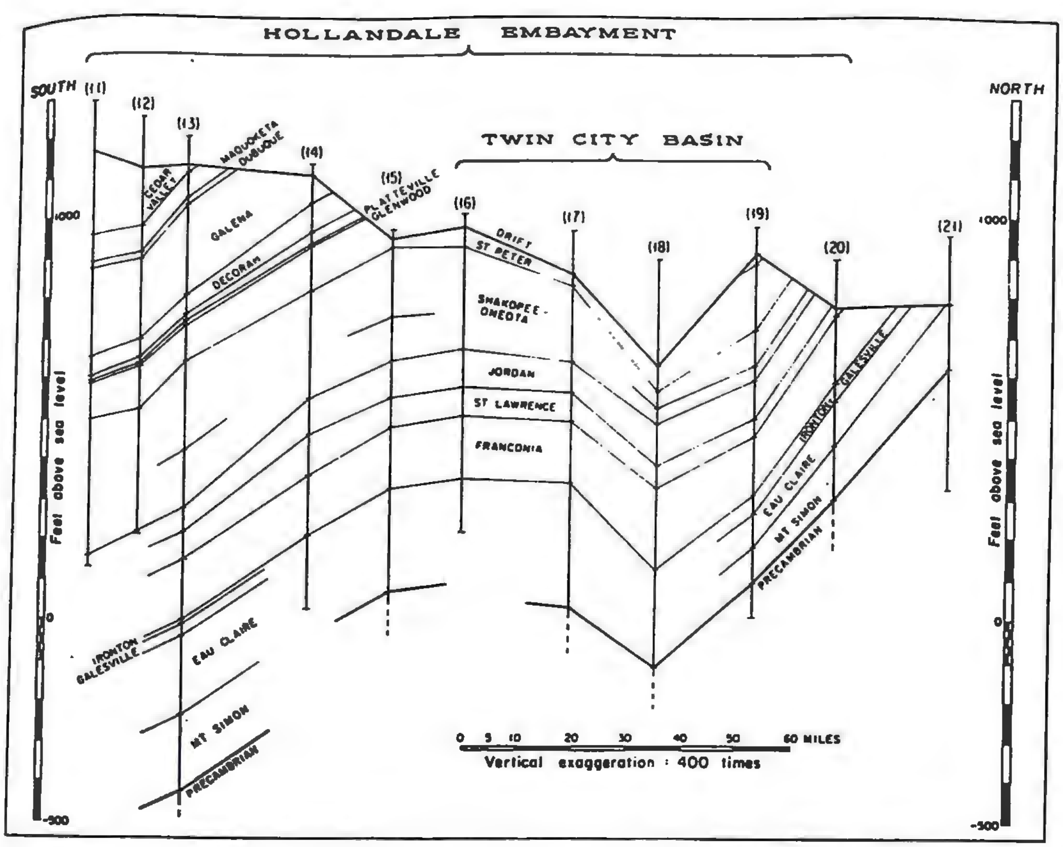

Fig. 13: Cross-section of the Hollandale embayment. The stratigraphically older units would have been exposed and available for recycling as the sea transgressed and regressed across southeastern Minnesota and southwestern Wisconsin. (From Austin, 1972).

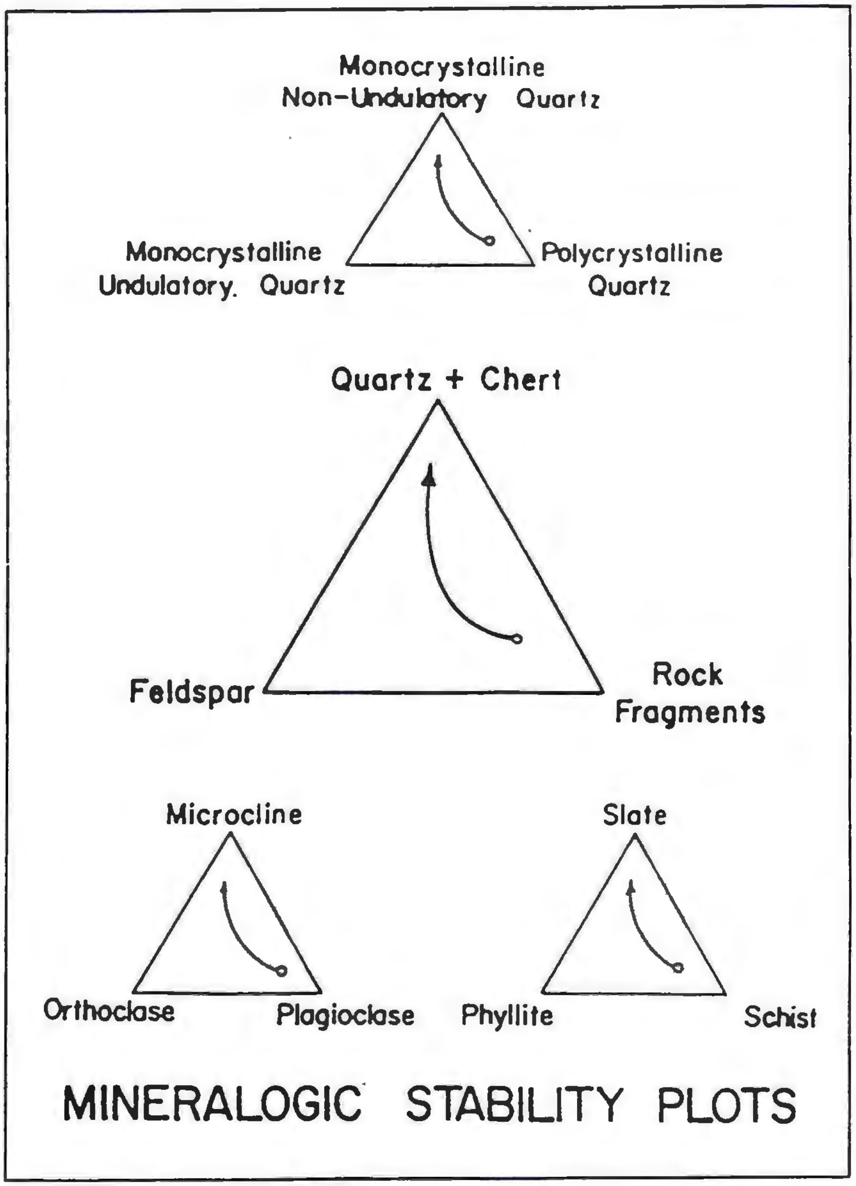

Fig. 14: Relative effects of sedimentary processes on sand-sized clastic grains. The circle within each triangle represents an arbitrary initial composition and the track shows the probable change in composition resulting from sedimentary processes (from Blatt, 1967).

examining how both first-cycle and multicycle quartz arenites are produced, it may then be possible to discuss the role of recycling in the Late Proterozoic - Early Paleozoic arenites.

Blatt (1967) conducted a study involving provenance determinations and the recycling of sediments. He stated that more effective methods need to be established to determine what percentage of an arenite is recycled. He suggested that the mechanical and chemical stability of minerals may provide a link as to the amount of sediment recycling (Figure 14).

The following discussion focuses on the possible mineralogic evidence for the recycling of quartz arenites as well as the role of tectonics and eustatic sea level change in the production of quartz arenites.

Presence, Mineralogy, and Abundance of Quartz:

Abraded quartz overgrowths:

Abraded quartz overgrowths are indicative of multicyclicity. An abraded overgrowth serves as an indicator that the grain was previously a framework grain in an older quartz arenite, cemented with silica cement. This grain was then removed from the arenite by erosion. As the grain is re-deposited to become part of a younger quartz arenite, it is then recemented with silica cement, thereby producing a second quartz overgrowth upon the abraded grain and overgrowth.

The fragile nature of the quartz overgrowth makes it difficult for it to withstand a great deal of abrasion and transport. It is the very presence of the abraded quartz overgrowth that provides the evidence for recycling. Kennedy and Arikan (1990) discussed the spalling of quartz overgrowths and have suggested that although quartz is physically stable, the boundary between the detrital core and the quartz overgrowth may be weak, along which breakage may take place, especially if a "dust" coating is present.

Sanderson (1984) studied the significance of inherited quartz overgrowths in arenites. He suggested that the proportion of inherited (an inclusive genetic term used by Sanderson, defined as any rounded overgrowth, double overgrowth, or pressure overgrowth) overgrowths may be underestimated. He explained that because an inherited overgrowth encompasses only a portion of a grain's surface, the probability of coming across a partially quartz-coated grain in a traverse is below average due to random grain orientations. He developed a method by which one can use whole rock mineralogy to estimate the percent of inherited overgrowths present. In the examples involved in his study, he concluded that the calculated whole rock inherited overgrowth quantity is twice as much as observed in thin section.

It is also necessary to examine the role of quartz overgrowths in diagenesis. The quartz overgrowths used as evidence for recycling in this study are abraded quartz overgrowths, indicating transportation and re-deposition of the grains. Austin (1974) studied multiple overgrowths on the detrital quartz sand grains of the New Richmond Member of the Shakopee Formation. He showed the important role of diagenesis on the creation of quartz overgrowths. The quartz overgrowth boundaries become increasingly euhedral away from the rounded detrital quartz grain, thereby indicating that the grain remained in place and no movement occurred between overgrowth stages. Such overgrowths are not evidence of recycling.

Decrease in polycrystalline quartz:

Other possible evidence for recycling is in the overall decrease of polycrystalline quartz. It has long been established that monocrystalline quartz has a much higher survival rate than that of polycrystalline quartz (Harrell and Blatt, 1978). They concluded that migrating sediment particles spend a great amount of time trapped in short-lived deposits, during which they suffer the effects of chemical weathering. In addition, polycrystalline quartz grains are chemically less stable than monocrystalline grains (Harrell and Blatt, 1978). This allows for weathered polycrystalline quartz grains to be preferentially destroyed over monocrystalline grains.

A decrease in polycrystalline quartz in a rock column would then indicate that the arenites underwent repeated abrasion and/or weathering during deposition. Therefore, if the older quartz arenites in a rock column are comprised of a fair amount of polycrystalline quartz, through repeated reworking and recycling of the arenites, one would expect the amount of polycrystalline quartz to decrease upward in the stratigraphic column, if recycled quartz was the major source for the new arenite.

Because of the transport and abrasion that the quartzose arenites of this study underwent as a result of the transgressing-regressing Late Cambrian and Ordovician seas, the possible recycling of the quartzose arenites could result in an overall decrease in the distribution of polycrystalline quartz.

Presence, Mineralogy, and Abundance of Feldspar:

The amount of feldspar present in an arenite is related to the source rock composition, chemical weathering in the source area, abrasion and solution during transportation, and solution and precipitation during diagenesis (Pettijohn et al., 1987, p. 155).

Mack (1978) found that marine sands contain significantly less mechanically unstable detrital feldspar than nonmarine (fluvial) sands, indicating that physical processes in the marine environment are active modifiers of the original feldspar population. However, Pettijohn et al. (1987, p. 36) also noted that some beaches and dunes can have considerable amounts of feldspar, counteracting the theory that quartz arenites are the products of the removal of feldspar in such environments. Obviously, residual time in a given environment is important.

The amount of feldspar present may also be a direct reflection of the grain size of the arenite. Odom (1975) concluded that the amount of feldspar present in the upper Mississippi Valley quartz arenites is related to the volume of very fine sand. He also stated that the amount of feldspar and glauconite present is related to the energy regime of the environment of deposition, with quartzose feldspathic arenites such as the Eau Claire and Franconia Formations representing low energy regime environments. If the amount of feldspar was modified by the possible recycling, it can then be hypothesized that the amount of feldspar will decrease with deposition of stratigraphically younger quartzose arenites. To further identify the possibility of recycling as a source for the sediment of the stratigraphically younger units, a comparison should be made between the amount of unaltered feldspar and altered feldspar. If the amount of altered feldspar surpasses the amount of unaltered feldspar, one can reasonably hypothesize that the unaltered feldspar of the stratigraphically older quartz arenites may have been reworked and recycled into the younger arenites.

Relationship between polycrystalline quartz and feldspar:

Both polycrystalline quartz and feldspar are relatively unstable minerals. Therefore, it should be possible to correlate the amount of polycrystalline quartz to the amount of feldspar, as one would expect that both should decrease through the processes of recycling.

Importance of the heavy mineral suite:

Other lines of evidence indicative of sediment recycling are high ZTR and ZTRG indices, high degrees of roundness (small grains, as heavy minerals are, are very difficult to round in an aqueous environment because of the protective water cushion) as well as similar heavy mineral concentrations (Morton, 1985). High ZTR indices are representative of intense weathering at the source and abrasion during transport, both of which could have occurred with the recycling of the Paleozoic sediments of the Hollandale embayment.

Heavy mineral concentrations in quartzose sandstones constitute less than 1 percent by weight of the entire sandstone. However, individual grains of tourmalines in this minor fraction may have abraded overgrowths which, similar to the presence of abraded quartz overgrowths, are indicators of a multicycle history with derivation from older sandstones. Some grains show abraded overgrowths beneath unabraded (authigenic) overgrowths whereas others do not have younger overgrowths present (Plate 5).

Tectonics and sedimentation:

In examining the tectonic framework of the Late Proterozoic - Early Paleozoic arenites, it is necessary to look at the amount of weathering/abrasion that occurred to produce such clean quartz arenites.

The amount of weathering of a source area can be linked to tectonics. The ratio of the amount of chemical weathering to the amount of mechanical weathering in the source area determines the survival of unstable minerals (Pettijohn et al., 1987, p. 37). Also, the ratio of chemical to mechanical weathering is directly related to the topography of the source area, with the topography being a function of tectonics.

The arenites occur as blanket deposits which laterally grade into fine-grained shaly sands and carbonates to the south and east across the craton (Ostrom, 1978). Paleocurrent measurements indicate that at the time and place of deposition of the arenites, the paleocurrents were moving mainly toward the south and southwest (Figure 15). However, Austin (1972) indicated that the direction of sediment transport and of the paleoslope in southeastern Minnesota may have varied over time as a result of uplift and degradation of various sections of the Transcontinental arch-Wisconsin dome positive area as well as the development of structures that affected sedimentation in the Paleozoic seas.

According to Austin (1972) the main source of clastic sediment during Late Cambrian time may have been the Wisconsin dome which extended to northeastern Minnesota. Erosion of the Wisconsin dome, as well as the subsidence of the Wisconsin arch (at a faster rate than the southeastern Minnesota) resulted in thicker sequences of Mt. Simon, Eau Claire, Galesville and Ironton in extreme southeastern Minnesota, Wisconsin, and northern Illinois than in the remainder of Minnesota; in the decrease in grain size in the Eau Claire and Galesville from Wisconsin toward southeastern Minnesota; and the reduction of easily degradable sediment (i.e. feldspar) in the Mt. Simon ranging from as great as 40 percent in Wisconsin to 1-7 percent in Minnesota (Austin, 1972) (see Figure 1).

The following paragraphs outline the environments of deposition of the units involved in this study as well as possible interpretations of the source areas for the quartz arenites in Late Cambrian and Early Ordovician time:

A major transgression and regression are noted during Dresbachian time (the lower stage of the St. Croixan Series or earliest Late Cambrian) (Lochman-Balk, 1970). The Mt. Simon Sandstone and the Eau Claire Formation were deposited over the Precambrian basement during Middle and Late Dresbachian time during this Late Cambrian transgression of the craton. Marginal marine and marine waters flooded the craton, as well as major depocenters including the Illinois and Iowa basins, and marginal areas such as the Hollandale embayment (Mossler, 1992). During the Late Cambrian regression, Early and Middle Dresbachian deposits were exposed as a flat coastal plain with scattered hills of resistant Precambrian rocks (Lochman-Balk, 1970). Evidence of this is recorded by the presence of Sioux quartzite fragments in the Mt. Simon Sandstone (Uribe, 1994) and in the disturbed dispersal patterns located around the Baraboo district of Wisconsin (Dott et al., 1980). The coarse detrital sediments of the Galesville Sandstone record this event (Mossler, 1992).

A second Late Dresbachian transgression marked the beginning of the Franconia Stage, with northwestern Wisconsin and possibly northeastern Minnesota serving as the origin of clastic material. The missing Mazomanie Member at the western edge of the Hollandale embayment implies that the section of the Transcontinental arch located in western and central Minnesota did not add sediment to the basin (Austin, 1972). As the sea spread to the west during St. Lawrence time, the dominant pattern of sediment transport was from the east to the west, with a majority of the sediment being derived from northwestern Wisconsin and northeastern Minnesota. By Early Ordovician time, the Transcontinental arch in central Minnesota was supplying sediment to the developing Hollandale depositional area, creating a crescent of New Richmond Sandstone around the embayment. During St. Peter time, the subsiding Twin Cities basin was filled with sand derived from northern, northwestern, and northeastern sources (Austin, 1972). Figure 15 shows the approximate southerly limits of the Galesville Sandstone, Jordan Sandstone, New Richmond Sandstone, and the St. Peter Sandstone.

The role of eustatic sea level rise:

The global supercontinent began to break up during Late Proterozoic time, and by Early Cambrian, all the continental segments were surrounded by slowly subsiding passive margins. Continuing subsidence and/or rising global sea levels produced great shallow seaways upon the continents themselves, so that by the Late Cambrian, at least three-fourths of the low surface of the North American continent (including the Hollandale embayment) was flooded. The epeiric sea that constituted the Sauk transgression continued to spread until Early Ordovician time (Dott and Prothero, 1994, p. 236). The average rate of transgression was approximately 18 kilometers per million years; however, the transgression was irregular, as suggested by the presence of unconformities.

After several million years of Early Ordovician dolomite deposition, a widespread unconformity occurred over a majority of the craton. The epeiric sea retreated to the margins of the continent, and the craton was subjected to extensive erosion. Above this well-developed unconformity lies the St. Peter Sandstone, which serves as the basal unit of the Tippecanoe Sequence. After deposition of the St. Peter Sandstone, major carbonate sediments were precipitated across the craton in the Late Ordovician epeiric sea (Dott and Prothero, 1994, p. 239).

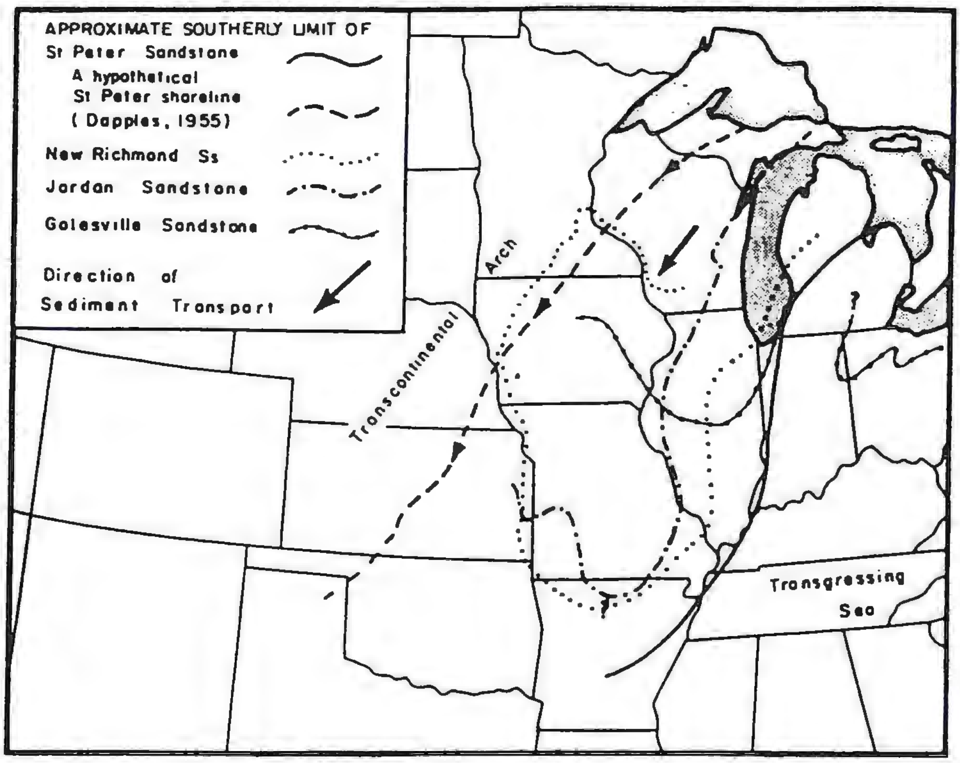

Fig. 15: Map showing approximate southern limit of occurrences of the quartzose arenites and the general direction of sediment transport. (From Ostrom, 1978).

CHAPTER VI

DISCUSSION: EVIDENCE FOR RECYCLING, LATE PROTEROZOIC - EARLY PALEOZOIC QUARTZ ARENITES

The principle objective of this chapter is to provide and discuss the petrographic evidence for the recycling of Late Proterozoic - Early Paleozoic quartzose arenites. Five main lines of evidence will be discussed: the presence of abraded quartz overgrowths, a decrease in polycrystalline quartz, the presence and abundance of feldspar, the relationship between polycrystalline quartz and feldspar, and the role of the heavy mineral suite.

Evidence: Abraded quartz overgrowths

All of the nine units contained grains with abraded overgrowths (see Plate 2). However, the overgrowths are not present in large quantities. It is evident that larger quantities of recycled quartz grains are present in the lower portion that the upper part of the stratigraphic column (Figure 16). Due to the amount of repeated abrasion that occurred through erosional processes and the fragile nature of the quartz overgrowths, the amount of abraded overgrowths generally decreases upward in the column.

Evidence: Decrease in polycrystalline quartz

In addition to the presence of abraded quartz overgrowths, an increasing maturity of the sediment can be seen in the overall reduction of less stable minerals, mainly polycrystalline quartz as well as feldspar. The overall distribution of polycrystalline quartz in the nine units of this study show a general trend of decreasing polycrystalline quartz upward in the stratigraphic column (Figure 17).

Evidence: Presence and abundance of feldspar

The amount of feldspar present in the quartzose arenites involved in this study is variable, ranging from 0-38% total feldspar (see Table 1).

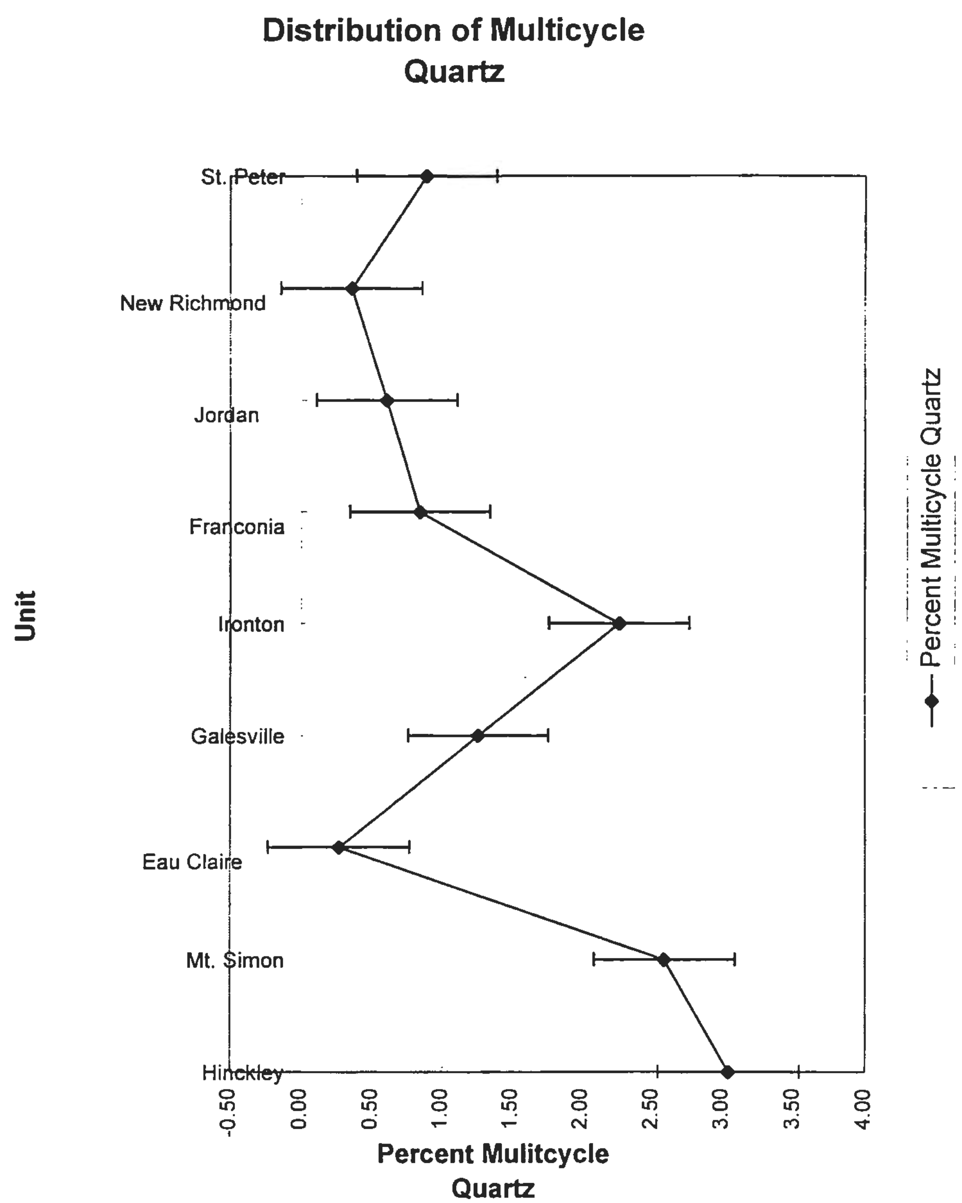

Fig. 16: Distribution of multicycle quartz (the bars indicate one standard deviation).

Distribution of Polycrystalline Quartz

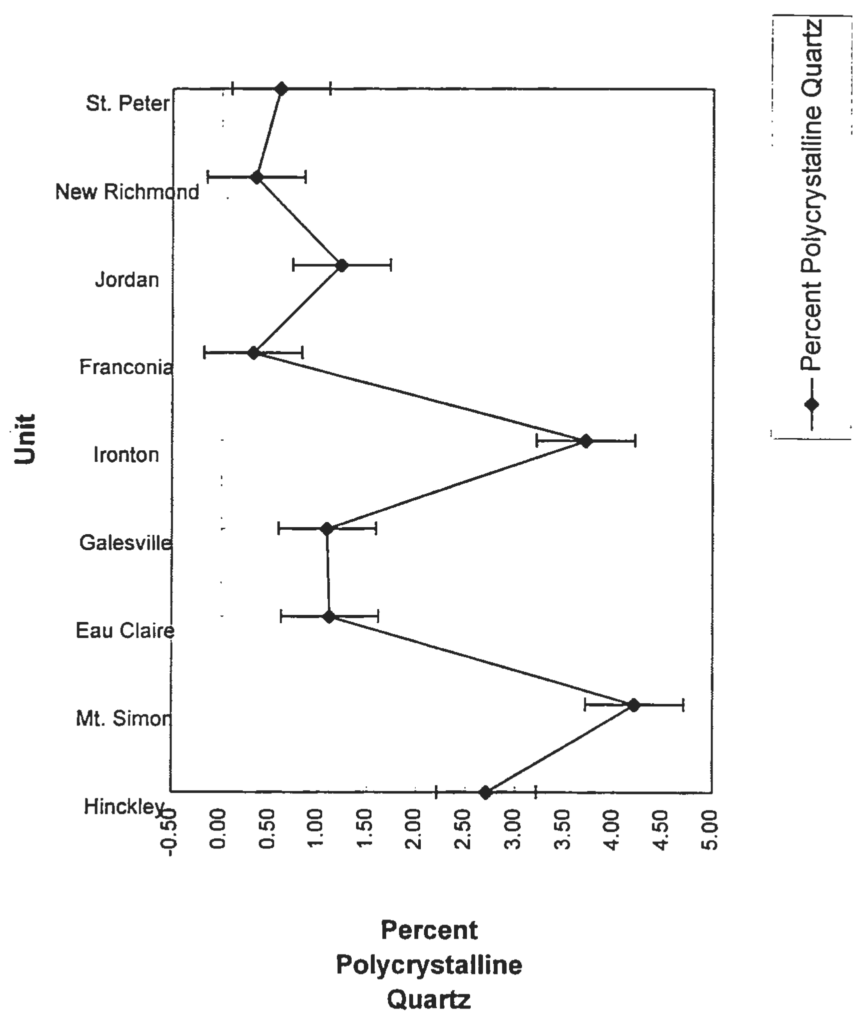

Fig. 17: Distribution of polycrystalline quartz (the bars indicate one standard deviation).

The amount of total feldspar present in most units, excluding the Eau Claire Formation and the Franconia Formation, is minimal, with approximately 3 percent present. However, there is no overall trend upwards through the sequences, but peaks of feldspar occur in the Eau Claire and the Franconia Formations (Figure 18).

During petrographic analysis, both unaltered and altered feldspar were counted. The distribution of unaltered feldspar vs. altered feldspar can be seen in Figure 19.

Evidence for the recycling of the quartzose arenites may also be interpreted through the distribution of unaltered feldspar vs. altered feldspar. In seven of the nine studied rock units, the amount of unaltered feldspar is less than or approximately 3% (Figure 19). However, in two units, the Eau Claire Formation and the Franconia Formation, the amount of unaltered feldspar increases sharply. It is possible that this sharp increase is due to an influx of fresh sediment from the Transcontinental arch/Wisconsin dome.

The amount of altered feldspar varies from 0-3% (Figure 19). Evidence for the recycling of the quartzose arenites by the redistribution of feldspar can be seen in the Ironton Sandstone. During Eau Claire time, the amount of unaltered feldspar peaks. Possibly through recycling, the amount of unaltered feldspar decreases in Galesville time, while the amount of altered feldspar increases. By Ironton time, so much possible recycling and reworking of the sediment has occurred that the amount of altered feldspar slightly surpasses the amount of unaltered feldspar.

A similar situation can be seen with the influx of fresh sediment during Franconia time, but it is not nearly as pronounced as that of the Eau Claire time. The notable difference is that the amount of altered feldspar does not surpass the amount of unaltered feldspar with the Franconia feldspar peak. However, the distribution of unaltered and altered feldspar mimic each other, which may indicate that some reworking of the feldspar was occurring.

Distribution of Total Feldspar

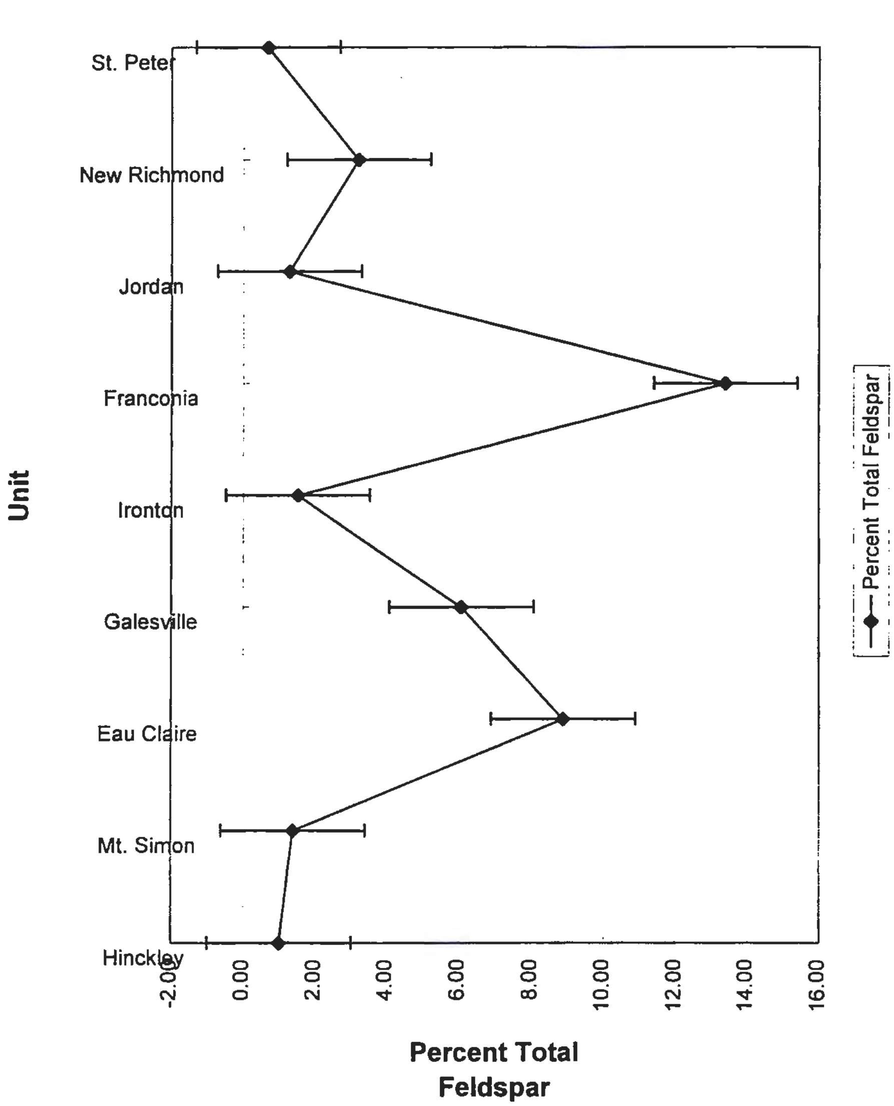

Fig. 18: Distribution of total feldspar (the bars indicate one standard deviation).

Distribution of Unaltered Feldspar vs. Altered Feldspar

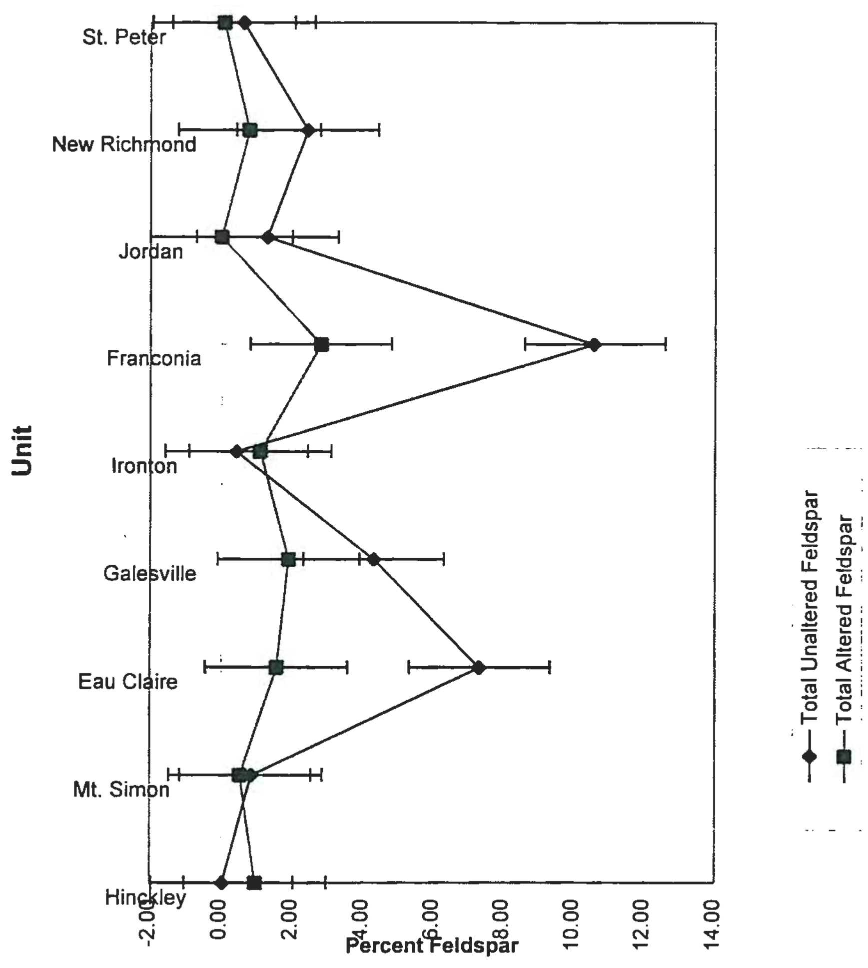

Fig. 19: Distribution of unaltered feldspar vs. altered feldspar (the bars indicate one standard deviation).

Evidence: Relationship between polycrystalline quartz and feldspar

There is an inverse relationship between polycrystalline quartz and unaltered feldspar (Figure 20). This seems to be the exact opposite of the hypothesis. However, polycrystalline quartz is derived from mainly metamorphic regions, such as the metasedimentary rock, schist-rich migmatite, and paragneisses that are present in northern Minnesota (Drew, 1993). If an influx of fresh sediment occurred during both Eau Claire and Franconia time, producing the peaks of unaltered feldspar in Figure 19, it can then be postulated that the fresh sediment was not derived from mainly metamorphic sources. As stated earlier, the paleocurrent direction was mainly to the south and southwest (Figure 15), and Austin (1972) indicated that the paleocurrent direction may have varied over time as a result of uplift and degradation of various sections of the Transcontinental arch-Wisconsin dome positive area as well as the development of structures that affected sedimentation in the Paleozoic seas. It is possible that the fresh sediment brought in during Eau Claire and Franconia time, both polycrystalline quartz and feldspar, was derived from a metamorphic source.

Evidence: Heavy mineral suite

Evidence for the recycling of the nine quartzose arenites is further supported by the heavy mineral analysis. Multicycle tourmaline grains are present in all nine formations (see Plate 5). These grains have abraded overgrowths, suggesting that the grains received tourmaline overgrowths in an older arenite, were removed from that setting, and were then reworked and recycled into a younger arenite. However, the number of tourmaline grains containing abraded overgrowths is very small.

Also noteworthy is that all of the units contain similar heavy mineral assemblages (Figure 21). All nine units contain significant amounts of subrounded green-brown tourmaline, unzoned round and subround zircon grains, as well as colorless and pink round and subround garnet grains. This indicates that although fresh sediment may have been brought into the Hollandale embayment during Eau Claire and Franconia time, that the overall heavy mineral concentrations did not vary much. The data also show that zircon, tourmaline, rutile, and garnet are stable heavy minerals.

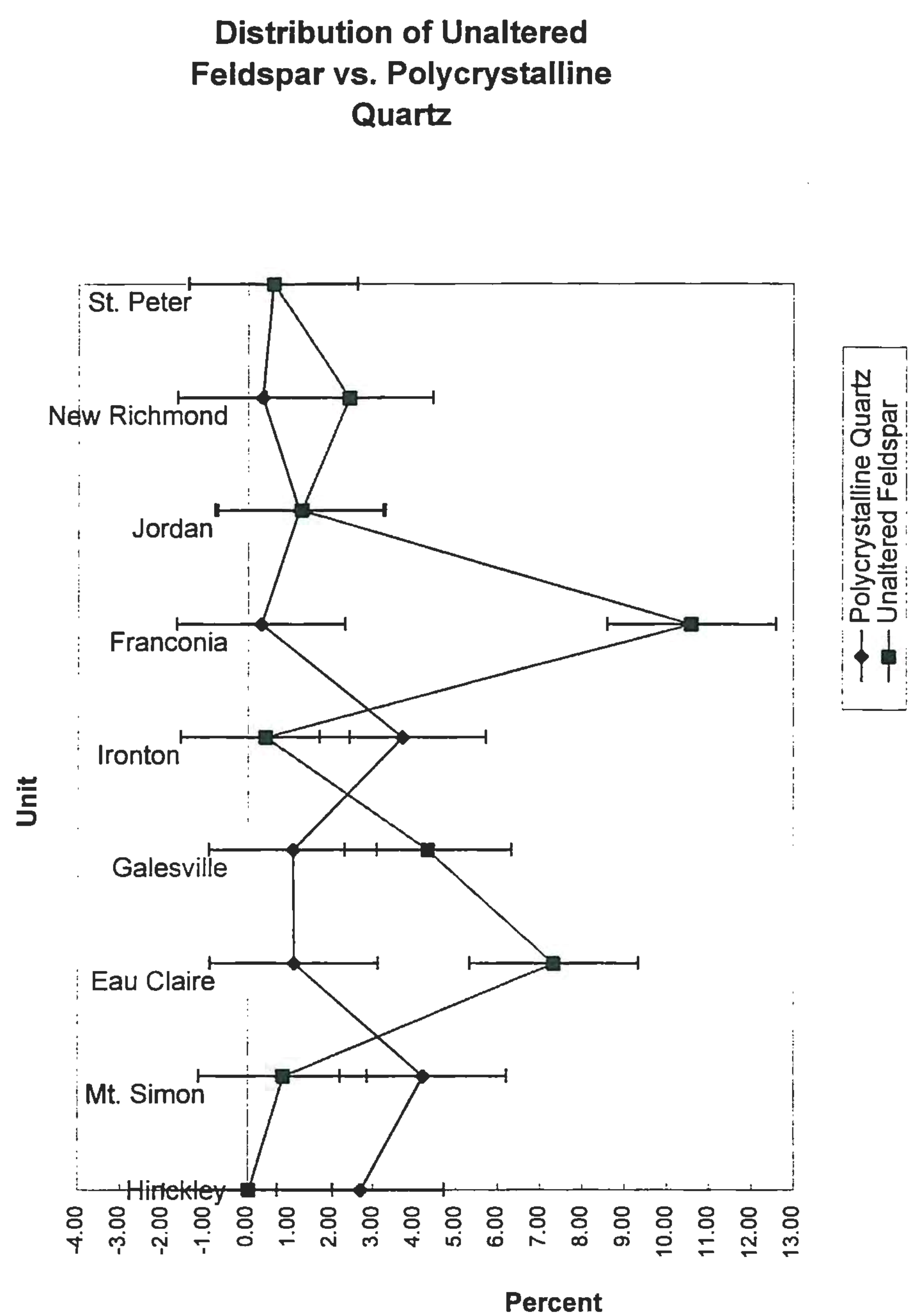

Fig. 20: Distribution of unaltered feldspar vs. polycrystalline quartz (the bars indicate one standard deviation).

Distribution of Heavy Minerals

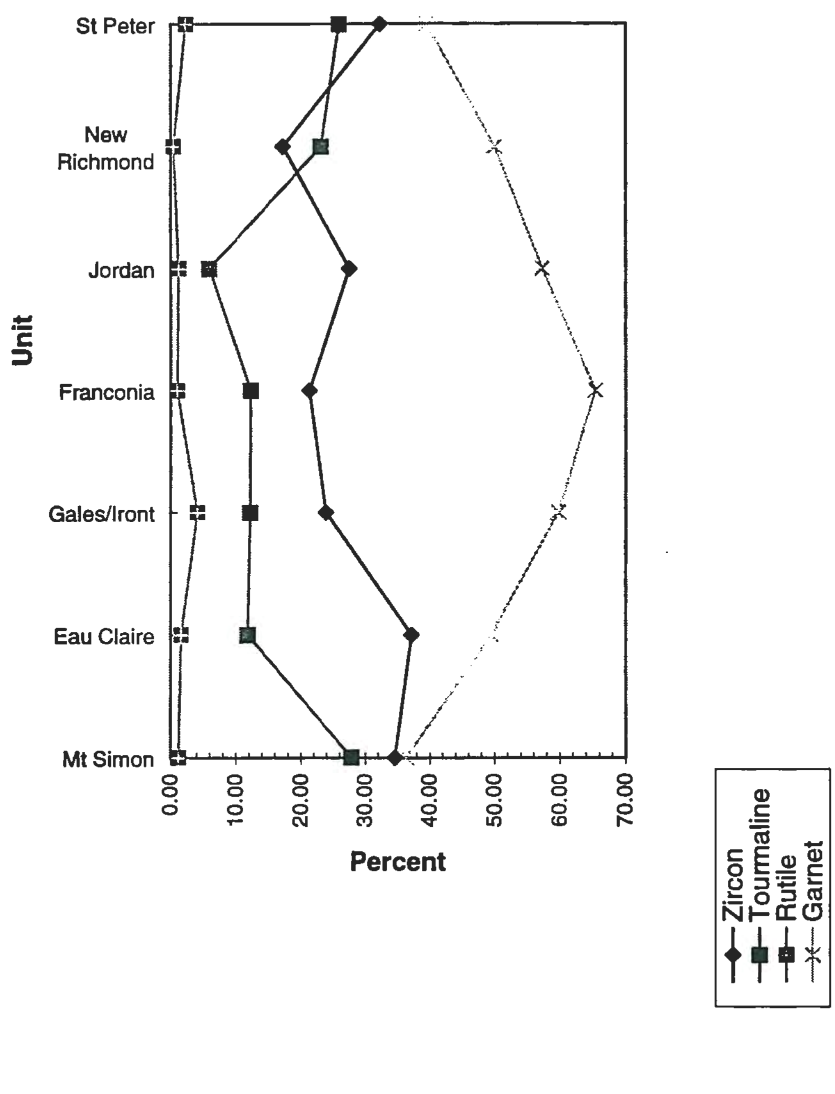

Fig. 21: Distribution of heavy minerals (the bars indicate one standard deviation).

Recycling of the units:

The following discussion examines possible evidence for recycling in each of the nine quartz arenites. For illustrative purposes, comparisons are made between a quartz arenite formation and the arenite formation that stratigraphically underlies it. However, one must realize that each stratigraphically older unit is a potential source for the recycling of the sediment (Figure 13).

Recycling to produce the Mt. Simon Sandstone:

The Mt. Simon Sandstone overlies many units of Precambrian age, primarily rift-fill sediments such as the Solor Church Formation, the Fond du Lac Formation, and the Hinckley Sandstone (Figure 21). Along the axis of the Hollandale embayment, the Mt. Simon overlies the Hinckley Sandstone. However, the Hinckley sand that directly underlies the Mt. Simon would not have served as a source for the recycling; only the Hinckley sand that was not covered by the transgressing sea would have been available for recycling.

The Hinckley and Mt. Simon Sandstones are both quartz arenites, and serve as the starting point for comparison of recycling of this study. The Fond du Lac and the Solor Church Formations were not studied herein because they are not quartz arenites. The Fond du Lac is arkosic and the Solor Church contains abundant rock fragments (Morey and Ojakangas, 1982). As a general comparison, the Late Proterozoic Hinckley Sandstone is well-cemented with quartz, whereas the Cambrian Mt. Simon Sandstone is friable.

The differences in detrital quartz composition between the two sandstones are minimal. The noticeable difference in quartz types is the increase in polycrystalline quartz in the Mt. Simon. If the Hinckley Sandstone was recycled to produce the Mt. Simon Sandstone, one would expect the amount of polycrystalline quartz to decrease. However, this slight increase can be explained by some sediment directly derived from the underlying Precambrian basement rock and not only from the Hinckley Sandstone.

Very little feldspar is present in the Hinckley Sandstone. The amount of total unaltered feldspar increases from the Hinckley to the Mt. Simon. Again, this is likely because some sediment was likely derived directly from the underlying Precambrian basement rock instead of just from recycled Hinckley Sandstone. The amount of total altered feldspar decreases due to continued reworking of the sediment. Although the amount of total feldspar decreases from the Hinckley to the Mt. Simon, the amount of authigenic feldspar and detrital cores increases from the Hinckley to the Mt. Simon.

The Mt. Simon Sandstone also shows a decrease in the amount of plutonic rock fragments present (average = 0.1 percent) in comparison to the Hinckley Sandstone (average = 0.9 percent) (Table 1).

Recycling to produce the Eau Claire Formation:

In comparison with both the underlying Hinckley Sandstone and Mt. Simon Sandstone, which may be possible sources for the sediment of the Eau Claire Formation, there is a decrease in the amount of detrital quartz present, due largely to an increase in detrital feldspar. Both multicycle quartz values and polycrystalline quartz values decrease in the Eau Claire Formation relative to lower units (Figures 16 and 17).

It is possible that the decrease in the amount of common quartz in the Eau Claire is due to the environment of deposition of the formation, located seaward of the littoral zone in the Hollandale embayment. In the littoral zone, there is a continuous reworking of the sediment by wave action. By moving away from the beach environment, it is possible to retain a greater amount of feldspar in the sediment due to the lower amounts of reworking and recycling. Also, the Eau Claire Formation has a smaller grain size relative to the Hinckley and Mt. Simon sandstones, which could also account for the differences in mineralogy.

Mossler (1992) indicated that small amounts of detrital sediment, combined with continued eustatic sea level rise, contributed to the overall increase in feldspar percentage. If this proves to be true, one would most likely expect the amount of polycrystalline quartz to increase in Eau Claire time along with the amounts of unaltered feldspar and rock fragments, as all of these minerals are unstable.

The amount of unaltered detrital feldspar sharply increases from the Mt. Simon to the Eau Claire. This supports the hypothesis of an influx of sediment. Also notable is the increase in the amount of altered feldspar and authigenic feldspar. Because the Eau Claire was deposited in a tidal flat environment (Byers and Huber, 1976), the possibility of reworking unstable minerals increases, so one would expect more altered feldspar in the Eau Claire Formation than in the Mt. Simon Sandstone.

Recycling to produce the Galesville Sandstone:

There is little variation in the amount of common and polycrystalline quartz present in the Galesville Sandstone in comparison to the underlying Eau Claire Formation. The only notable difference is in the increased amount of multicycle quartz present in the Galesville. With a renewed transgression, sediment from the underlying arenites may have been moved shoreward, producing a higher amount of multicycle quartz in the Galesville.

The Galesville Sandstone has a lower feldspar percentage than the underlying Eau Claire Formation. If recycling of the Eau Claire Formation occurred to produce the Galesville Sandstone, one would expect that feldspar percentages would decrease, and to some extent, they do. The amount of unaltered feldspar decreases . This is perhaps due to the fact that sediment supply was lower during the second progradation than the first progradation (Mossler, 1992). As further evidence of recycling, the amount of altered feldspar increases in the Galesville, thereby indicating reworking of the greater percentage of unaltered feldspar in the Eau Claire Formation.

Recycling to produce the Ironton Sandstone:

The overall percentage of total quartz increases with the deposition of the Ironton Sandstone (average = 98.4 percent) when compared to the underlying Galesville Sandstone (average = 93.4 percent). This might be surprising, as Austin (1972) noted that the sediment was not sorted as effectively in Ironton time as it was during Galesville. However, an increase in the percentage of polycrystalline quartz would be an expected result of lower energy bottom currents as evidenced by the Ironton's environment of deposition. The ability to mechanically abrade polycrystalline quartz grains would decrease in a lower energy environment. Also worth noting is the increase in the amount of multicycle quartz present. Perhaps the lower energy currents and the decrease in wave activity allowed for enhanced preservation of the delicate quartz overgrowths.

There is little feldspar present in the Ironton Sandstone. Unaltered feldspar is present only in trace amounts, while altered feldspar has decreased. This may be due to the continued recycling of the influx of sediment that was brought into the Hollandale embayment during Eau Claire time. During Galesville time, the amount of unaltered feldspar decreased, while the amount of altered feldspar increased. Finally, during Ironton time, enough recycling had occurred so that the amount of altered feldspar surpassed the amount of unaltered feldspar.

The amount of matrix present is also greater in the Ironton Sandstone (average = 19.1 percent) as compared to the Galesville Sandstone (average = 7.2). This further supports Austin's (1972) theory of a lower energy environment of deposition.

Recycling to produce the Franconia Formation:

The sediment of the Franconia Formation was derived from a different source than that of the Ironton Sandstone. Northwestern Wisconsin and possibly northeastern Minnesota served as the source of clastic material during Franconia time (Austin, 1972). The absence of the Mazomanie Member on the western edge of the Hollandale embayment suggests that the section of the Transcontinental arch located in western and central Minnesota did not contribute sediment to the basin (Austin, 1972). The Franconia was also deposited during a marine transgression (Austin, 1969). If northwestern Wisconsin and northeastern Minnesota served as the sources of clastic material, perhaps sediment input from rivers added to the overall decrease in common quartz percentages and the overall increase in feldspar percentages.

Evidence for the recycling of underlying quartzose arenites to produce the Franconia Formation is weak. Total quartz percentages in the Franconia Formation are much lower (average = 84.5 percent) in comparison to the immediately underlying Ironton Sandstone (average = 98.4 percent). However, one also needs to remember that it is not only the Ironton sediment that is available to produce the Franconia, but rather all of the underlying arenites as well as the likely contribution of a influx of fresh sediment.

Direct petrographic evidence for the recycling of the feldspar of the underlying arenites to produce the Franconia Formation is also lacking. If the feldspar was recycled, one would expect the unaltered feldspar percentage to be even lower, and it is not (average = 10.6 percent). It is possible that this increase of unaltered feldspar is due to an influx of sediment being derived from the different source areas. Northwestern Wisconsin and possibly northeastern Minnesota served as the origin of clastic material during Franconia time. The missing Mazomanie Member at the western edge of the Hollandale embayment implies that the section of the Transcontinental arch located in western and central Minnesota did not add sediment to the basin (Austin, 1972).

Recycling to produce the Jordan Sandstone:

Runkel (1994) interpreted the Jordan lithofacies to represent a regressive sequence deposited as part of a shoreline system that prograded across the Hollandale embayment, with the lower Jordan being a feldspathic sandstone and the upper Jordan being a quartzose sandstone. During this marine regression, it is likely that the sediments deposited during the Franconian transgression were allowed ample time to be reworked and recycled into the lower Jordan. In upper Jordan time, more abrasion eliminated the feldspars (supporting Runkel's classification). Why are there polycrystalline quartz grains present in the Jordan Sandstone (average = 1.1 percent)? If indeed Runkel's interpretation of the environment of deposition of the Jordan is accurate, it is possible that addition of polycrystalline quartz grains occurred with a river influx as the shoreline prograded. Again, the amount of multicycle quartz grains present has decreased, and that seems logically due to the fragility of the overgrowths.

The overall lack of both altered and unaltered feldspar in the upper Jordan provides direct evidence that the Franconia sands were recycled, eliminating the feldspar. Relative to the underlying Franconia Formation, a minimal amount of unaltered feldspar is present (average = 1.3 percent), whereas the Franconia contains 10.6 percent.

Recycling to produce the New Richmond (Sandstone) Member of the Shakopee Formation:

Evidence for the recycling of the underlying quartz arenites to produce the New Richmond (Sandstone) Member of the Shakopee Formation is minimal. The amount of multicycle quartz decreases slightly, due possibly to the fragility of the quartz overgrowths.

Surprisingly, though, the amount of feldspar also increases with the New Richmond Sandstone (average = 3.2 percent), with an average of 2.4 percent consisting of unaltered feldspar. Perhaps a larger portion of the recycled sediment that was contributed to the New Richmond was derived from the Franconia Formation.

Recycling to produce the St. Peter Sandstone:

The St. Peter Sandstone serves as a classic example of a clean quartz arenite. However, it is not possible that the thin New Richmond Sandstone could have served as the sole sediment contributor for the production of the St. Peter Sandstone. Where did the sediment come from? Is it a first cycle quartz arenite produced from sediments derived from the Wisconsin dome and Transcontinental arch? According to Suttner et al's (1981) specified conditions necessary to produce a first cycle quartz arenite (Suttner (1981) determined that first cycle quartz arenites are produced through a specific and complex combination of extreme conditions consisting of a tropical climate, low relief, and slow sedimentation rates.), conditions during St. Peter time were ideal for the production of a quartz arenite. However, after the Early Ordovician dolomite deposition, a widespread unconformity occurred over a majority of the craton (Dott and Prothero, 1994, p. 239), thereby exposing the underlying arenites for a great deal of time, increasing the likelihood for the possibility of recycling to occur.

All of the detrital grains present are indicative of possible recycling of the underlying sandstones. Total quartz percentages increase from the New Richmond Sandstone (average = 95.4 percent) to the St. Peter Sandstone (average = 99.3 percent).

Feldspar content in the St. Peter Sandstone is also minimal (average = 0.7 percent). Amounts of unaltered feldspar decrease, while a trace amount of altered feldspar is present.

CHAPTER VII

CONCLUSIONS

Data collected in this study support the following conclusions:

1) Petrographic analyses support the hypothesis that the Late Proterozoic - Early Paleozoic quartzose arenites of this study (Late Proterozoic Hinckley Sandstone, the Upper Cambrian Mt. Simon Formation, Eau Claire Sandstone, Galesville Sandstone, Ironton Sandstone, and Jordan Sandstone, and the Ordovician New Richmond Member of the Shakopee Formation and the St. Peter Sandstone) were produced in part by recycling. All of the nine units of this study contain multicycle quartz grains, or quartz grains with abraded quartz overgrowths, which provide evidence for the recycling of the arenites.

2) All of the units of this study were petrographically examined, using consistent operational definitions. Through this process, it is possible to draw conclusions about the concentrations of the various quartz types. An overall decrease in the amount of polycrystalline quartz present through geologic time can be used to further support that recycling of the quartzose arenites occurred. Because of the unstable nature of polycrystalline quartz, as further abrasion and transportation of the sediment occurred through the reworking and recycling of the arenites, polycrystalline quartz was virtually eliminated by latest Cambrian and Ordovician time.

3) The concentrations of the unaltered and altered feldspar types can also be used to support the recycling of the quartzose arenites. Again, using consistent operational definitions during the point counting of the thin sections allows for the comparison of the relative amount of feldspar to be made from unit to unit through geologic time. Peaks of unaltered feldspar occur during Eau Claire and Franconia time, indicating that influxes of fresh sediment may have occurred during these times. Further evidence of the recycling of the quartzose arenites in relation to the feldspar concentrations can be found in the Ironton Sandstone, in which unaltered

feldspar of Eau Claire time was reworked and recycled to the point that during Ironton time, the amount of altered feldspar surpassed the amount of unaltered feldspar.

4) Quantitative heavy mineral analyses indicate that subrounded to rounded garnet, zircon, tourmaline, and rutile are the most abundant detrital non-opaque heavy minerals present in the nine quartzose arenites. Also present in minor quantities are apatite, pyroxene, epidote, staurolite and anatase. The most common opaque minerals present are magnetite, pyrite, and hematite.

5) All nine of the units included in this study contain tourmaline grains with abraded overgrowths; their presence also indicates that the arenites are multicycle in origin.

6) Because of the high concentration of garnet present in all nine of the arenites, a ZTRG index is utilized (modified from the ZTR index of Hubert, 1962). The ZTRG index is the total percentage of zircon, tourmaline, rutile, and garnet among the non-opaque, non-micaceous detrital heavy mineral concentration in an arenite (Uribe, 1994).

7) It has long been speculated that the Late Proterozoic - Early Paleozoic quartz arenites are multicycle in origin because of the presence of clean quartz sand (e.g. Matsch and Ojakangas, 1982, p. 65; Dott and Batten, 1982, p. 283; Dott and Prothero, 1994, p. 236). The surface of the craton was eroded for nearly 500 million years, and was certainly affected by rivers, tides, winds, and glacial ice before being deposited in the epeiric sea (Dott and Batten, 1982, p. 283). This study now provides petrographic evidence that erosional processes during the Late Cambrian - Early Ordovician marine transgressions and regressions played a substantial role in the creation of these quartz arenites, thereby recycling grains from older exposed units within the Hollandale embayment.

REFERENCES CITED

Andrew, J.A., 1965. Size distribution of the sand and heavy minerals in the Ironton Sandstone: Unpublished MS Thesis, University of Wisconsin, Madison.

Austin, G.S., 1972. Paleozoic lithostratigraphy of southeastern Minnesota: in Geology of Minnesota: A Centennial Volume, P.K. Sims and G.B. Morey, editors, p. 459-473.

Austin, G.S., 1971. The stratigraphy and petrology of the Shakopee Formation, Minnesota: Unpublished Ph.D. dissertation, University of Iowa, Iowa City.

Austin, G.S., 1974. Multiple overgrowths on detrital quartz grains in the Shakopee Formation (Lower Ordovician) of Minnesota: Journal of Sedimentary Petrology, v. 44, no. 2, p. 358-362.

Berg, R.R., 1954. Franconia Formation of Minnesota and Wisconsin: Geological Society of America Bull., v. 66, p. 857-882.

Berg, R.R., Nelson, C.A., and Bell, W.C., 1956. Upper Cambrian rocks in southeastern Minnesota: in: Lower Paleozoic geology of the upper Mississippi Valley, Geol. Soc. America Guidebook Series, G.M. Schwartz, editor, Field Trip No. 2, p. 1-23.

Blatt, H., 1967. Provenance determinations and the recycling of sediments: Journal of Sedimentary Petrology, v. 37, no. 4, p. 1031-1044.

Bunker, B.J., Witzke, B.J., Watney, W.L., and Ludvigson, G.A., 1988. Phanerozoic history of the central midcontinent, United States: In: Sloss, L.L., ed., Sedimentary Cover- North American Craton, USA: Geological Society of America, The Geology of North America, v. D-2, p. 243-260.

Byers, C.W., and Huber, M.E., 1976. The Eau Claire Formation in Wisconsin: a Cambrian tidal flat, Geol. Soc. Am. Abstracts, North-Central Section, p. 469.

Chase, C.G., and Gilmore, T.H., 1973. Precambrian plate tectonics: The Midcontinent Gravity High: Earth and Planetary Sci. Let., v. 21, p. 70-78.

Churchill, R., in prep. The Stratigraphy and Petrology of the Upper Cambrian Mt. Simon, Eau Claire, and Galesville Formations in southeastern Minnesota: Unpublished MS Thesis, University of Minnesota, Duluth.

Craddock, C., 1972. Late Precambrian: Regional Geologic Setting in: Geology of Minnesota: A Centennial Volume, P.K. Sims and G.B. Morey, editors, p. 281-291.

Distefano M., 1973. The mineralogy and petrology of the Eau Claire Formation, west-central Wisconsin: Unpublished MS thesis, Northern Illinois University, DeKalb.

Pettijohn F.J., Potter, P.E., and Siever, R., 1987. Sand and Sandstone, second edition: New York, Springer Verlag, 553 p.

Dott, R.H., and Batten, R.L., 1988. Evolution of the Earth, fourth edition: New York, McGraw-Hill, 643 p.

Dott, R.H., and Prothero, D.R., 1994. Evolution of the Earth, fifth edition: New York, McGraw-Hill, 569 p.

Harrell, J., and Blatt, H., 1978. Polycrystallinity: Effect on the durability of detrital quartz: Journal of Sedimentary Petrology, v. 48, p. 25-30.

Hubert, J.F., 1962. A zircon-tourmaline-rutile maturity index and the interdependence of the composition of heavy mineral assemblages with the gross composition and texture of sandstones: Journal of Sedimentary Petrology, v. 32 (3), p. 440-450.

Lochman-Balk, C., 1970. Upper Cambrian Faunal Patterns on the Craton, Geological Society of American Bulletin, v. 81, p. 3197-3224.

Kennedy, S.K., and Arikan, F., 1990. Spalled quartz overgrowths as a potential source of silt: Journal of Sedimentary Petrology, v. 60, no. 3, p. 438-444.

Mack, G.H., 1978. The survivability of labile light-mineral grains in fluvial, aeolian and littoral marine environments: the Permian Cutler and Cedar Mesa Formations, Moab, Utah: Sedimentology, v. 25, p. 587-604.

Mazullo, J.M., 1988. Nature and causes of transgressive and regressive cycles in a Lower Paleozoic quartzose sheet sand [abs]: AAPG Bulletin, v. 72, p. 219.

Miller, R., 1970. Northern Natural Gas Company, written comm., in: Austin, G.S., 1972. Paleozoic lithostratigraphy of southeastern Minnesota in Geology of Minnesota: A Centennial Volume, P.K. Sims and G.B. Morey, editors, p. 459-473.

Morey, G.B., 1993. Geologic Map of Minnesota: Bedrock Geology, State Map Series S-19, University of Minnesota, Minnesota Geological Survey, P.C. Drew, Director.

Morey, G.B., 1972. Petrology of Keweenawan sandstones in the subsurface of southeastern Minnesota: in Geology of Minnesota: A Centennial Volume, P.K. Sims and G.B. Morey, editors, p. 436-449.

Morton, A.C., 1985. Heavy Minerals in Provenance Studies: in Provenance of Arenites, G.G. Zuffa, editor, NATO ASI Series, D. Reidel Publishing Company, Boston, p. 249-277.

Mossler, J.H., 1987. Paleozoic lithostratigraphic nomenclature for southeastern Minnesota: Minnesota Geological Survey, Report of Investigations 36, 36 p.

Mossler, J.H., 1992. Sedimentary rocks of Dresbachian age (Late Cambrian), Hollandale Embayment, Southeastern Minnesota: Minnesota Geological Survey Report of Investigations 40, 71 p.

Odom, I.E., 1975. Feldspar-grain size relations in Cambrian arenites, Upper Mississippi Valley: Journal of Sedimentary Petrology, v. 45, no. 3, p. 636-650.

Ojakangas, R.W., and Matsch, C.L., 1982. Minnesota's Geology: Minneapolis, University of Minnesota Press, 243 p.

Ojakangas, R.W., and Morey, G.B., 1982. Keweenawan prevolcanic quartz sandstones and related rocks of the Lake Superior region. Geol. Soc. Am. Mem. 156: 85-96.

Ojakangas, R.W., 1963. Petrology and sedimentation of the Upper Cambrian Lamotte

Sandstone in Missouri: Journal of Sedimentary Petrology, v. 33, p. 860-873.

Ostrom, M.E., 1964. Pre-Cincinnati Paleozoic cyclic sediments in the Upper Mississippi Valley: a discussion: in Symposium on cyclic sedimentation, Kansas Geol. Survey Bull. 169, v. 2, pp. 381-398.

Ostrom, M.E., 1966. Cambrian stratigraphy in Western Wisconsin: Wis. Geological and Natural History Survey Info. Circular 7.

Ostrom, M.E., 1970. Lithologic Cycles in Lower Paleozoic Rocks of Western Wisconsin: Wis. Geol. and Nat. History Survey Info. Circular 11.

Ostrom, M.E., 1978. Lithostratigraphy, petrology, and sedimentology of Late Cambrian - Early Ordovician rocks near Madison, Wisconsin: Field Trip Guide Book Number 3, Eighth Annual Meeting, Great Lake Section, Society of Economic Paleontologists and Mineralogists.

Ostrom, M.E., 1981. Bedrock Geology Map of Wisconsin: University of Wisconsin - Extension, Geological and Natural History Survey.

Parham, W.E., 1970. Petrography of St. Peter Sandstone [abs.]: in Summary of fieldwork, 1969: Minnesota Geological Survey Information Circular 8, p. 10.

Pettijohn F.J., Potter, P.E., and Siever, R., 1987. Sand and Sandstone, second edition: New York, Springer Verlag, 553 p.

Potter, P.E., and Pryor, W.A., 1961. Dispersal centers of Paleozoic and later clastics of the Upper Mississippi Valley and adjacent areas, Geological Society of America, v. 72, p. 1195-1250.

Pride, D.E., 1966. Size and heavy mineral analysis of the New Richmond Sandstone of Lower Ordovician age: Unpublished MS Thesis, University of Wisconsin, Madison.

Runkel, A.C., 1994. Deposition of the uppermost Cambrian (Croixan) Jordan Sandstone, and the nature of the Cambrian-Ordovician boundary in the Upper Mississippi Valley: Geological Society of American Bulletin, v. 106, p. 492-506.

Sanderson, I.D., 1984. Recognition and significance of inherited quartz overgrowths in quartz arenites: Journal of Sedimentary Petrology, v. 54, no. 2, p. 473-486.

Sloan, R.F., and Danes, Z.F., 1962. A geologic and gravity survey of the Belle Plaine Area, Minnesota: Minn. Acad. Sci. Proc., v. 30, p. 41-45.

Squillace, P.J., 1979. The geology of the New Richmond Member of the Shakopee Formation (Lower Ordovician), upper Mississippi Valley: Unpublished MS thesis, University of Minnesota, Duluth.

Suttner, L.J., Basu, A., and Mack, G.H., 1981. Climate and the origin of quartz arenites: Journal of Sedimentary Petrology, v. 51 (4), p. 1235-1246.

Tryhorn, A.D., and Ojakangas, R.W., 1972. Sedimentation and petrology of the Upper Precambrian Hinckley Sandstone of east-central Minnesota: in Geology of Minnesota: A Centennial Volume, P.K. Sims and G.B. Morey, editors, p. 459-473.

Tucker, M.E., 1991. Sedimentary Geology: An Introduction to the Origin of Sedimentary Rocks, second edition: Oxford, Blackwell Scientific Publications, 259 p.

Uribe A., R.D., 1994. Petrography and diagenesis of the Mt. Simon Sandstone, Southeastern Minnesota: Unpublished MS Thesis, University of Minnesota, Duluth.